Deltares

Enabling Delta Life

Analysis of Breach Flow Slides with HMBreach

December 2011

Frank Tabak

Supervisor:
ir. D.R. Mastbergen

PREFACE

This report is a result of my internship with Deltares. My name is Frank Tabak and study Applied Mathematics at Delft University of Technology. As part of my study I have to do an internship to gain experience of what it is like to work as a mathematician in a company. Deltares offered me the change to carry out this internship.

I have learned a lot during my time at Deltares, the most valuable experience is in my opinion to work with not only mathematicians, but also with people from other disciplines, mainly civil engineering. I have noticed that the view of a civil engineer on certain matters differs from that of my view, as a mathematician. The challenge is to bridge the gap between the understanding of a mathematician and that of a more practical oriented civil engineer. Although I study *applied* mathematics I have learned that my definition of *Applied* is very different from that of civil engineers who really *apply* the mathematics.

I enjoyed working for Deltares and I would like to thank some people for helping me during my time here: Arno Rozing, Geeralt van den Ham, Jan van Zanten, Bert Jagers, Maarten de Groot and above all, my supervisor Dick Mastbergen.

Frank Tabak
29 December 2011, Delft

TABLE OF CONTENTS

PREFACE **3**

1 INTRODUCTION **6**

2 FLOW SLIDES **7**

2.1 LIQUEFACTION FLOW SLIDE 7

2.2 BREACH FLOW SLIDE 9

3 HMBREACH **12**

3.1 THE COMPUTATIONAL MODEL 12

3.1.1 Boundary Condition *13*

3.2 THE APPLICATION 15

3.2.1 General *15*

3.2.2 Input *15*

3.2.3 Output *16*

3.2.4 Charts *17*

3.2.5 Constants *17*

3.3 SENSITIVITY ANALYSIS HMBREACH 18

3.3.1 Porosity *19*

3.3.2 D_{50} *20*

3.3.3 $D_{50}D_{15}$ *20*

3.3.4 Δn *20*

3.3.5 Thickness Top *21*

3.3.6 Concentration *21*

3.3.7 Retrogression Velocity *21*

3.3.8 f_0 ..... *22*

3.3.9 Initiation *22*

3.3.10 Conclusion *23*

3.4 SENSITIVITY ANALYSIS HMTURB 24

3.4.1 Porosity *26*

3.4.2 D_{50} *27*

3.4.3 $D_{50}D_{15}$ *27*

3.4.4 Δn *28*

3.4.5 Thickness Top *28*

3.4.6 Concentration (%) *28*

3.4.7 Retrogression Velocity *28*

3.4.8 Froude Number *29*

3.4.9 f_0 ..... *29*

3.4.10 Conclusion *30*

3.5 SPECIFY ΔN PER LAYER 31

4 ANALYSIS OF SLOPE FAILURES **32**

4.1 ROOMPOT 32

4.1.1 Simulation with HMTurb *34*

4.1.2 Proneness of the Slope to Breach Flow Slides *40*

4.2 ROGGENPLAAT 41
4.2.1 Simulation with HMTurb *43*
4.2.2 Proneness of the Slope to Breach Flow Slides *45*
4.3 PLAAT VAN OUDE TONGE 47
4.3.1 Simulation with HMTurb *50*
4.3.2 Proneness of the Slope to Breach Flow Slides *52*
4.4 SPIJKERPLAAT 53
4.4.1 Simulation with HMTurb *54*
4.4.2 Proneness of the Slope to Breach Flow Slides *56*
4.5 CONCLUSION 58

5 APPENDIX: FIGURES 59
5.1 SENSITIVITY ANALYSIS 59
5.2 ROOMPOT 63
5.3 ROGGENPLAAT 72
5.4 PLAAT VAN OUDE TONGE 87
5.5 SPIJKERPLAAT 93

6 APPENDIX: TABLES 108
6.1 SENSITIVITY ANALYSIS HMBREACH 108
6.2 SENSITIVITY ANALYSIS HMTURB 109
6.3 ROGGENPLAAT 110
6.4 SPIJKERPLAAT 111

7 BIBLIOGRAPHY 112

1 INTRODUCTION

Flow slides are a major issue in subaqueous slopes. A flow slide can cause a large bank to collapse, and if a dyke is located on top of the bank this dyke can even collapse, which of course can cause a flooding. Two kinds of flow slides can be identified: breach flow slides and liquefaction flow slides. Although the two are intricately different they seem to be closely connected.

HMBreach is a computational model which, given a slope, can calculate the resulting, if any, breach flow slide. This model will be used to attempt to simulate major slope failures in the province of Zeeland, the Netherlands. This enables us to conclude if the failure was the result of a breach flow slide or perhaps some other process. This knowledge can then be used to predict if a certain slope is prone to breach flow slides.

Section 2 introduces the process of two types of flow slides; breach and liquefaction flow slides. Subsequently the reader is familiarized with HMBreach in Section 3. This section will also include some sensitivity analysis of the computational model. Finally, Section 4 will consider four slope failures which are attempted to recreate using the model.

This project was carried out as a part of the Deltares project *SBW Faalmechanismen in losgepakt zand (1204202).* The subproject which concerns this work is *1204202.019: Narekenen opgetreden oevervallen met bresgroeimodel*.

2 FLOW SLIDES

A Flow slide in sandy slopes is a physical phenomenon in which a subaqueous slope fails due to sand which becomes in suspension. Until recently the term 'flow slide' was used as a cause of numerous slope failures. A better understanding about the physical processes behind this phenomenon however has lead to the understanding that there are different types of flow slides. In this section we will familiarize ourselves with two types of flow slides:

- Liquefaction Flow Slides;
- Breach Flow Slides.

We are mainly interested in the latter type, the breach flow slide. It needs to be noted that, although a lot of progress has been made about understanding these processes, there still is much to be learned about these processes.

2.1 LIQUEFACTION FLOW SLIDE

A flow slide is a liquefaction flow slide when a slope suddenly, without any apparent reason, becomes unstable, a large part of the sand liquefies and the suspension will flow as a liquid down the slope and will settle down on a very shallow part of the bed. This whole process will make the slope much shallower then it was before. If the subaqueous slope is part of a dyke this process might cause (a part of) the dyke to collapse, see figure below (Groot, Stoutjesdijk, et al. September 2007).

Figure 2.1-1: Slope failure which resulted in damage to a dyke.

The cause of a liquefaction flow slide is the sudden occurrence of a large excess pore water pressure in a large part of the sandy slope. This causes the effective stress between the sand particles to decrease which in turn causes the sand to turn into a viscous fluid which will begin to flow. The pressure increase is assumed to be due to some load on the bed. Liquefaction flow slides typically

occur in loosely packed chunks of sand. For more information about this sort of flow slide the reader is referred to (Groot, Stoutjesdijk, et al. September 2007).

2.2 BREACH FLOW SLIDE

As mentioned earlier we are more interested in the process of a breach flow slide. Hence we will give somewhat more details about the process.

Figure 2.2-1: Result of a breach flow slide (2008).

A breach flow slide, in contrast to a liquefaction flow slide, can also occur in slopes that consist of compactly packed sand. The breach flow slide begins with an initial disturbance somewhere on the slope. This disturbance creates a *breach*. The breach is a small portion of the slope which has a steeper slope than the slope itself, it could even be vertical. From this breach sand crumbles down and creates a turbidity current. If this current is strong enough it can turn into an erosive turbidity current meaning that the current causes more erosion than sedimentation and thus erodes the slope. The breach meanwhile continues to produce the current. Because of the sand falling down the breach slowly retrogrades onto the slope. A small initial disturbance can ultimately result into a major slope failure because of this process (Figure 2.2-1). The process itself is relatively slow; the whole collapse of the slope can take up to several hours or even days, depending on the height of the slope. In contrast, a liquefaction flow slide is more or less instant. Figure 2.2-2 shows a picture of an experiment in which a breach flow slide is simulated (on small scale). Note the vertical wall from which sand rains down and creates a turbidity current. The breach will slowly travel upslope, represented by the arrow with label V_wal.

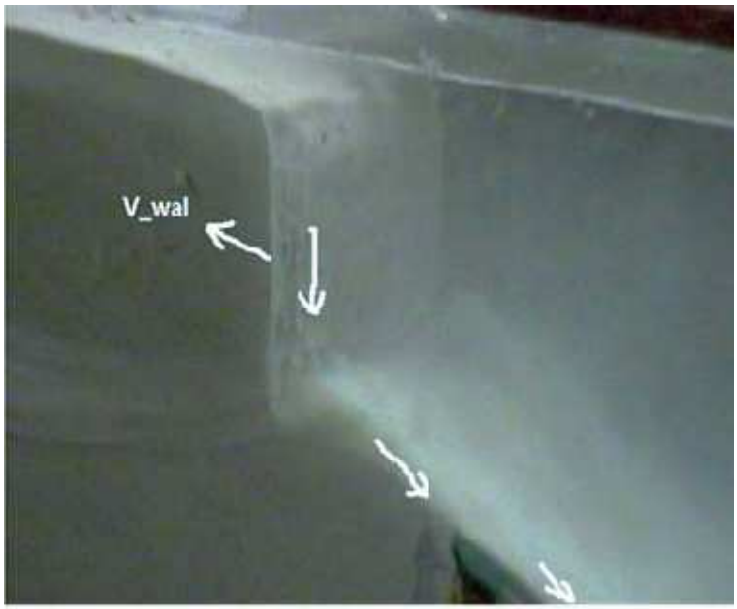

Figure 2.2-2: The process of a breach flow slide.

Breach flow slides can occur as a result of dredging. A dredger uses the process of a breach flow slide. Dredging at the toe of the (the initial disturbance) slope results in a breach. This breach creates a small turbidity current. The current is dredged so that it cannot settle down at the toe of the slope. By carefully monitoring the speed at which the sand is dredged the dredger can control the process. It can, however, happen that the process becomes unstable, thus that the turbidity current becomes a self-sustaining erosive turbidity current. This could ultimately result into a bank collapse.

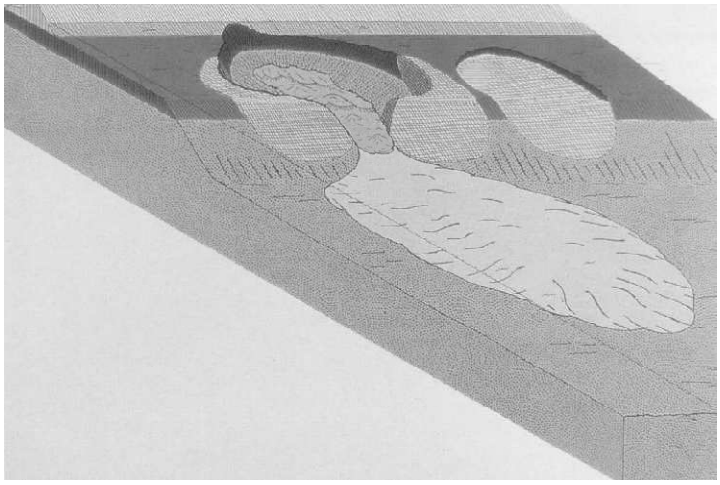

Figure 2.2-3: Sketch of the slope after a breach flow slide.

Breach flow slides have a typical ‘hourglass’ shape. The flow slide first converges to a certain point in what is called the erosion area and thereafter diverges in the sedimentation area. This shape can be seen in Figure 2.2-3.

It seems that the breach flow slide is greatly affected by the type of sediment (sand) of which the slope consists. The porosity, a measure of how loosely packed the sand is, seems to be import. Also the grain size of the sand is a big influence on the flow slide. In the next section we will investigate the influence of these aspects using the computational model HMBreach.

More information regarding breach flow slides can be found in (Groot., et al. July 2009) and (Mastbergen 2009).

3 HMBREACH

In a subaqueous slope a small disturbance (e.g. caused by dredging) can cause a breach, an upslope retrograding density current which can result in a bank collapse.

HMBreach is a computational model developed at WL | Delft Hydraulics for dredging applications and was validated with flume tests. Its purpose is to predict the shape of slope after dredging given the composition of the soil in sand layers. The ultimate goal of the model is to compute if a certain slope is stable what the equilibrium slope would be.

In this section some background on the model is given, for a more extensive (mathematical) description of the model and software one is referred to (Mastbergen 2009). Furthermore, we will investigate the sensitivity of the model with respect to various parameters. Lastly we will look at a refinement of the application.

3.1 THE COMPUTATIONAL MODEL

HMBreach is a 1 dimensional 2-layer model for stationary non-uniform depth averaged density flows. It describes a supercritical erosive 2-layer turbidity flow over a sand bed which consists of several layers of sand. The model requires only an upper boundary condition since the flow is supercritical. The boundary condition is defined as a slowly retrograding breach. This breach generates a small but steady sand flow which may transform into an erosive and turbulent sand-water density flow that causes more erosion than sedimentation and thus ultimately can cause a slope to fail. Note that this breach is not actually present in the model, only the resulting turbidity current is. This current starts on the top of the slope. The actual process of a retrograding breach on the slope itself is not modeled since the model is stationary. HMBreach has been calibrated and validated under laboratory conditions with maximal slope heights of 2 meters.

HMBreach consists of two computational models: HMBreach and HMTurb. One should note that the name 'HMBreach' is both used for the whole application as for one of the two computational models, it should be clear from the context which one is referred to. Now the two models will be explained:

- **HMBreach**, this model takes soil composition consisting of different sand layers as input. For these layers one has to specify the thickness, porosity of the sand and the D_{50} of the sand (a measure for the grain size). Optionally one can also give in the D_{15} of the layer, this together with D_{50}, gives a measure for the distribution of the grain size. With this input and the boundary condition the model calculates the slope under which the slope is balanced (equilibrium), i.e., the erosion and sedimentation are balanced given a stationary dredging process.

- **HMTurb**, this model has the same input as HMBreach but one can now also specify the angle of sand layer, hence one gives in an actual slope. With this information and the boundary condition the model calculates the resulting flow. This flow can transform into an erosive and turbulent sand-water density flow that causes more erosion than sedimentation.

3.1.1 Boundary Condition

As mentioned the upstream boundary condition is represented as a slowly retrograding breach. Such a breach creates a small but steady sand-water mixture current. Only this resulting current is actually used as the boundary condition of the model, the breach is not actually present in the model. The user needs to specify four aspects for the boundary condition; height of the breach dbr_0, retrogression velocity of the breach v_z , concentration $c_0$and Froude number Fr_0. The height and velocity are clear. The concentration is the concentration of sand in the initial current. Froude number is the Froude number of the initial flow, in order for the flow to be supercritical (which we need) we have to have that $Fr_0 > 1$. From these four values the initial sand-water mixture flow can be calculated.

The initial specific sand transport, i.e. the mass of sand transported every second per unit width is computed as:

$$sz_0 = \rho_s v_z (1 - n_0) dbr_0$$

Where ρ_s is the density of sand grains, we have $\rho_s = 2650$ kg/m^3. The term n_0 is the volume porosity of the sand bed, i.e. how loosely the sand is packed, for normally packed sand we have $n_0 \approx 0.4$. Note that the sz_0 is measured in kg/sm.

From sz_0 one can compute the initial specific discharge of the flow in m^3/sm as:

$$q_0 = \frac{sz_0}{\rho_s c_0}$$

The initial relative density difference between the sand-water mixture and the ambient water is computed as:

$$\varepsilon_0 = \frac{\Delta c_0}{1 + \Delta c_0}$$

with

$$\Delta = \frac{\rho_s - \rho_w}{\rho_w}$$

is the relative density difference between sand grains and water.

From this we can compute the initial sand-water mixture flow velocity in m/s:

$$u_0 = \sqrt[3]{Fr_0^2 \varepsilon_0 g q_0}$$

From this initial current the rest of the computations are done. These differ for which computational model is used.

For HMTurb the user has to give in a certain slope and a boundary condition. The computational model then computes the resulting sand-water mixture flow on this specific slope.

In HMBreach the user only gives in certain layers of sand and a boundary condition (thus not the geometry of the slope). The computational model then computes for every layer the angle for which the slope is stable given the boundary condition. That is, the boundary condition results in a sand-water mixture flow and for this flow the stable angle is computed. This computation is actually done by running HMTurb multiple times as a subroutine.

We will not give the complete details of all the computations the model does, interested readers are referred to (Mastbergen 2009).

3.2 THE APPLICATION

The implementation of HMBreach is done in C# which allows for a quite user friendly GUI. In the coming sections the workings of the applications are explained.

3.2.1 General

As one executes HMBreach he or she is presented with the window shown in Figure 3.2-1. There are three menus: *File, Edit* and *Run*. In the File menu one can open and save the input for a certain slope as well as open a new input screen (which will be identical to the figure). In the edit menu one can insert, remove, copy and paste layers of the input (see below). With the run menu one can run the model.

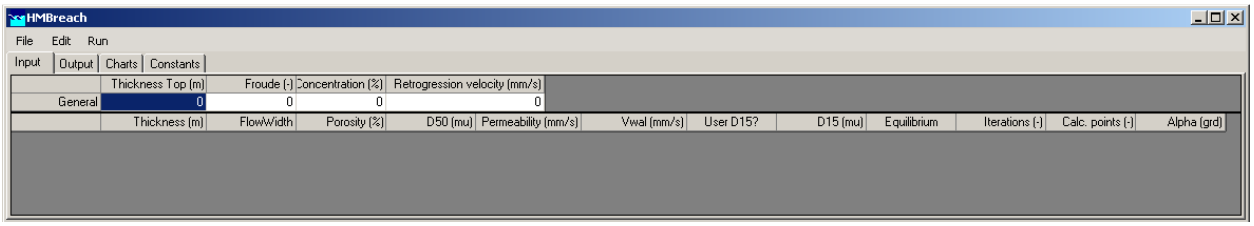

Figure 3.2-1: HMBreach on start-up.

Furthermore one is presented with four tabs: *Input, Output, Charts* and *Constants.* These tabs will now be explained one by one.

3.2.2 Input

The input screen is shown in Figure Figure 3.2-2. As mentioned earlier one can specify per layer the different properties of the sand. If one uses HMTurb one can also specify the angle of said layer in the column 'Alpha', if one uses HMBreach, then after running, this column shows the angles per layer of the slope. The columns *Permeability, Vwal, Equilibrium, Iterations* and *Calc. points* are not editable and will be filled after running. Permeability is calculated through the porosity, D_{50} and D_{15} of the sand. The Vwal is the retrogression velocity of the breach in that specific layer. Equilibrium is only used for HMBreach and is checked if the resulting angle of the slope in that layer is stable. Iterations and Calc. points are results of the numerical model.

	Thickness (m)	FlowWidth	Porosity (%)	D50 (mu)	Permeability (mm/s)	Vwal (mm/s)	User D15?	D15 (mu)	Equilibrium	Iterations (-)	Calc. points (-)	Alpha (grd)
Layer 1	0,8	1	43	165	0,116737	0,0000E+000	☐	0	☑	6	409	42,1875
Layer 2	0,7	1	43	165	0,116737	0,0000E+000	☐	0	☑	6	20	29,0039
Layer 3	0,7	1	43	165	0,116737	0,0000E+000	☐	0	☑	7	14	24,4720
Layer 4	0,95	1	41,4	190	0,130707	0,0000E+000	☐	0	☑	8	15	24,0897
Layer 5	0,85	1	41,4	190	0,130707	0,0000E+000	☐	0	☑	8	12	19,9493
Layer 6	0,85	1	41,4	190	0,130707	0,0000E+000	☐	0	☑	6	12	16,2088
Layer 7	1,05	1	40,4	175	0,099612	0,0000E+000	☐	0	☑	5	21	10,1305
Layer 8	1,05	1	40,4	175	0,099612	0,0000E+000	☐	0	☑	7	22	7,9144

Figure 3.2-2: Input screen for HMBreach.

The model was updated in 2008 that made it possible to also calculate the width of the flow because of free-fanning, this made the model quasi 2 dimensional. From then on it was also

possible to specify the width of each layer and make the model fit this width, or one could simply choose the width to be constant. In this report we will only investigate flows with constant width. In that case one cannot alter the value in the column 'FlowWidth'.

One also needs to give in a boundary condition (Figure 3.2-3). This boundary condition is specified on top of the slope and can be thought of as a breach, which provides a small but steady sand-water mixture flow. 'Thickness Top' represents the thickness of the breach and 'Retrogression velocity' the speed in which this breach travels upslope. 'Concentration' is the concentration of sand in the initial sand-water mixture and 'Froude' is the Froude number of this flow. The Froude number should be bigger than 1 in order for this flow to be supercritical. If the flow is subcritical (Froude < 1) then one also needs a boundary condition at the bottom of the slope, which cannot be done with this model.

	Thickness Top (m)	Froude (-)	Concentration (%)	Retrogression velocity (mm/s)
General	0,5	2	12	1

Figure 3.2-3: The input for the boundary condition.

3.2.3 Output

After the user has given in all the information and chosen which model to use, he or she can run the application. As mentioned earlier several columns in the input screen will be filled. Furthermore all the columns in the output screen will be filled, Figure 3.2-4.The different columns are:

- X (m) – The horizontal length of the slope;
- Z (m) – The vertical distance to the bed;
- ZW (m) – The vertical distance to the top of the flow;
- H (m) – The thickness of the flow;
- U (m/s) – The flow velocity;
- C (-) – The sand volume concentration;
- Fr (-) – The Froude number of the flow;
- VEros (m/s) – The Erosion velocity;
- Q (m^3/s) – The flow rate;
- SZ (kg/sm) – The sand transport rate;
- VSed (m/s) – The sedimentation velocity;
- VEntr (m/s) – The entrainment velocity;
- b (m) – The flow width.

	Index	X (m)	Z (m)	ZW (m)	H (m)	U (m/s)	C (-)	Fr (-)	VEros (m/s)	Q (m3/s)	SZ (kg/s)	VSed (m/s)	VEntr (m/s)	b (m)
	1	0,0000E+000	-2,5000E+000	-2,4646E+000	3,6932E-002	4,8546E-001	1,2000E-001	2,0000E+000	4,3625E-004	1,7813E-002	5,6644E+000	2,1663E-003	2,9128E-003	1,0000E+000
	2	2,1568E-003	-2,5020E+000	-2,4778E+000	3,5896E-002	4,9626E-001	1,1997E-001	2,0570E+000	4,3625E-004	1,7814E-002	5,6636E+000	2,1661E-003	3,1498E-003	1,0000E+000
	3	4,3137E-003	-2,5039E+000	-2,4803E+000	3,5163E-002	5,0669E-001	1,1995E-001	2,1222E+000	4,3625E-004	1,7816E-002	5,6630E+000	2,1659E-003	3,4230E-003	1,0000E+000
	4	6,4705E-003	-2,5059E+000	-2,4827E+000	3,4494E-002	5,1664E-001	1,1991E-001	2,1850E+000	4,3625E-004	1,7821E-002	5,6628E+000	2,1656E-003	3,6999E-003	1,0000E+000
	5	8,6274E-003	-2,5078E+000	-2,4851E+000	3,3881E-002	5,2617E-001	1,1987E-001	2,2457E+000	4,3625E-004	1,7827E-002	5,6629E+000	2,1653E-003	3,9805E-003	1,0000E+000
	6	1,0784E-002	-2,5098E+000	-2,4874E+000	3,3315E-002	5,3534E-001	1,1982E-001	2,3045E+000	4,3625E-004	1,7835E-002	5,6632E+000	2,1649E-003	4,2646E-003	1,0000E+000
	7	1,2941E-002	-2,5117E+000	-2,4897E+000	3,2792E-002	5,4416E-001	1,1977E-001	2,3616E+000	4,3625E-004	1,7844E-002	5,6636E+000	2,1645E-003	4,5522E-003	1,0000E+000
	8	1,5098E-002	-2,5137E+000	-2,4920E+000	3,2305E-002	5,5268E-001	1,1972E-001	2,4170E+000	4,3625E-004	1,7854E-002	5,6642E+000	2,1640E-003	4,8431E-003	1,0000E+000

Figure 3.2-4: The output screen for HMBreach.

3.2.4 Charts

In the charts screen one can plot, after running, charts of all the output as a function of the horizontal distance. It is possible to plot two graphs in one as can be seen in Figure 3.2-5 which shows both the vertical distance to the bed (left axis) as the flow velocity (right axis) as a function of the horizontal length of the slope. Afterwards the user can save the chart as an image with the button *Save Picture As…*.

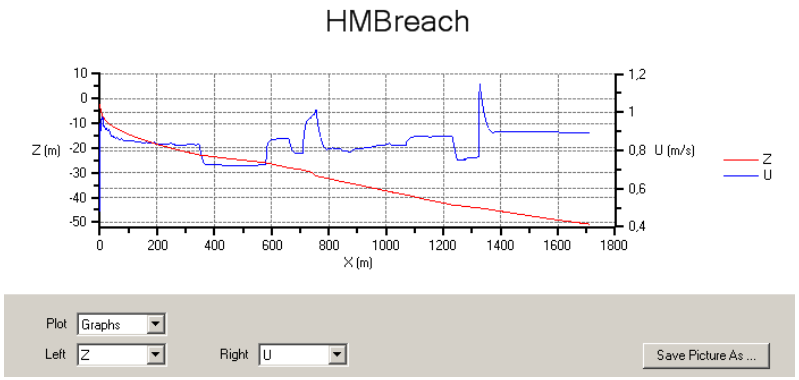

Figure 3.2-5: The chart screen of HMBreach.

3.2.5 Constants

In the constants tab one can give in all the different constants and coefficients for the model. Here one can also chose between HMBreach and HMTurb as for which model one wants to use for the calculation of the width of the flow. When the user clicks on a constant or coefficient he or she is presented with a small description of the constant in the bottom of the screen (Figure 3.2-6). Furthermore one can load and save the defaults of all the values with the corresponding buttons.

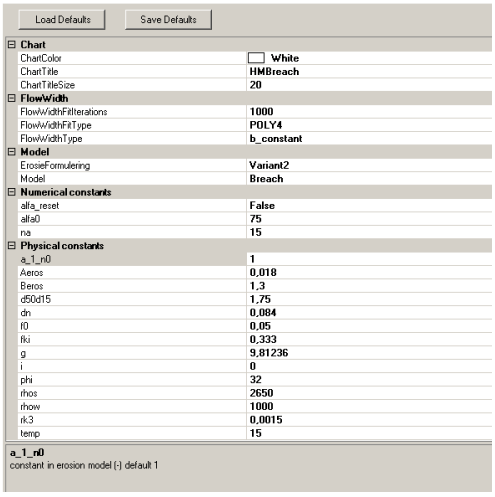

Figure 3.2-6: The constants screen of HMBreach.

3.3 SENSITIVITY ANALYSIS HMBREACH

This section investigates the sensitivity of the model with the HMBreach variant of certain parameters. To that extent a homogeneous slope of 20 meters deep is taken consisting fine sand, D_{50} = 200µm, with a porosity of 40% (Table 6.1-1). Subsequently parameters are changed one at a time to investigate the influence on the resulting slope when HMBreach is executed. The upper boundary condition and default coefficients and constants are listed in Table 3.3-1 and Table 3.3-2. In HMBreach there are two formulas for erosion, variant 1 and variant 2. Each erosion formula has three parameters, A, B and f_0. A and B are two constant coefficients in the erosion model and f_0 is the Darcy-Weisbach bed friction coefficient. Variant 1 is newer than variant 2 but has not been fully tested yet, hence we use variant 2.

	Thickness Top (m)	Froude (-)	Concentration (%)	Retrogression velocity (mm/s)
General	0.5	2	12	0.5

Table 3.3-1: Upper boundary conditions for the sensitivity experiment.

FlowWidth		**Physical constants**	
FlowWidthFiltrations	1000	a_1_n0	1
FlowWidthFitType	POLY4	Aeros	0,012
FlowWidthType	b_constant	Beros	1,3
Model		d50d15	1,75
ErosieFormulation	Variant2	dn	0,04
Model	Breach	f0	0,05
Numerical constants		fki	0,333
alfa_reset	FALSE	g	9,81236
alfa0	75	i	0
na	15	phi	32
		rhos	2650
		rhow	1000
		rk3	0,0015
		temp	15

Table 3.3-2: Coefficients and constants for the sensitivity experiment.

The parameters which will be varied are:

Porosity (%)	**40**	36	43			
D_{50} (µm)	**200**	350	125			
$D_{50}D_{15}$ (-)	**1.75**	1.33	2.5			
Δn (-)	**0.04**	0.06	0.02			
Thickness Top (m)	0.3	0.4	**0.5**	1.0	2.0	
Concentration (%)	**12**	15	9			
Retrogression Velocity	0.25	**0,5**	1	2	2,	3
f_0 (-)	0.2	0.3	0.4	**0.5**	0.75	0.1

The bold entries are the default values of the parameter. The slope for the default case, i.e. all the values of the parameters are the bold ones in the table, is visualized in Figure 3.3-1. One can see that the slope is steep at first but will become gentler further down. In this scenario the average angle of the slope is approximately 25° or 1:2.5 but the maximal slope is 35°. The average retrogression velocity of the breach is about 6 mm/s and the slope is 50 meters long. In this scenario one would expect a longer slope than this; about 80 meters would be more realistic. For the purpose of this analysis however this is not of vital importance, we are only interested in the sensitivity of the various parameters.

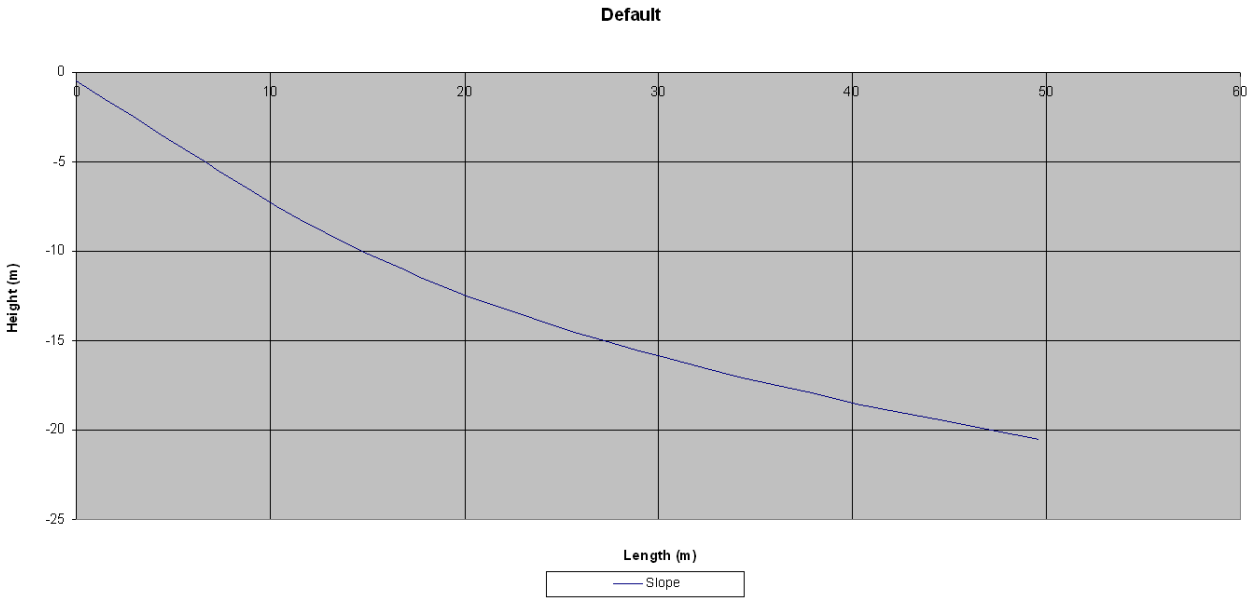

Figure 3.3-1: The default slope.

3.3.1 Porosity

The porosity is a measure of the void fraction of the sand. A high porosity means that the sand grains are not optimally stacked upon each other and thus there is a lot of void space in between the grains. Normally the porosity of sand lies between 43% and 36%, this means that said percentage of the sand is void space. Dense sand has a low porosity while loose sand has a higher porosity.

In Figure 5.1-1 one can see the resulting slope if the porosity is varied (note that a porosity of 40% corresponds to the default case). Apparently this factor does not influence the shape of the slope much since the slopes all have the similar length and shape. It does, however, have influence on the computed retrogression velocity of the breach since this is directly related to the permeability of the sand and higher porosity yields higher permeability and thus a faster retrogression speed. For dense sand, thus a porosity of 36%, this velocity is 4 mm/s on average. For the loose sand (43%) this speed is 8 mm/s on average.

3.3.2 D_{50}

As mentioned earlier, the D_{50} gives a measure for the grain size. Since sand always contains grains of different sizes it is hard to quantify what 'the' grain size of the sand is. Therefore D_{50} is used. It means that 50% of the grains in the sand have a diameter which is smaller than the D_{50} value; hence it is the median grain size. Similarly, D_{15} means that 15% of the grains are smaller than that value; hence it is the 15^{th} percentile of the grain size. High values of D50 stand for coarse sand (≥ 300 μm) while small values stand for fine sand (≤ 150 μm).

Figure 5.1-2 displays the resulting slopes of the varied D_{50} sizes, 200 μm is the default scenario. Clearly the shape of the resulting slope is very much influenced by the grain size. The coarse sand results in a 31 meter long slope which has an angle of 32° on average. On the other hand the fine sand results in a very gentle 138 meter long slope with an angle of only 16° or 1:3. The grain size also has influence on the permeability of the sand and thus also on the retrogression speed. It is easy to see that coarse sand has a high permeability, therefore the computed retrogression speed is also higher, approximately 19 mm/s. And on the other hand, fine sand has a lower permeability and thus the speed is only 2 mm/s.

3.3.3 $D_{50}D_{15}$

The $D_{50}D_{15}$ is a factor which gives the ratio between the D_{50} and D_{15}. If the user only gives in D_{50} the model assumes a distribution $D_{50}D_{15}$ of 1.75, which means that $D_{15} = D_{50} / 1.75$. Thus for D_{50} = 200 μm one has default $D_{15} = 200 / 1.75 \approx 114$ μm. One can also give in the D_{15} of the particular sand-layer itself, in which case the specified $D_{50}D_{15}$ (in the coefficients and constants, Table 3.3-2) is ignored and $D_{50}D_{15} = D_{50}/D_{15}$ is taken. If $D_{50}D_{15}$ is close to 1 (but still bigger than 1 since smaller values would yield a contradiction) the D_{15} is close to the D_{50}. In that case the sand consists of grains which have size that are very close to the D_{50}. If $D_{50}D_{15}$ is greater than the distribution of the grain sizes is wider and so is the mixture of the sand.

In the experiment we have chosen $D_{50}D_{15}$ of 1.75 (default), 1.33 and 2.5 which corresponds to D_{15} of 114, 150 and 80 respectively. One can see the resulting slopes in Figure 5.1-3. Apparently the distribution of the grain sizes has very little effect on the length of the slope. The retrogression velocity of the breach is affected by the $D_{50}D_{15}$ though. For $D_{50}D_{15}$ = 1.33 the sand is mostly consisting of grains with approximately the same size (200 μm) and thus the permeability of the sand is higher which result in an average computed retrogression speed of 11 mm/s. For $D_{50}D_{15}$ = 2.5 it is the other way around and the average speed is 3 mm/s.

3.3.4 Δn

This parameter stands for the relative porosity increase during dilation. The breach consists of a (almost) vertical wall. The wall moves upward along the slope because little layers of sand separate from the wall and create a turbidity-current. Before this sliding can occur the porosity of the sand in the wall needs to increase. The Δn factor, which is a property of the sand, is a measure for this increase.

Figure 5.1-4 depicts the slopes after HMBreach has been executed. It is clear that Δn has almost no influence on the resulting slope. The computed retrogression velocity on the other hand is affected by the factor. If Δn = 0,02 (2%) than very little porosity increase has to take place in order for the layer to flow down and thus the speed is on average 11 mm/s. For Δn = 0.06 the porosity of the sand needs to increase more which results in a computed retrogression velocity of approximately 5 mm/s.

3.3.5 Thickness Top

The thickness top is part of the upper boundary condition. This boundary is defined as a slowly retrograding breach above the slope which gradually moves upslope generating a small but steady sand flow down the slope. Thickness top is the height of this breach.

In Figure 5.1-5 one can see the resulting slopes if the thickness of the initial breach is varied. It appears that the influence of this parameter is very limited; the slope is longer if the thickness is higher. Varying the height of the breach has no effect on the computed retrogression velocity; this was to be expected since that velocity is directly related to the permeability of the sand. Changing the thickness of the breach does not change the permeability and hence not the computed retrogression velocity.

3.3.6 Concentration

The concentration is part of the upper boundary condition and gives the percentage of sand present in the initial sand-water mixture flow.

Figure 5.1-6 illustrates the result when HMBreach is executed with different concentrations. Again the effect is very little on the length and shape of the slope. Since changing the concentration of the boundary condition does not affect the permeability of the sand also the computed retrogression velocity does not change.

3.3.7 Retrogression Velocity

This retrogression velocity should not be confused with the computed retrogression velocity of the breach that has been analyzed throughout this section. This velocity is part of the boundary condition and concerns the breach that acts as upper boundary condition. Consequently, it has effect on the velocity of the turbidity flow but not on the permeability of the sand.

In Figure 5.1-7 one can see the resulting slopes when this velocity is altered. It is clear that the length of the slope is dependent on the retrogression velocity. Higher velocities result in long slopes, e.g. if the velocity is 3 mm/s the resulting slope is 229 meters long. If one chooses a low velocity than the resulting slope will be short. A velocity of 0.25 mm/s results into a slope of 31 meters. The computed retrogression velocity of the breach is not affected, as was expected.

3.3.8 f_0

The coefficient f_0 stands for the Darcy-Weisbach bed friction coefficient and is part of the erosion-model. Higher f_0 lead to more friction and thus erosion. Obviously increasing the friction has no influence on the permeability of the sand and thus so on the computed retrogression velocity of the breach. This value represents the bed friction so it is a measure for irregularities on the slope. The parameters A and B in the erosion formula and f_0 are dependent on each other. For every f_0 there is another A and B. In (Mastbergen 2009) erosion formulation variant 2 is said to have A = 0.012, B = 1.3 with corresponding f_0 = 0.1. Unfortunately, the values of A and B are not precisely known and there is some uncertainty.

In Figure 5.1-8 one can see the resulting slopes for different f_0. It is clear that changing this coefficient has effect on the resulting slope. For f_0 = 0.1 the resulting slope is 108 meters long. Smaller f_0 result in shorter slopes since less erosion takes place. As stated earlier in this section one would expect a slope of about 80 meters long, but we got a slope of about 50 meters when everything else was default. If one chooses f_0 = 0.075 however, we obtain a slope of 83 meters long. Thus it seems that this might be a good value for f_0 in variant 2 of the erosion-formula.

3.3.9 Initiation

The upper boundary condition acts as an initiation of erosive sand-water mixture flow. It can occur that the chosen condition results in a flow which will go extinct since it cannot cause enough erosion on the slope. If one for example chooses the boundary conditions as in Table 3.3-3 the resulting flow is not capable of erosion and thus will go extinct. As a result the slope will be as in Figure 3.3-2. This slope has an angle of 32° which is not incidentally equal phi (Table 3.3-2), the critical angle of repose of sand. This is the angle in which the sand on the slope is on the verge of sliding. Hence, one small disturbance in this slope can cause it fail.

	Thickness Top (m)	Froude (-)	Concentration (%)	Retrogression velocity (mm/s)
General	0.1	2	12	0.1

Table 3.3-3: Upper boundary conditions for which no turbidity flow occurs.

Figure 3.3-2: Resulting slope when no turbidity flow is present.

3.3.10 Conclusion

It seems that the length of the resulting slope is mainly affected by the grain size of the sand, the D_{50}. Also the retrogression velocity of the boundary condition and Darcy-Weisbach bed friction coefficient, f_0, have strong influence on this length. The other parameters and coefficients have very little to none effect on the shape and steepness of the slope. Note that this dependent on erosion model used in HMBreach.

The computed retrogression velocity of the breach is also very dependent on the D_{50} of the sand and to some extent by the fraction $D_{50}D_{15}$ and the Δn. The porosity affects the retrogression velocity, but the influence is very little. The other parameters and coefficient have no influence on the velocity.

Clearly the composition of the sand is very important to the model. The Retrogression velocity and in a small degree the thickness of the boundary condition have some influence. The Froude number and concentration have virtually no influence as long as one makes sure that the Froude number is bigger than 1.

3.4 SENSITIVITY ANALYSIS HMTURB

As in the previous section we will perform a sensitivity analysis on the variant HMTurb. Recall that HMTurb computes the resulting turbidity current from the given boundary conditions on a certain slope which one has to give in. The slope that we will investigate is depicted in Figure 3.4-1, the input for this slope can be found in section 6.2, Table 6.2-1. Note the long shallow part at the toe of the slope. HMTurb computes a current, if the boundary conditions are sufficiently high this current will transform in a breach flow slide, such a current will not stop directly after the slope has become shallower but will rather travel some distance before it will die out. This shallow part allows us to investigate the whole flow.

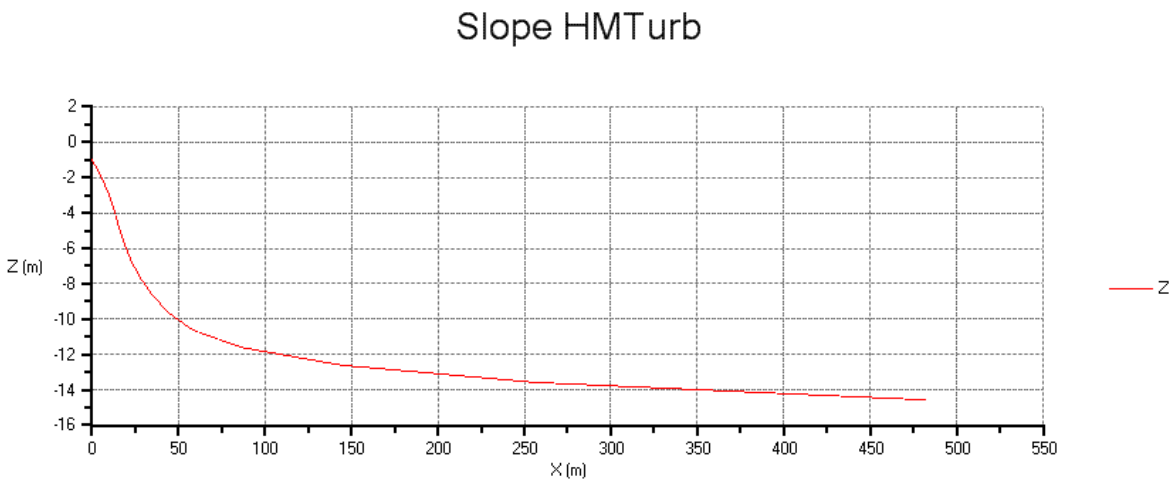

Figure 3.4-1: Slope used for the HMTurb sensitivity analysis.

As in the case of the HMBreach sensitivity analysis we will choose a certain default boundary condition. Then parameters are changed one by one to investigate what influence it has on the resulting breach flow slide. These default boundary conditions are listed in the table below.

	Thickness Top (m)	Froude (-)	Concentration (%)	Retrogression velocity (mm/s)
General	1	2	12	20

Table 3.4-1: Upper boundary conditions for the sensitivity experiment.

For this experiment the constants and coefficients also need to be adapted slightly for HMBreach to use the HMTurb computational model. In Table 3.3-1 one can find the full list of constants and coefficients used for the experiment. Note that again we have chosen to use erosion formulation Variant2 rather than the newer Variant1 since the latter has not been fully tested yet. For A and B we again choose 0.012 and 1.3 respectively and the default value of f_0 is 0.05, but this value will also be investigated in the sensitivity analysis.

FlowWidth		Physical constants	
FlowWidthFiltrations	1000	a_1_n0	1
FlowWidthFitType	POLY4	Aeros	0,012
FlowWidthType	b_constant	Beros	1,3
Model		d50d15	1,75
ErosieFormulation	Variant2	dn	0,04
Model	Breach	f0	0,05
Numerical constants		fki	0,333
alfa_reset	FALSE	g	9,81236
alfa0	75	i	0
na	15	phi	32
		rhos	2650
		rhow	1000
		rk3	0,0015
		temp	15

Table 3.4-2: Coefficients and constants for the sensitivity experiment.

The parameters that we will vary will be the same as for the HMBreach sensitivity experiment with the addition of the Froude number which, as we will see, now does have influence on the resulting current, as long as it is higher than 1. In the table below the various parameters are listed, again the bold values are the default values.

Porosity (%)	**40**	36	43
D_{50} (µm)	**200**	350	125
$D_{50}D_{15}$ (-)	**1,75**	1,33	2,5
Δn (-)	**0,04**	0,06	0,02
Thickness Top (m)	0.5	**1**	2
Concentration (%)	**12**	15	9
Retrogression Velocity	10	**20**	40
Froude Number (-)	1,5	**2**	3
f_0 (-)	0,25	**0,5**	0,1

We measure the magnitude of the resulting breach flow slide (if any results) by the sand transport in kg/sm and the velocity of the flow. Note the dimension of the transport; it represents the total sand transport in kg per second over 1 meter of width of the slope. We will look at the maximum of the sand transport and the mean value of the transport over the slope as well as for the velocity.

It can occur that the upper boundary conditions are not sufficient to bring about a breach flow slide; in that case the sand transport will be very low. Figure 3.4-2 shows a plot of the velocity and sand transport along the horizontal distance of the slope in case a breach flow slide does occur. This is the plot for the default case. In Figure 3.4-3 one can see the velocity and sand transport in case a breach flow slide is absent. Note that the disturbance due to the boundary condition quickly dies out and thus does not create an erosive turbidity current.

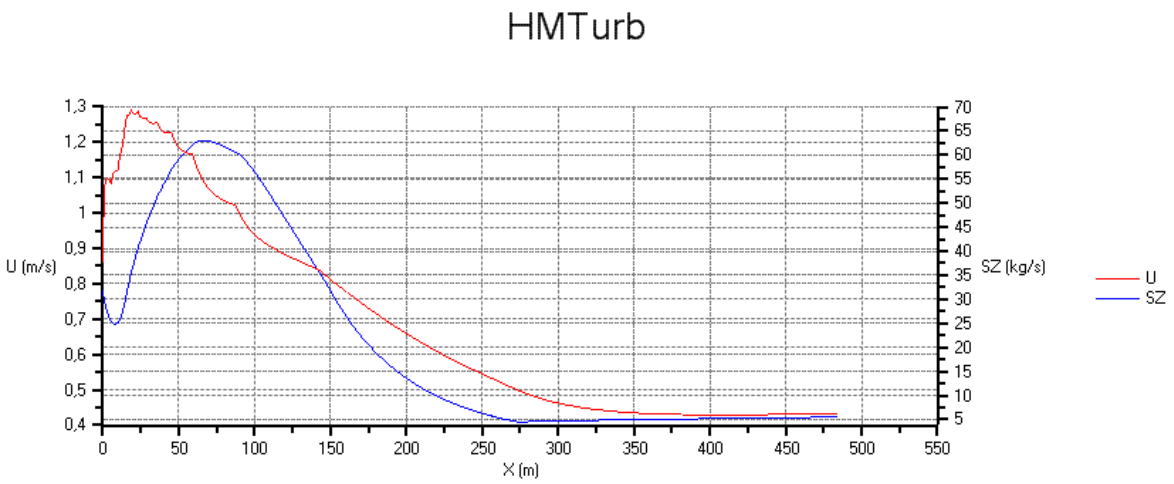

Figure 3.4-2: The velocity (left axis) and the sand transport (right axis) if a breach flow slide does occur.

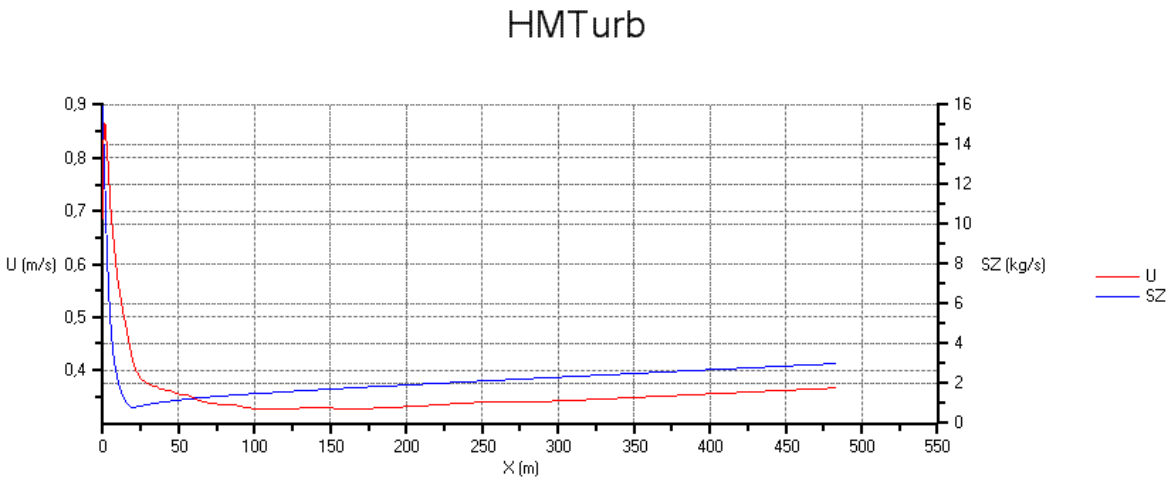

Figure 3.4-3: The velocity (left axis) and the sand transport (right axis) if a breach flow slide does not occur.

3.4.1 Porosity

Table 3.4-3 shows the results of the analysis when the porosity is varied. In all the cases a breach flow slide does occur. A lower porosity will result in a bigger flow slide, though the difference is not really significant. The velocity exhibits the same behavior as the sand transport, for the lower porosity it is slightly higher than the default case and the other way around for a higher porosity.

Porosity (%)	40	36	43
S_{max}	63,01	67,07	56,80
S_{mean}	20,78	23,09	17,77
U_{max}	1,29	1,34	1,25
U_{mean}	0,68	0,70	0,65

Table 3.4-3: Results sensitivity analysis for the porosity.

3.4.2 D_{50}

The table below lists the results for different values of the median grain size D_{50}. Note that the values in the column of 350 µm are printed italic; this is because no breach flow slide occurred. Apparently the grain size influences the flow very much. A higher D_{50} means that the sand grains will be bigger on the whole and thus harder to pick up by a current, it simply was not strong enough to cause enough erosion and thus no breach flow slide occurred. On the other hand if the median grain size is smaller the sand transport is nearly tripled with respect to the default case. The velocity for the smaller D_{50} has a higher maximum than the default case but a lower mean value. This indicates that the resulting density current is of great magnitude on a small distance of the slope.

D_{50} (µm)	200	350	125
S_{max}	63,01	*15,51*	157,80
S_{mean}	20,78	*3,10*	81,25
U_{max}	1,29	*1,09*	1,47
U_{mean}	0,68	*0,44*	0,61

Table 3.4-4: Results sensitivity analysis for D_{50}.

3.4.3 $D_{50}D_{15}$

The distribution of the sand grain seems to influence the flow only little. Recall that lower values of $D_{50}D_{15}$ (close to 1) mean that the distribution is narrow and situated around D_{50}. Lower values will result in a stronger flow while higher values of $D_{50}D_{15}$ yield a weaker flow, but the difference is not big. The velocities of the flows are similar for all values.

$D_{50}D_{15}$ (-)	1,75	1,33	2,50
S_{max}	63,01	66,06	56,25
S_{mean}	20,78	21,59	18,45
U_{max}	1,29	1,29	1,30
U_{mean}	0,68	0,68	0,66

Table 3.4-5: Results sensitivity analysis for $D_{50}D_{15}$.

3.4.4 Δn

The Δn also seems to have little effect on the resulting breach flow slide. A lower Δn yields a higher sand transport. The flow velocities, both the maximum and the mean, for the three values are practically the same.

Δn (-)	0,04	0,06	0,02
S_{max}	63,01	60,89	64,67
S_{mean}	20,78	20,07	20,92
U_{max}	1,29	1,30	1,28
U_{mean}	0,68	0,67	0,68

Table 3.4-6: Results sensitivity analysis for Δn.

3.4.5 Thickness Top

The thickness of the upper boundary seems to affect the resulting current in a high degree. If the top is smaller, than the resulting initial flow will be smaller, hence a thickness of 0.5 meters does not result into a breach flow slide. On the other hand, if the top is higher, than the initial flow will be much bigger and thus so the resulting breach flow slide. Also note that the velocity of the flow is significantly higher.

Thickness Top (m)	0,5	1,0	2,0
S_{max}	*11,79*	63,01	150,83
S_{mean}	*2,16*	20,78	78,86
U_{max}	*0,87*	1,29	1,72
U_{mean}	*0,36*	0,68	0,97

Table 3.4-7: Results sensitivity analysis for the Thickness Top.

3.4.6 Concentration (%)

The concentration of sand in the initial flow does have some effect on the resulting breach flow slide but the effect is small. A lower concentration will result in a flow with a higher velocity and discharge; hence the breach flow slide is larger.

Concentration (%)	12	15	9
S_{max}	63,01	57,27	69,72
S_{mean}	20,78	18,04	24,18
U_{max}	1,29	1,27	1,33
U_{mean}	0,68	0,66	0,71

Table 3.4-8: Results sensitivity analysis for the concentration.

3.4.7 Retrogression Velocity

The retrogression velocity and the thickness of the top are both part of the boundary condition. The product of the two is used to compute the properties of the initial flow which will traverse along the

slope, hence a boundary condition with a thickness of 1 m and retrogression velocity of 40 mm/s will result in exactly the same breach flow slide as if one would choose a top of 2 m and velocity of 20 mm/s. This can be seen if Table 3.4-7 is compared to Table 3.4-9. Hence, a higher retrogression velocity results in a bigger breach flow slide.

Retrogression Velocity (mm/s)	10	20	40
S_{max}	*11,79*	63,01	150,83
S_{mean}	*2,16*	20,78	78,86
U_{max}	*0,87*	1,29	1,72
U_{mean}	*0,36*	0,68	0,97

Table 3.4-9: Results sensitivity analysis for the Retrogression Velocity.

3.4.8 Froude Number

If the Froude number of a flow is bigger than 1 the flow is supercritical. As explained earlier HMBreach can only compute with supercritical flows, hence we have to chose the Froude number of the boundary condition bigger than 1. If the number is bigger, than the initial velocity of the flow will be higher and thus the resulting breach flow slide will be larger. This can also be deduced from the table below.

Froude Number (-)	1,5	2,0	3,0
S_{max}	58,64	63,01	68,21
S_{mean}	18,77	20,78	23,26
U_{max}	1,27	1,29	1,32
U_{mean}	0,66	0,68	0,70

Table 3.4-10: Results sensitivity analysis for the Froude number.

3.4.9 f_0

The Darcy-Weisbach friction coefficient f_0 gives a measure for how smooth the bed surface is, i.e. a lower f_0 means less friction between the flow and the bed and less erosion. This obviously has a large influence on the resulting flow. If there is more friction between the bed and the flow more erosion will take place and thus the sand transport will be higher. The table below confirms this. Note that a very smooth bed (low f_0) does not result in an erosive turbidity current.

f0 (-)	0,25	0,50	0,10
S_{max}	*23,89*	63,01	150,30
S_{mean}	*4,15*	20,78	46,30
U_{max}	*1,14*	1,29	1,43
U_{mean}	*0,47*	0,68	0,42

Table 3.4-11: Results sensitivity analysis for f_0.

3.4.10 Conclusion

We've seen that a parameter in the HMTurb computational model either has a large effect on the resulting flow or a minor effect. The porosity, $D_{50}D_{15}$, Δn, concentration and Froude number all do not have a big influence on the resulting flow; however, a combination of these parameters can have a big influence on the resulting flow. The D_{50}, thickness of the top, retrogression velocity and f_0 all have a large effect on the flow and a slight change in these parameters will result in a noticeable effect on the magnitude of the flow.

3.5 SPECIFY ΔN PER LAYER

The Δn is very dependent on the properties of the sand. Since the soil is made up of different layers of sand and the Δn can usually be computed per layer using measurements it would be reasonable to be able to also give in the Δn per layer. Unfortunately the user could only give in one Δn for the whole slope. Therefore, it was decided to add this feature to the application.

The application is written in C# and was edited using Microsoft Visual Studio 2008 Professional Edition. In order to be able to give in the Δn per layer the input screen needs two extra columns similar to the columns for the user specified D_{15}. In one column the user can check a box if he or she wishes to put in the Δn for that layer, in the other column the user can then specify the Δn for this layer. In the case that the user does not wish to specify the Δn of the layer the Δn is taken which is specified in the constants-tab. In Figure 3.5-1 one can see the new input screen.

	Thickness (m)	FlowWidth (m)	Porosity (%)	D50 (mu)	User dn?	dn (-)	Permeability (mm/s)	Vwal (mm/s)	User D15?	D15 (mu)	Equilibrium	Iterations (-)	Calc. points (-)	Alpha (deg)
Layer 1	0,8	1	43	165	☑	0,084	0,116737	0,0000E+000	☐	0	☑	8	136	50,3906
Layer 2	0,7	1	43	165	☑	0,084	0,116737	0,0000E+000	☐	0	☑	8	20	41,7297
Layer 3	0,7	1	43	165	☑	0,084	0,116737	0,0000E+000	☐	0	☑	10	12	40,5887
Layer 4	0,95	1	41,4	190	☑	0,089	0,130707	0,0000E+000	☐	0	☑	10	13	38,5275
Layer 5	0,85	1	41,4	190	☑	0,089	0,130707	0,0000E+000	☐	0	☑	9	9	34,0126
Layer 6	0,85	1	41,4	190	☑	0,089	0,130707	0,0000E+000	☐	0	☑	9	8	30,0267
Layer 7	1,05	1	40,4	175	☑	0,125	0,099612	0,0000E+000	☐	0	☑	7	11	23,4584
Layer 8	1,05	1	40,4	175	☑	0,125	0,099612	0,0000E+000	☐	0	☑	8	11	18,6934

Figure 3.5-1: The new input screen of HMBreach.

Changing the Δn per layer however has very little effect on the end result, which also could be expected from the sensitivity analysis. It has to be noted that we used the erosion formula variant 2 and that the newer variant 1 also has to factor Δn in it, the effect for that erosion formula is most likely bigger.

4 Analysis of Slope Failures

In this section we look at real-world slope failures from which some data is known and attempt to reconstruct the failure with HMBreach. If this is possible then we can conclude that the slope failure could be caused by a breach flow slide which in turn can be caused by other physical phenomena. If one compares Figure 2.1-1 with Figure 2.2-1 then one should note that the results of a liquefaction flow slide and breach flow slide are quite similar. Some of the collapses considered here were also investigated to be the result of a liquefaction flow slide.

4.1 Roompot

The Roompot is part of the Oosterschelde, an estuary in Zeeland, the Netherlands. This estuary has been closed by a storm surge barrier and dam called the Oosterscheldekering. Because of this (partial) closure the water that enters the Oosterschelde during ebb and leaves during flood will flow faster than it formerly did and as a consequence more erosion will occur in the estuary. This erosion can cause very steep subaqueous slopes that can collapse as a result of a breach flow slide and the Oosterscheldekering could be endangered. To prevent this, as part of the Deltaworks, the bed land inbound is covered with protective mats.

Figure 4.1-1: Location of the collapse.

A breach flow slide is a relatively slow process; it can take up to several hours. In 2004 such a flow slide probably occurred very close to the Oosterscheldekering on the edge of the bed protection (see Figure 4.1-1), during this collapse 850 000 m^3 of sand was moved. This collapse was discovered from annual measurements by Rijkswaterstaat that monitors the water depth in the Oosterschelde. In Figure 4.1-2 one can see the difference of the bed depth between April 2004 and March 2005. The red part shows a depth decrease of about 7 meters, the blue part is a depth increase of about 16 meters. Note that the left of the figure is the South from Figure 4.1-1. That means that the collapse was from North to South (right to left in the Figure below). The turbidity current first is converging; this part (blue) is called the erosion-area, and subsequently diverges, called the

sedimentation-area (red). The bit in between both areas is referred to as the gully. This shape is typical for a slope failure. The length of the blue part is called the length of the collapse and as such with the width. Although the red and blue part have approximately the same area the depth decrease is considerably lower than the increase, this is most likely because of erosion which moved sand to the east (through the bottom of the below image), recall that the measurements are a year apart.

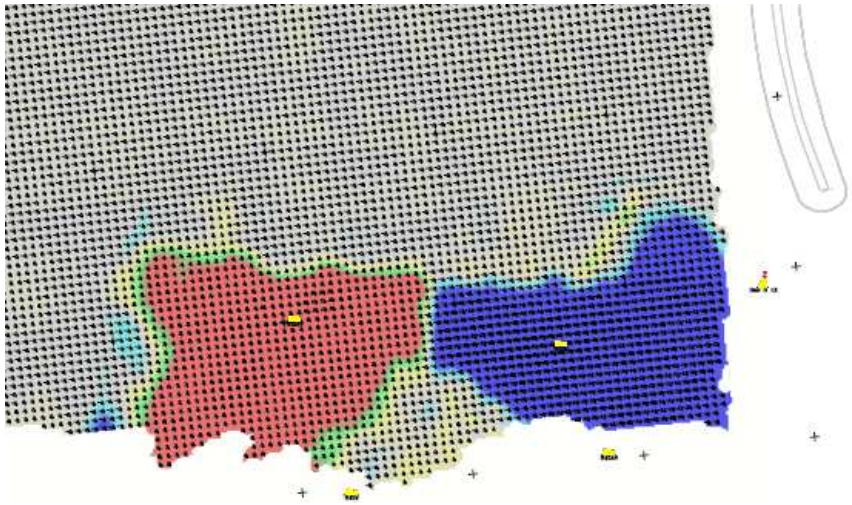

Figure 4.1-2: The depth difference in the Oosterschelde between April 2004 and March 2005.

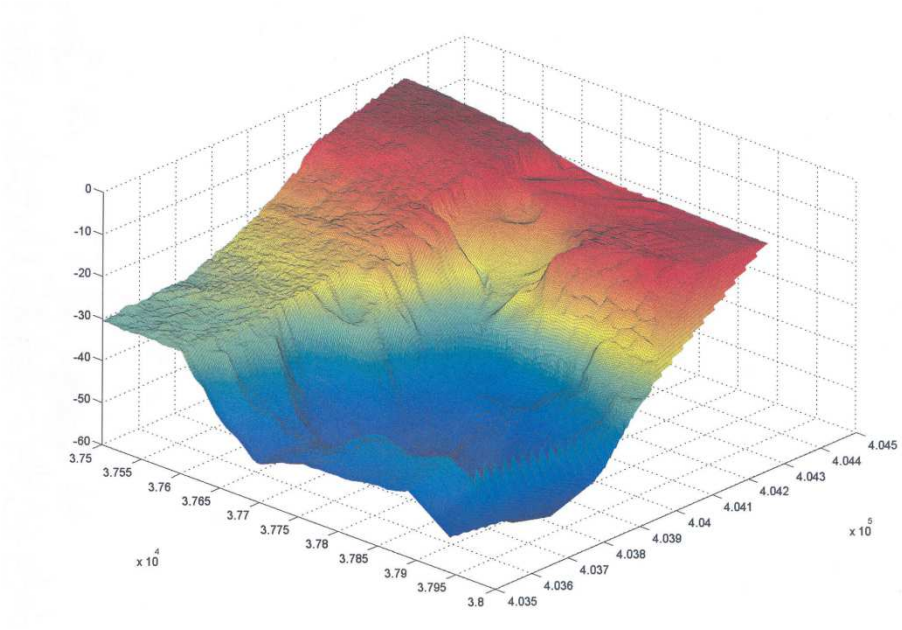

Figure 4.1-3: Bed of the Roompot before the collapse, note that the red and blue do not correspond to the above figure.

4.1.1 Simulation with HMTurb

In 2008 this phenomenon was simulated with different models including HMTurb **(Groot, Ruyt, et al. 2008)**. During the project this slope failure was compared to one which occurred in the Hollandsch Diep in 2007. Many aspects of this collapse were known such as the time and the width of the gully. With Froude scaling laws, the knowledge about the Hollansch Diep collapse, which thus was a very well documented and measured breach flow slide, and the estimation of the total volume of sand that had been flowed down the slope in the Oosterschelde, 850 000 m^3, one can estimate the lengthscaling factor by $\sqrt[3]{\mathbf{850\,000}/\mathbf{111\,681}} \approx \mathbf{1.97}$. From this al other aspects such as the length, width and so on can be estimated. The timescalingfactor is computed as $\sqrt{\mathbf{1.97}} \approx \mathbf{1.40}$. Hence we have the following table:

Description	Quantity	Roompot	H. Diep	Unit
Volume of sand	V	*850 000*	*111 681*	m^3
Length of collapse	L	301	*153*	m
Width of collapse	W	350	*178*	m
Height of slope	H	45	*23*	m
Gully width	B	81	*41*	m
Time of collapse	T	30.5	*21.75*	h
Volume total mixture (sand + water)	V_m	8 500 000	1 117 000	m^3
Time-averaged maximum spatial mixture discharge	$Q = V_m / T$	77.4	14.3	m^3/s
Q per unit of width	$q = Q / B$	0.96	0.35	m^2/s
Time-averaged maximum sand-transport per unit width	$s = q \cdot c \cdot 2650$ kg/m^3	153	56	kg/sm

Table 4.1-1: Estimation of the Roompot collapse properties, the italic entries are known values, the normal entries are deduced from known values.

Recall that we only used the estimated volume to obtain the rest of the properties (hence it is the only value in the Roompot column which is italic). If we compare the estimated length, width and gully width to Figure 4.1-2 then we find that the estimation is reasonably accurate. Note that the time of the collapse is estimated by $21.75 \cdot 1.40 \approx 30.5$ hours. We are mainly interested in reconstructing s, the time-averaged maximum sand-transport per unit width, with HMTurb. For c, the concentration, we have taken 6% which is quite a realistic value for a breach flow slide.

The slope from before the collapse and the properties of the slope, which were known from measurements, were put into HMTurb (see Table 4.1-2). Layer 2, 4 and 9 are layers that contain clay, these have been modelled as sand layers with a low permeability. Note that layer 7 and 8 consist of very coarse sand with high porosity, this means that the retrogression speed of a breach will be very high. From Layer 10 and on it is assumed that the sand is homogeneous with the properties as shown in the table. Layer 14 and 15 are added to be able to see what the flow looks like in the sedimentation area and how fast the flow dies out.

Firstly we take variant 2 as erosion formula with parameters A = 0.012 and B = 1.3. From the sensitivity analysis we deduced that f_0 = 0.075 is a realistic value. Changing parameters in the erosion-model has a very large effect on the outcome of HMTurb. Unfortunately, it is very hard and expensive to determine the values A, B and f_0 from experiments thus so far the coefficients are not determined accurately yet. That is why we will investigate three values of f_0: 0.05 (default according to the application), 0.075 (from sensitivity analysis) and 0.1 (default according to (Mastbergen 2009)). In Table 4.1-3 the constants and coefficients used for this experiment are listed.

Input:	Thickness (m)	Porosity (%)	D50 (mu)	D15 (mu)	Angle (deg)
Layer 1	2,5	42	230	140	4,97
Layer 2	3	42,5	63	40	12,26
Layer 3	2	41	175	105	12,26
Layer 4	3	41	63	40	9,86
Layer 5	2	41	195	120	9,86
Layer 6	3	41	250	150	12,26
Layer 7	2	41	380	230	12,26
Layer 8	3	41	380	230	23,49
Layer 9	2	41	63	40	23,49
Layer 10	5	41	250	150	23,49
Layer 11	5	41	250	150	6,2
Layer 12	5	41	250	150	6,2
Layer 13	5	41	250	150	5,52
Layer 14	5	41	250	150	1
Layer 15	5	41	250	150	0,2

Table 4.1-2: Input HMTurb for the slope before collapse.

FlowWidth		**Physical constants**	
FlowWidthFiltrations	1000	a_1_n0	1
FlowWidthFitType	POLY4	Aeros	0,012
FlowWidthType	b_constant	Beros	1,3
Model		d50d15	1,75
ErosieFormulation	Variant2	dn	0,04
Model	Turb	f0	0,05 / 0,075 / 0,1
Numerical constants		fki	0,333
alfa_reset	FALSE	g	9,81236
alfa0	75	i	0
na	1	phi	32
		rhos	2650
		rhow	1000
		rk3	0,0015
		temp	15

Table 4.1-3: Coefficients and constants for HMTurb.

A small disturbance in sand with a low porosity can cause an initial flow which in turn can evolve into a breach flow slide. It can occur that if this disturbance occurs somewhere on the slope that is not steep enough the resulting initial flow will not result in a breach flow slide. In that case the resulting sand-water mixture current will fade out and almost no sand transport will be present. The sand transport output of such an event in HMTurb will typically look like Figure 4.1-4. Note that the sand transport is maximal about 2.2 kg/sm while the maximal sand transport for the Roompot we would expect should be around 150 kg/sm. In case a breach flow slide does not begin when the disturbance is on the shallow part of the slope, the same disturbance, i.e. boundary condition, can create a breach flow slide on steeper parts of the slope. To simulate this effect one would take the input from Table 4.1-2 from layer 6 and on for example. When a breach flow slide results the typical output of HMTurb is something like Figure 4.1-5. Note the peak at about 650 kg/sm which corresponds to the time-averaged maximal sand transport per unit width, this is about 4 times as high as what we are looking for.

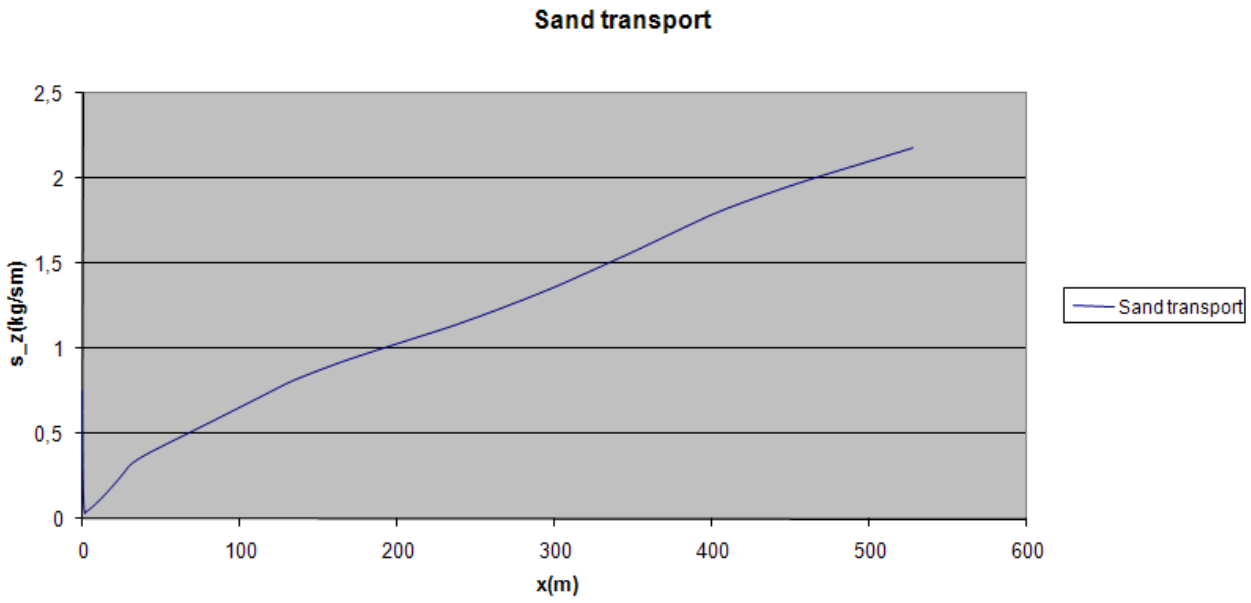

Figure 4.1-4: Sand transport in case no erosive turbidity current is present.

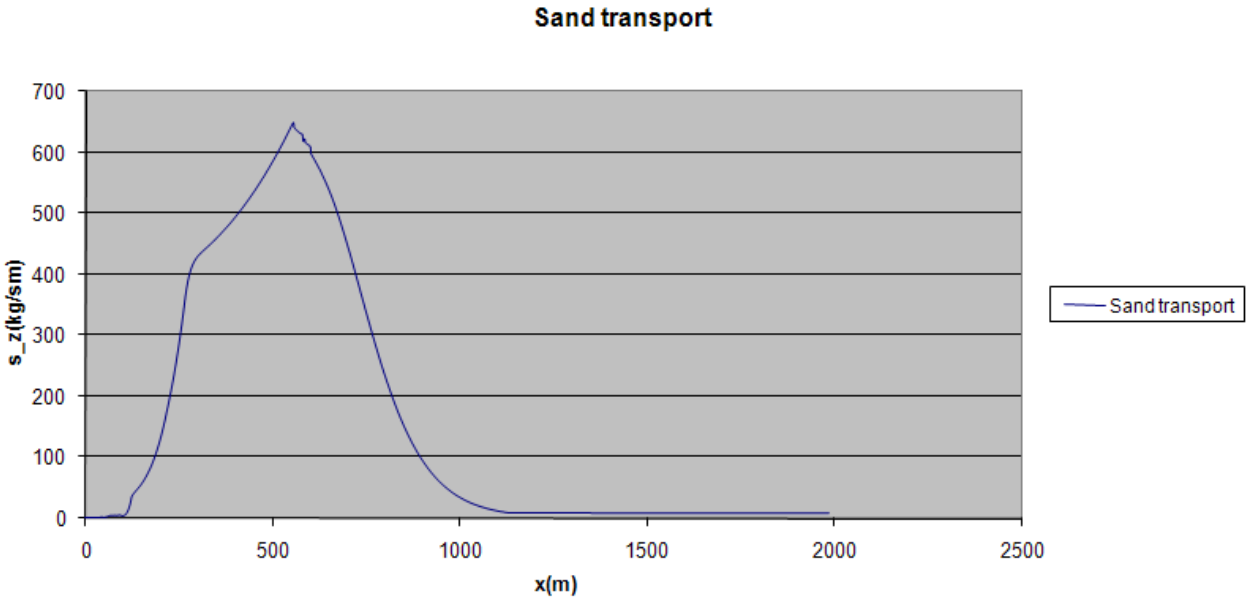

Figure 4.1-5: Sand transport in case an erosive turbidity current is present.

We want to investigate whether is possible in HMTurb to create a turbidity current which is comparable to that of the Roompot, i.e. has a comparable sand transport. Up to that extent 3 locations on the slope are chosen in which the initial disturbance can occur, and then, for each f_0, it is investigated for which disturbance a comparable flow results. The 3 locations are above layer 1 (the whole slope), above layer 6 (where the slope has an angle of 12°) and above layer 8 (slope of 23°). Figure 4.1-6 shows the slope of the Roompot before the collapse with the locations marked.

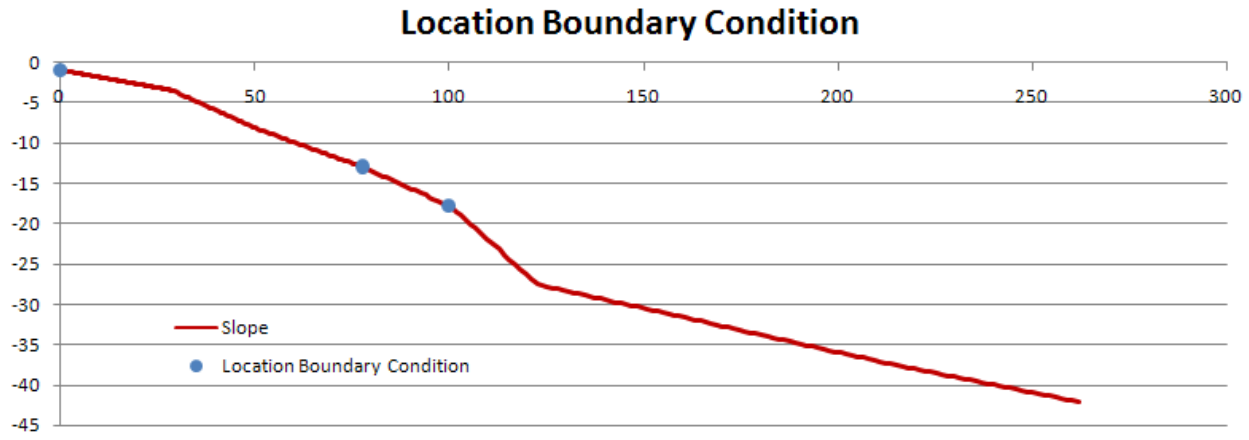

Figure 4.1-6: The slope before the collapse with the locations of the boundary condition for the experiment.

The mentioned disturbance is the boundary condition in the model. As seen in the sensitivity analysis of HMTurb, a boundary condition with an initial height of 2 m and velocity of 5 mm/s is the same as a boundary condition with height of 1 m and velocity 10 mm/s, since the product of the

two is used for the initial flow. Note that this is only the case when HMTurb is used, this does not hold for HMBreach. Hence we fix the thickness at 1 meter and vary the retrogression velocity. Recall that the Froude number (provided it is larger than 1) and concentration have less influence on the resulting flow than the retrogression velocity (Section 3.4). The goal is to end up with a breach flow slide with a maximal sand transport which is as close to 153 kg/sm (the estimated average maximal sand transport) as possible by varying the retrogression velocity. The velocity will be varied with a precision of 0.1 mm/s, i.e. if a velocity of 17.1 gives better result than 17.0 and 17.2 mm/s then 17.1 mm/s is the best estimate for the sought after flow (e.g. we won't look at the flow for 17.15 mm/s). Doing this yields the results as depicted in Table 4.1-4.

In Appendix 5.2 one can find a plot of the sand transport and flow velocity of all the flows from Table 4.1-4. Note that in the figures both the slope and the sand transport (or flow velocity) are plotted. The right axis corresponds to the slope height, the left to the sand transport (or flow velocity). Note that the maximal sand transport occurs when the slope steadily becomes shallower and transport rapidly decreases from then on. This is because the flow velocity decreases, the Froude number of the flow becomes less than 1 and thus the flow becomes sub critical, the sand in the mixture will slowly settle on the bed. The mean of the sand transport is taken over 1000 meters, after this distance the sand transport is virtually not and thus no turbidity current is present.

Location	Retrogression Velocity (mm/s)	s_{max} (kg/sm)	S_{mean} (kg/sm)	V (m^3)	f0
1	28.3	193	102	1 419 714	0.05
1	20.8	288	128	1 781 601	0.075
1	18.6	750	216	3 006 453	0.1
2	29.1	138	54	751 613	0.05
2	18.6	174	65	904 719	0.075
2	14.0	155	48	668 100	0.1
3	19.3	152	58	807 288	0.05
3	11.8	162	56	779 450	0.075
3	8.7	188	57	793 369	0.1

Table 4.1-4: The maximal sand transport corresponding to the initial velocity.

Table 4.1-4 also lists the approximated volume of moved sand V. This is computed from the s_{mean}. We have found several flows, which are listed in the table, with a comparable maximal sand transport. If such a flow with constant sand transport s_{mean} were to flow for T time over a width of (W + B)/2 (approximately the average flow width, Figure 4.1-2) we want to find that the total volume of moved sand is equal to V. Hence we use the following formula to compute V:

$$V = \frac{s_{mean} \cdot (T \cdot 3600) \cdot \frac{W + B}{2}}{1700}$$

We know s_{mean} has unit kg/sm, T is in hours and hence T*3600 is in seconds. Both W and B are in meters. Multiplying these gives us the mass of the moved sand in kilograms. The bulk density of (wet) sand is dependent on a lot of factors and is computed as $2650*(1-n_0)$ kg/m^3 where 2650 kg/m^3 is the density of a sand grain and n_0 is the void fraction of the sand, thus the porosity. For $n_0 \approx 0.36$ we find 1700 kg/m^3. Thus dividing the mass of the moved sand by this density we get the volume in m^3. Applying this equation to our data we find the fifth column in the table

We see that, when $f_0 = 0.075$ and disturbance is above the first layer, then a retrogression velocity of 20.8 mm/s is needed to create a breach flow slide with a maximal sand transport of 288 kg/sm. The model is very sensitive for this case. If the speed is 20.7 mm/s (a difference of less than 1%) the disturbance does not even result in a breach flow slide. If the speed is 20.9 mm/s then s_{max} is 352 kg/sm. Also for the other f_0 we see this phenomenon; the values in the table are thus closest to 153 kg/sm (the estimated sand transport) as possible (when the speed is varied no more than 0.1 mm/s at a time). Therefore it is unlikely that the initial disturbance in the Roompot was in the shallow part. The fact that the estimated volumes are much higher than what was recorded for the Roompot collapse confirms this.

If we take the disturbance further down the slope, above layer 6, then changing the velocity slightly has not as much effect on the sand transport as earlier but is still significant. For example, if $f_0 = 0.05$ and the velocity is 29.0 mm/s then $s_{max} = 125$ kg/sm, for 29.2 mm/s we have $s_{max} = 175$ kg/sm. It seems more likely an initial disturbance in this layer would create a collapse as the one observed in the Oosterschelde, also the estimated volumes are close to what was found in the Roompot.

For the last location the disturbance is taken right above the steepest part of the slope. Also here the effect on the sand transport by altering the velocity slightly is still significant. But the disturbance needed to create an erosive turbidity current is smaller. It is also more likely that a disturbance will occur on the steeper part of the slope rather than on a shallow part since the slope is less stable. For the flow on the last location with $f_0 = 0.05$, with $s_{mean} = 57$ we find $V \approx 805\,000$ m^3, which is particularly close to 850 000 m^3. For the other two values of f_0 we find similar (good) results.

In (M.B. de Groot, 2008), which investigated this slope failure, it was predicted that the initial disturbance was located above layer 8, thus in layer 7. Our experiments have shown that a disturbance above layer 8, location 3, is very likely to cause a breach flow slide. We already saw that layer 7 consists of sand with a high porosity and somewhat coarse grains (Table 4.1-2) and therefore a small disturbance (which can be caused by some sand or clay crumbling of) in this layer could have caused a small liquefaction flow slide (a process in which sand suddenly flows down as a liquid) or an initial flow. This can be the initial disturbance which begins the breach flow slide. It has to be noted that liquefaction flow slides are less likely to occur in coarse sand.

Hence we can conclude that the flows that we have found with HMTurb indeed mimic the flow that would have originated if a breach flow slide caused the collapse in the Roompot. Both the maximal sand transport as the volume of moved sand is comparable. It thus seems fairly possible that the collapse indeed was the result of a breach flow slide.

If we take variant 1 of the erosion-model with A = 0.018 and B = 0.06 then very small initial disturbances cause huge amounts of sand transport. Varying f_0 does not solve this problem. For example, if f_0 = 0.05 a boundary condition with height 0.5 m and velocity 1 mm/s causes an s_{max} of about 5700 kg/sm. With a lower velocity of 0.9mm/s the maximal sand transport is about 10500 kg/sm, when one would actually expect it to be lower. This is an indication that the parameters for this erosion formula are not correct or accurate enough. It needs to be noted though that the f_0 corresponding to the chosen values for A and B is 0.1 and not 0.05 according to (Mastbergen 2009).

4.1.2 Proneness of the Slope to Breach Flow Slides

In the previous section we were able to simulate the slope failure in the Roompot as a breach flow slide. We found that an initial disturbance in location 3 could easily produce a breach flow slide which has the magnitude of the slope failure in the Oosterschelde. This initial disturbance could for example be the result of a liquefaction flow slide or some clay crumbling of. In this section we investigate if the initial disturbance found is also the (close to) the minimum needed to create a breach flow slide. If this is the case it explains why the breach flow slide did not happen sooner, since a smaller initial disturbance could also have created a breach flow slide.

We carry out this experiment by taking the initial disturbances for location 3 from the previous section and lower to retrogression velocity until there is just a small erosive turbidity current with an acceptable sand transport. We do this for the three f_0. The results are listed in the table below. In the first column the retrogression velocities found in the previous section are listed, in the next column the minimal velocities for which a breach flow slide occurs.

Old Velocity (mm/s)	New Retrogression Velocity (mm/s)	s_{max} (kg/sm)	S_{mean} (kg/sm)	V (m^3)	f0
19.3	18.7	70.8	20.9	290 770	0.05
11.8	11,7	129	37.2	517 810	0.075
8.7	8.7	188	57	793 369	0.1

Table 4.1-5: The minimal initial disturbance to create a breach flow slide.

Note that the values differ very little and for f_0 = 0.1 we even find that there is no breach flow slide if the retrogression velocity is lower than 8.7 mm/s. This is an indication that a breach flow slide does not occur very easily and needs some significant initial disturbance.

4.2 ROGGENPLAAT

The Roggenplaat is a sandbank in the Oosterschelde (Figure 4.2-1). Between the 6th and 9th of April 1973 a collapse of a 50 meter deep slope moved 1 260 900 m^3 of sand (Deltadienst, Plaatval in de Roggenplaat 1973). Figure 4.2-2 shows a sketch of the depth difference, the red part indicates a depth decrease while the blue part indicates a depth increase; hence the flow was from south to north. In Figure 4.2-3 the slope of the Roggenplaat is depicted before, on the 27th of August 1971, and three days after the collapse. Note that the left part of the figure depicts the slope; the steep right part is a strengthened bank (which was done between 1860 and 1880). Because of the strengthening of this bank (north in Figure 4.2-1) the flowing water around the Roggenplaat, which could not erode the bank more land inbound, was forced to cut deeper and deeper. The water on the Roggenplaat side was flowing more slowly and dropped sediment on the bank. Eventually the slope became very shallow at the beginning and steep further away from the Roggenplaat, as can be seen in the figure below.

Figure 4.2-1: The Roggenplaat.

Figure 4.2-2: Depth difference sketch Roggenplaat.

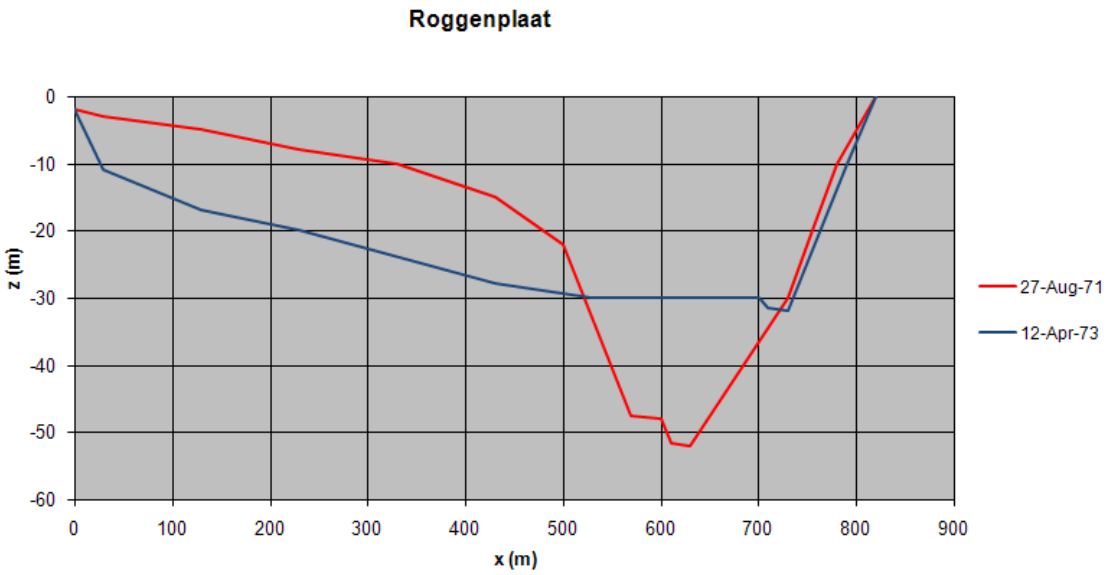

Figure 4.2-3: The Roggenplaat slope before and after collapse.

Through measurements the composition of the different sand layers was determined; these were listed in (Stoutjesdijk en Groot 1994). Some of these layers contained clay and sand which are not modeled by HMBreach. The layers were broken down into layers of approximately 1 meter thick for computational purposes. Furthermore, the steep slope was removed and replaced by a long gentle piece in order to be able to better investigate the properties of the flow. Table 6.3-1 (Section 6.3) was put into HMTurb, the Δn is now specified per layer. Note that layer 59 and on were added to create the gentle part. The constants and coefficients were as in Table 4.1-3 except Δn = 0.084 (the average of the measured values) instead of 0.04, this does not have any influence since the Δn are specified per layer and thus this value is ignored.

Description	Quantity	Roggenplaat	H. Diep	Unit
Volume of sand	V	*1 260 900*	*111 681*	m^3
Length of collapse	L	343 (*520*)	*153*	m
Width of collapse	W	399 (*535*)	*178*	m
Height of slope	H	52	*23*	m
Gully width	B	92	*41*	m
Time of collapse	T	32.6	*21.75*	h
Volume total mixture (sand + water)	V_m	12 609 000	1 117 000	m^3
Time-averaged maximum spatial mixture discharge	$Q = V_m / T$	107.6	14.3	m^3/s
Q per unit of width	$q = Q / B$	1.17	0.35	m^2/s
Time-averaged maximum sand-transport per unit width	$s = q \cdot c \cdot 2650$ kg/m^3	186	56	kg/sm

Table 4.2-1: Estimation of the Roggenplaat collapse properties, the italic entries are known values, the normal entries are deduced from known values.

4.2.1 Simulation with HMTurb

As with the Roompot case we estimate the time-averaged sand-transport of the collapse by scaling the Hollandsch Diep collapse to the Roggenplaat. As stated the volume of the sand moved during the collapse in the Roggenplaat was 1 260 900 m^3 and thus the length scale factor is estimated to be $\sqrt[3]{1\,260\,900/111\,681} \approx 2.24$. The timescalingfactor therefore is estimated to be $\sqrt{2.24} \approx 1.50$. The result is listed in Table 4.2-1. Note that again only the volume is used for the scaling. The length and width differ somewhat from what was measured. The measured length (as also can be seen in Figure 4.2-3) was about 520 meters and the measured width was about 535 meters, these two values are also included in the table, italic between brackets.

We attempt to create an erosive turbidity current with HMTurb that has a maximal sand-transport s_{max} ≈ 186 kg/sm. Again we take multiple locations on the slope as the initial disturbance and investigate for f_0 = 0.05, 0.075 and 0.1. The locations are above layer 1 (about 1° slope), layer 16 (about 8°), layer 24 (about 14°), layer 32 (about 10°) and layer 38 (about 21°), see Figure 4.2-4. Note that the slope first gets steep to about 14 degrees but after that is somewhat shallower, about 10° before becoming very steep. Note that the initial disturbance is the boundary condition with thickness 1 meter, Froude number 2, concentration 12% and we vary the retrogression velocity to create the sought after breach flow slide. The experiment which was done in Section 4.1 is repeated. Thus we vary the speed no more than 0.1 mm/s to create a flow which has a maximal sand transport as close as possible to 186 kg/sm.

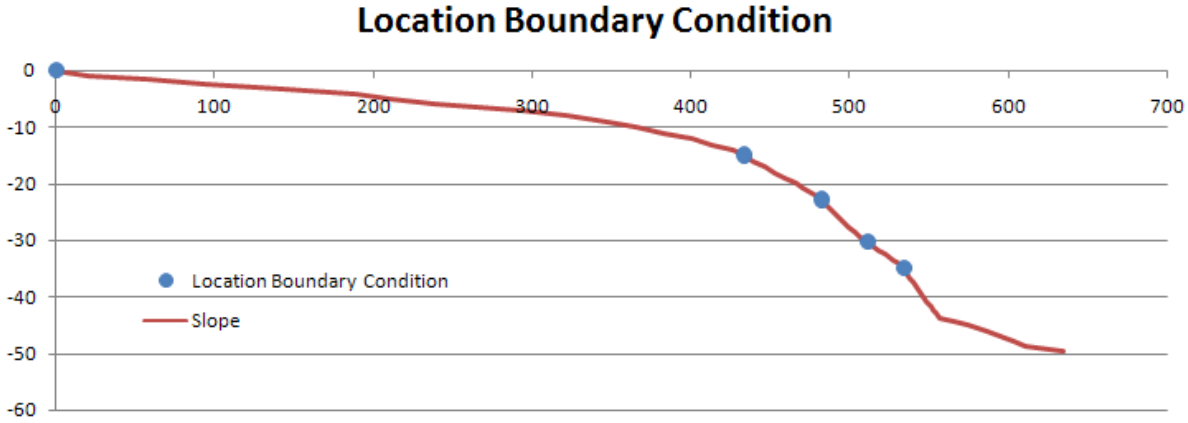

Figure 4.2-4: The location of the boundary conditions.

The results are listed in Table 4.2-2. Section 5.3 contains the plot of the sand transport and flow velocity of all the corresponding flows. Note that in the figures both the slope and the sand transport (or flow velocity) are plotted. The right axis corresponds to the slope height, the left to the sand transport (or flow velocity). Note that the maximal sand transport occurs when the slope steadily becomes shallower and transport rapidly decreases from then on. The reason for this is that

the flow velocity decreases and the sand in the mixture will slowly settle on the bed. The mean of the sand transport is again taken over a distance of 1 km. Also note that the required retrogression velocity to create a breach slide on location 4 is higher than on location 3. This is because location 4 is just above a somewhat shallower part of the slope than location 3 and thus the flow will sooner fade out. In the figures one can observe that the sand transport peak is much thinner for f_0 = 0.1 than for the other two values, consequently the mean sand transport will be lower, as can be seen in the table below. The effect was not found for the Roompot case.

Location	Retrogression Velocity (mm/s)	s_{max} (kg/sm)	S_{mean} (kg/sm)	V (m^3)	f0
1	90.3	458	191	3 237 099	0.05
1	75.5	584	221	3 745 544	0.075
1	69	130	39	660 978	0.1
2	16	184	84	1 423 645	0.05
2	10.9	535	244	4 135 352	0.075
2	8.6	456	74	1 254 164	0.1
3	9.9	172	78	1 321 956	0.05
3	4.8	173	67	1 135 527	0.075
3	3.1	209	34	576 237	0.1
4	22.1	186	86	1 457 542	0.05
4	11	186	70	1 186 371	0.075
4	8.5	185	28	474 548	0.1
5	30.9	185	86	1 457 542	0.05
5	16.7	197	74	1 254 164	0.075
5	14.3	187	27	457 600	0.1

Table 4.2-2: The maximal sand transport corresponding to the initial velocity.

We now, as in the Roompot case, can investigate if the flows we found indeed produce the same volume of sand as the flow in the Roggenplaat collapse did. To that extent we again use the following formula to produce the estimated volume of moved sand V (fifth column in the table above):

$$V = \frac{s_{mean} \cdot (T \cdot 3600) \cdot \frac{W + B}{2}}{1700}$$

Obviously an initial disturbance in the first location, the shallow part, can result in a breach flow slide but it is highly unlikely that this has happened during the collapse of 1973 since the disturbance is particularly high and the volume of moved sand is either much too high or too low.

The second location seems more prone to be able to create the current we seek. Note that the flow with f_0 = 0.1 seems to be almost of the same volume as the real collapse in the Roggenplaat. The maximal sand transport however is much higher. If we look at the plot of the sand transport, Figure 5.3-6, we see that indeed it has a peak but is very thin which causes the mean of the transport to be

quite low. That the volume is quite good mimicked is thus more or less a coincidence, the flow, although they have the same volume, is most likely not the same as in the Roggenplaat.

Location three is very prone for a breach flow slide; the initial disturbance needed is low in comparison to the other location and the volumes for f_0 = 0.05 and 0.075 also come close to the sought after value.

When one places the initial condition just above layer 32, thus the fourth location, the resulting flows for f_0 = 0.05 and 0.075 are very similar to what probably happened in 1973. Again f_0 = 0.1 produces a flow with a very thin peak and thus yields a too low volume.

The fifth location also produces quite nice flows for the first two f_0 but the magnitude of the disturbance needs to be higher, this is probably because the flow needs some time (distance) to grow but the slope becomes shallow very soon on this location, hence a bigger initial flow is needed to meet the required sand transport.

Especially the third and fourth location seems to produce the sought breach flow slide for a quite small initial disturbance. If we also take a closer look at the composition of the sand at location 4 of the slope then we see that layer 29-31 consist of slightly coarser sand with a high porosity. A small disturbance in this layer can create a small liquefaction flow slide which can act as the boundary condition and thus consequently can cause the breach flow slide leading to the failure of the slope. Although it has to be noted that a liquefaction flow slide is less likely to occur in coarse sand.

It needs to be noted that we took the slope of the Roggenplaat here and added a shallow part. This meant that the sand flowing down the slope could sediment farther away then was the case in 1973. During the real collapse the flowing sand-water mixture was trapped between the Roggenplaat and the strengthened bank on the opposite of the Roggenplaat.

4.2.2 Proneness of the Slope to Breach Flow Slides

Old Velocity (mm/s)	Retrogression Velocity (mm/s)	s_{max} (kg/sm)	S_{mean} (kg/sm)	V (m^3)	f0
9.9	9.2	71.3	20.8	352 350	0.05
4.8	4.8	173	67	1 135 527	0.075
3.1	3.1	209	34	576 237	0.1
22.1	14.8	68.3	17.9	303 540	0.05
11	9.7	93.1	29.2	494 730	0.075
8.5	8.5	118	14.3	242 440	0.1

Table 4.2-3: The minimal initial disturbance to create a breach flow slide.

We investigate, as in the Roompot case, the proneness of the slope to breach flow slides. We investigate this for two location, the third and fourth since a disturbance in these locations seem the most likely to bring forth a breach flow slide. The results are depicted in the table above. Note

that for location 3 the initial disturbance needed to mimic the 1973 collapse seem to just be on the verge of creating a breach flow slide. Only for $f_0 = 0.05$ a lower retrogression velocity brings forth a breach flow slide, the velocities on the other two locations already are as low as they can be. The initial disturbance on the fourth location with $f_0 = 0.05$ can be lowered quite a lot and still a breach flow slide occurs. The other two values for f_0 seem to be just on the verge of creating a breach flow slide.

4.3 PLAAT VAN OUDE TONGE

As a part of the Delta Works the Grevelingendam was built which connected Schouwen-Duiveland and Goeree-Overflakkee. The building began in 1958 and would take up about 7 years so that the dam was opened in 1965. The dam runs over the Plaat van Oude Tonge (Figure 4.3-1). The Krammer is a body of water which formerly flowed perpendicular to the dam (which obviously was not there at the time) but since the building of the dam the flow direction became parallel to the dam, along the Plaat van Oude Tonge, which can be seen in the figure below. This caused a lot of erosion on the sand bank and in the period from 1958 to 1973 multiple slope failures have been reported. In 1973 it was decided to enforce the Plaat van Oude Tonge to prevent any further failures (Deltadienst, Bescherming van de Plaat van Oude Tonge 1974).

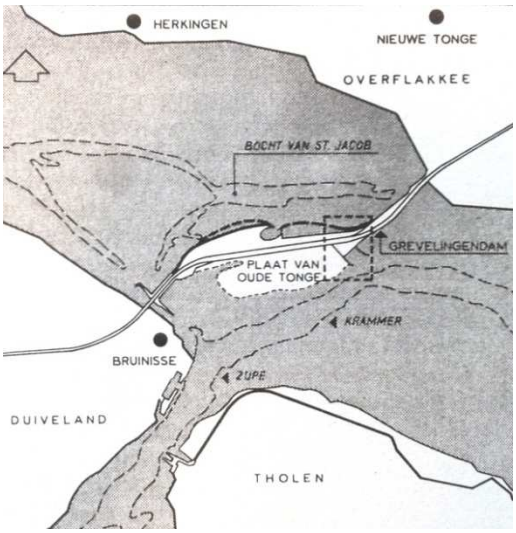

Figure 4.3-1: Old map which shows the Plaat van Oude Tonge and the Grevelingendam.

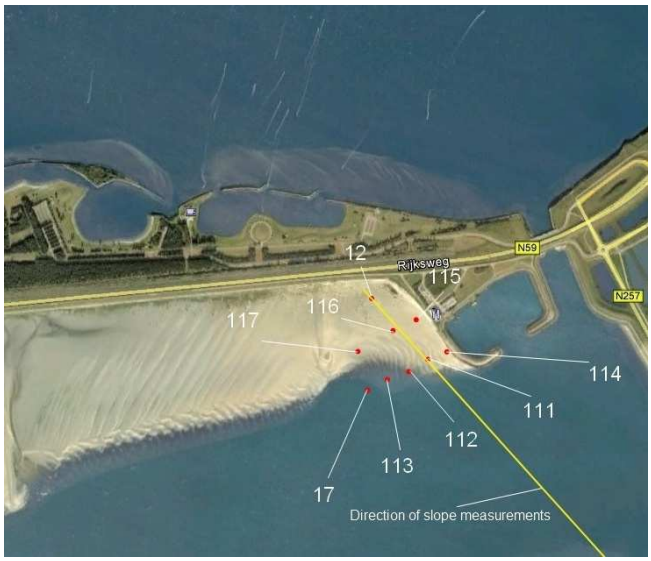

Figure 4.3-2: Location of the samples and the direction in which the slope depth was determined.

One of the failures is of particular interest since just before the collapse measurements were done from which the composition of the soil was deduced, this failure took place between February and October 1972. Figure 3.3 2 shows the location of the measurements. The results of these measurements are taken from (Stoutjesdijk & de Groot, 1994). Measurement 111 consists of the most samples, 10, which range from 5 meter depth to 27 meter depth. It is also assumed that the center of the collapse was located (roughly) on the yellow line in the above figure. Therefore the samples from measurement 111 are used to determine the layer composition of the slope. For the layers in the first 5 meters one sample is taken from measurement 113 since this was the only one in this range. The boundaries of the layers are determined by averaging over the sample depth, i.e., if one sample is from 5,20 to 5,55 meter deep and the next one is from 6,25 to 6,60 meters then the boundary of the two layers is (6,25+5,55)/2 = 5,90 meter. Since the slope that we are interested in is only approximately 20 meters deep we can ignore the samples deeper than 20 meters. The resulting slope composition and consequently, the HMTurb input, is given in Table 3.3 1.

Input:	From (m)	To (m)	Thickness (m)	Porosity (%)	D50 (mu)	Δn (-)	D15 (mu)	Angle (deg)
Layer 1	0,00	4,20	4,20	41	175	0,116	125	6,65
Layer 2	4,20	5,90	1,70	41,5	220	0,065	140	8,06
Layer 3	5,90	7,13	1,23	42,1	240	0,057	180	8,71
Layer 4	7,13	8,53	1,40	44	195	0,045	150	9,93
Layer 5	8,53	10,45	1,93	40	200	0,100	155	6,46
Layer 6	10,45	12,55	2,10	42	140	0,111	110	3,08
Layer 7	12,55	15,00	2,45	41,3	125	0,144	105	17,03
Layer 8	15,00	18,15	3,15	41	170	0,101	125	9,41
Layer 9	18,15	19,23	1,08	43	150	0,127	115	6,84

Table 4.3-1: Composition of the slope before collapse.

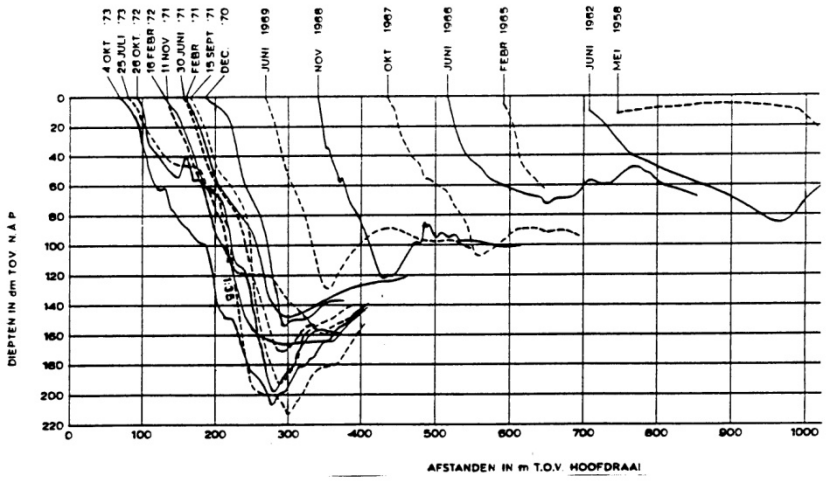

Figure 4.3-3: The geometry of the slope for multiple dates.

The shape of the slope along the yellow line in Figure 4.3-2 was also known on multiple dates including just before and after the collapse, these are all drawn in Figure 4.3-3 (note that the vertical axis has unit dm). The hierboven figure is taken from (Deltadienst, Bescherming van de Plaat van Oude Tonge 1974). Note that the Plaat van Oude Tonge has retracted over 900 meters in just 15 years time. It is also apparent that the slope has become a lot deeper because the Krammer changed its flow direction which from 1958 on was perpendicular to these slopes, hence the erosion of the slope.

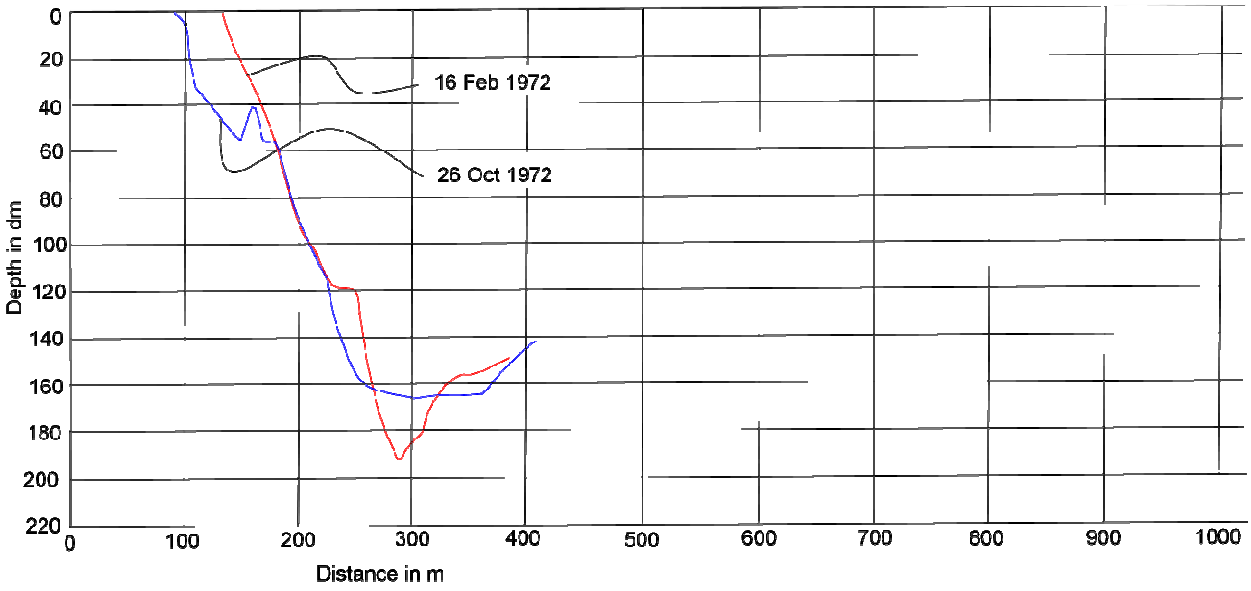

Figure 4.3-4: The slope before and after the collapse.

Figure 4.3-4 shows the slope before and after the collapse acquired from Figure 4.3-3. The angles in Table 4.3-1 are determined from this figure and the layer thickness. A couple of things are notable about this picture. The top of the slope has been retrograded over about 42 meters and on two-thirds of the slope a part disappeared (of about 27 meters long). The part in between however seems to be untouched. This is an indication that maybe the slope failure was not caused by a breach flow slide, or that there were two separate breach flow slides (where one can cause the other).

As with the Roggenplaat case we add a shallow part at the end of the slope to monitor the flow fully until it fades away. To that extent we added two layers with the same sand properties as layer 9, the first has an angle of 1 degree, the second of 0.2 degree.

Input:	From (m)	To (m)	Thickness (m)	Porosity (%)	D50 (mu)	Δn (-)	D15 (mu)	Angle (deg)
Layer 10	19,23	20,23	1,08	43	150	0,127	115	1,00
Layer 11	20,23	21,23	1,08	43	150	0,127	115	0,20

Table 4.3-2: The two added layers to create a shallow toe.

4.3.1 Simulation with HMTurb

Description	Quantity	Plaat van Oude Tonge	Hollandsch Diep	Unit
Volume of sand	V	32 484	*111 681*	m^3
Length of collapse	L	64	*153*	m
Width of collapse	W	149	*178*	m
Height of slope	H	*19.2*	*23*	m
Gully width	B	34.2	*41*	m
Time of collapse	T	19.9	*21.75*	h
Volume total mixture (sand + water)	V_m	324 840	1 117 000	m^3
Time-averaged maximum spatial mixture discharge	$Q = V_m / T$	4.54	14.3	m^3/s
Q per unit of width	$q = Q / B$	0.13	0.35	m^2/s
Time-averaged maximum sand-transport per unit width	$s = q \cdot c \cdot 2650$ kg/m^3	21.1	56	kg/sm

Table 4.3-3: Estimation of the Plaat van Oude Tonge collapse properties, the italic entries are known values, the normal entries are deduced from known values.

As in the previous cases we use the Hollansch Diep collapse to approximate the scope of the collapse. Note that this case is much smaller than the Roompot and Roggenplaat case. Unfortunately there are only a few details known about the morphology of the Plaat van Oude Tonge, actually, the above figure is the only data we have at our disposal. From the figure we learn that the height of the slope is 19.2 meters. The height of the slope in the Hollandsch Diep was 23 meters, thus we can estimate the scaling factor to be $19.2/23 \approx 0.83$. Using this scaling factor we can determine the rest of the properties of the collapse. Note that this factor would give us a length L of$153 \cdot 0.83 \approx 127.7$ m. However, from the above figure we deduced that the length can be no more than 42+27 = 69m (the two parts that disappeared). For the volume we take thus not 50

$0.83^3 \cdot 111\,681\ \mathrm{m}^3$ but rather $\frac{0.83^3 \cdot 111\,681}{2} = 32\,848\ \mathrm{m}^3$ to correct for the length. The time the collapse would have taken is $\sqrt{0.83} \cdot 21.75 \approx 19.9$ h. The properties are listed in Table 4.3-3. Again it is stressed that only the height of collapse was known with some certainty. The rest is estimated using this height and Froude scaling. We corrected for the length according to our findings from Figure 4.3-4 and divided the scaled value by 2.

Now we can investigate if we can create a breach flow slide on this slope in HMTurb which has a maximal sand-transport of 21 kg/sm. We repeat the experiment we did in the previous two cases. Two locations will be taken for the boundary condition, at the top of the slope and just above layer 7; this is the part that is almost horizontal two-thirds down the slope (Figure 4.3-4). The results are shown in the table below. For the mean sand transport for the first location we take the sand transport over 500 m distance, for the second location a distance of 150 meters.

Location	Retrogression Velocity (mm/s)	s_{max} (kg/sm)	S_{mean} (kg/sm)	V (m^3)	f0
1	20.1	48.1	21.52	83 074	0.05
1	13.6	97.4	32.41	125 089	0.075
1	10.8	129.7	35.59	137 396	0.1
2	8.5	20.9	10.24	39 540	0.05
2	4.7	21.1	9.74	37 592	0.075
2	3	21.0	8.87	34 245	0.1

Table 4.3-4: The maximal sand transport corresponding to the initial velocity.

The first location, corresponding to the top of the slope, seems to be unlikely to be the location of the initial disturbance since the resulting erosive turbidity current would be much grander than what possibly happened. The second location however does seem likely to produce a breach flow slide which has the desired maximal sand transport. The volume of moved sand also comes close to what is predicted.

Although we were able to create a comparable breach flow slide to the collapse in HMTurb we cannot conclude that the collapse was caused by a breach flow slide. It is however also not possible to exclude a breach flow slide from the possible causes. First of all there is too little information about the morphology of the Plaat van de Oude Tonge at the time of the collapse to accurately predict the magnitude of a possible flow. Secondly, we assumed that the flow direction of the collapse was over the yellow line in Figure 4.3-2, on this line we knew the depth of the slope. It is very possible that a breach flow slide occurred somewhere on the bank but what we see in the measurements is next to the gully. This scenario is depicted in Figure 4.3-5, the blue part is the erosion area and the red part is the sedimentation area. Note that the depth measurements are not taken in the heart of the collapse. This could also explain the bit on the slope from 6 to 12 meters which seemed untouched by the flow (Figure 4.3-4), this would correspond to the bit of yellow line which first is inside the blue area, then outside and then again inside.

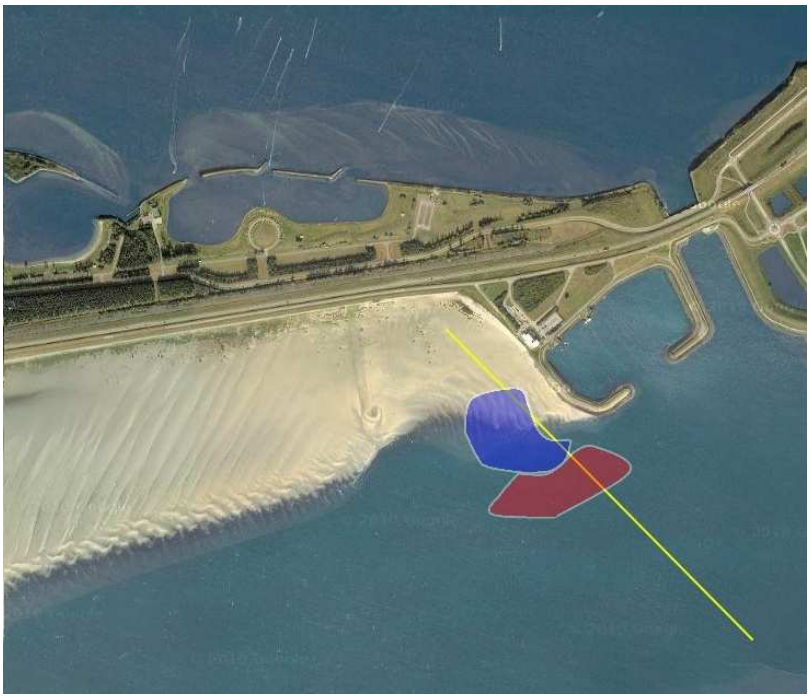

Figure 4.3-5: A possible scenario of the breach flow slide.

4.3.2 Proneness of the Slope to Breach Flow Slides

Again we will investigate the proneness of this slope to breach flow slides. The minimal disturbances needed for the first location are already in Table 4.3-4 and these yield very high volumes. Hence we can conclude that if there ever was any breach flow slide at the Plaat van Oude Tonge, the initial disturbance wouldn't be on the first location. The table below lists the results of the experiment. Note that again the values for the found breach flow slide are close to the minimal values.

Old Velocity (mm/s)	Retrogression Velocity (mm/s)	s_{max} (kg/sm)	S_{mean} (kg/sm)	V (m^3)	f0
8.5	7.8	16.2	7.84	30 258	0.05
4.7	4.0	11.84	4.65	17 947	0.075
3	2.6	12.44	4.88	18 830	0.1

Table 4.3-5: The minimal initial disturbance to create a breach flow slide.

4.4 SPIJKERPLAAT

In the Westerschelde, near Borssele, a sand bank called the Spijkerplaat is located. In the period from 1955 to 1967 a total of four collapses took place on this bank; Figure 4.4-1 shows the location of these four failures. All these failures have in common that the slope was relatively shallow (average slope of only 3°) and very high (more than 50 meters). Again we want to investigate if a breach slide could have been the cause for these collapses. In particular we will investigate the collapse between August 1963 and March 1964 since the slope of this collapse is the shallowest of all the collapses.

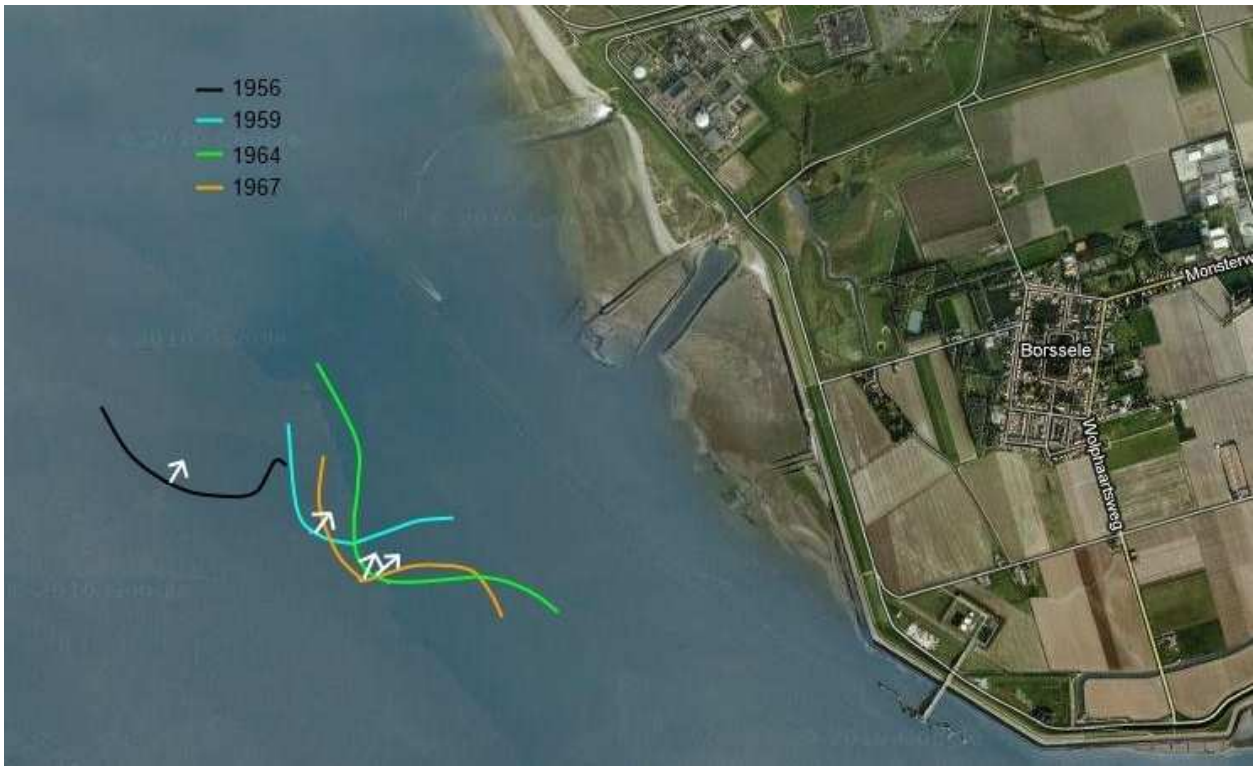

Figure 4.4-1: Locations of the different collapses.

Figure 4.4-2 is from (Stoutjesdijk en Groot 1994) and depicts the slope before and after the collapse in 1964. Note that the slope is very shallow, at its steepest it is about 8° (15 m – N.A.P.). In the previous cases we encountered slopes which had relatively steep parts, it were these parts which seemed prone to creating a breach flow slide, hence our interest in this slope which lacks really steep parts.

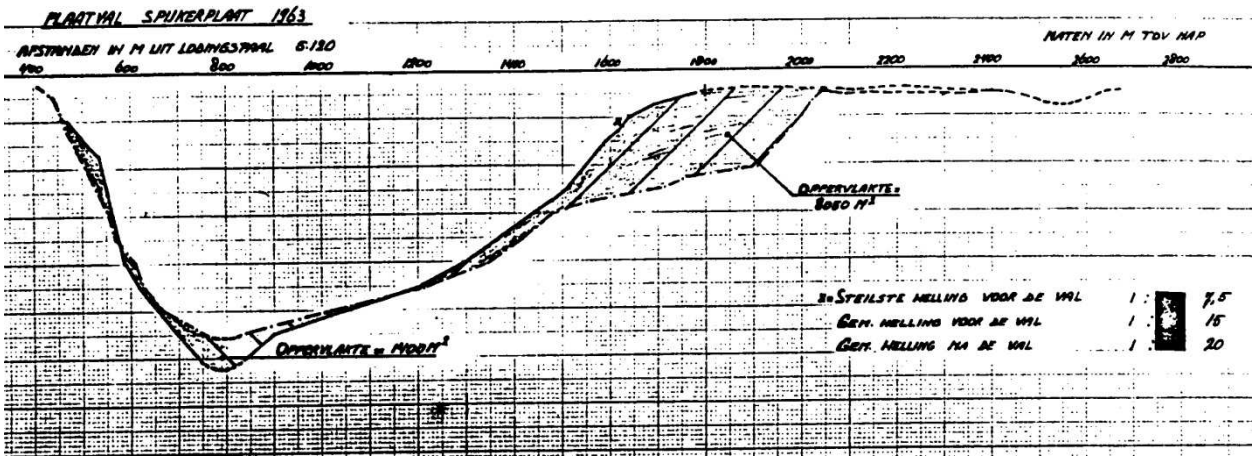

Figure 4.4-2: The slope before and after the collapse in 1964.

Unfortunately not much is known about the soil composition of the slope. The porosity is known to a depth of 27 m – N.A.P., but not on precisely the same location, but something is better than nothing. The porosity from 27 m – N.A.P. to the bottom of the slope is assumed to be 41.5%. The grain size is only known from two samples at about 10 m – N.A.P. and 11 m – N.A.P. It is therefore assumed that the sand from the top of the slope (5 m – N.A.P.) to 11 m – N.A.P. has a distribution according to the first sample and the rest of the slope has a distribution according to the second sample. The HMTurb input and consequently slope composition is listed in Table 6.4-1. The angles of the different layers are deduced from Figure 4.4-2. Note that again a shallow part is added to investigate the flow as it slows down in the sedimentation area.

4.4.1 Simulation with HMTurb

Froude scaling again is used to scale the Hollandsch Diep collapse to this one on the Spijkerplaat, assuming a breach flow slide occurred of course. As in the Plaat van Oude Tonge case we have very little information at our disposal about the geometry of the slope and collapse. From (Wilderom 1979) we know that the total volume of moved sand is 3 500 000 m^3. Hence we can deduce the scaling factor as $\sqrt[3]{\frac{3\,500\,000}{111\,681}} \approx 3{,}15$. From this factor all the other spatial aspects of the collapse can be computed and from those the rest of the information. The results are listed in Table 4.4-1. Note that the volume is very high and hence the collapse of the Spijkerplaat was extremely big. This is the biggest collapse ever measured in the Netherlands.

Description	Quantity	Spijkerplaat	Hollandsch Diep	Unit
Volume of sand	V	*3 500 000*	*111 681*	m^3
Length of collapse	L	482	*153*	m
Width of collapse	W	561	*178*	m
Height of slope	H	73	*23*	m
Gully width	B	129	*41*	m
Time of collapse	T	38.6	*21.75*	h
Volume total mixture (sand + water)	V_m	35 000 000	1 117 000	m^3
Time-averaged maximum spatial mixture discharge	$Q = V_m / T$	251.7	14.3	m^3/s
Q per unit of width	$q = Q / B$	1.95	0.35	m^2/s
Time-averaged maximum sand-transport per unit width	$s = q \cdot c \cdot 2650\ kg/m^3$	310	56	kg/sm

Table 4.4-1: Estimation of the Spijkerplaat collapse properties, the italic entries are known values, the normal entries are deduced from known values.

As in all the previous cases we choose a number of locations which can act as a possible initial disturbance. The locations are at the top of the slope above layer 1 (slope of 1.8°), above layer 6 (4.8°), above layer 11 (8.1°, the steepest part of the slope), above layer 21 (4.1°) and at the toe of the slope above layer 51 (4.6°). These locations are shown on the slope in the figure below, note that the shallow part is left out of this picture. Also note that the overall slope is very gentle.

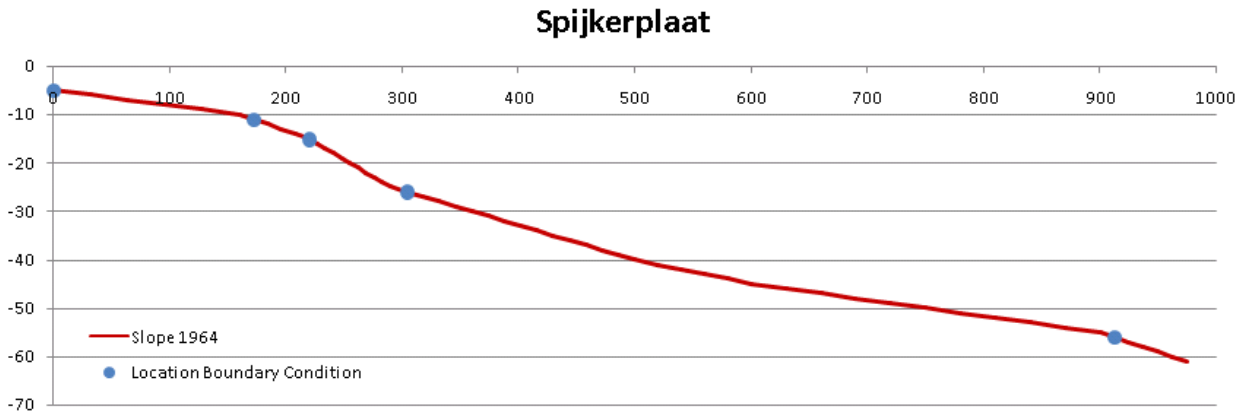

Figure 4.4-3: The slope and locations of the boundary condition for the Spijkerplaat.

The results of the experiment are listed in Table 4.4-2, figures with the sand transport and flow velocity of all the flows can be found in section 5.5. For the first four locations we calculated the mean over a distance of 1200 meters, for location five this distance was 500 meters. Note that the maximal sand transport and hence the estimated volume for the first four locations are much higher than the values we would like to mimic. HMTurb was only able to create a breach flow slide with minimally these initial disturbances. Although the slope in location 3 seems fairly prone to an initial disturbance, the resulting breach flow slide would simply be much too big to mimic the 1964

collapse. Also if one takes a look at for example Figure 5.5-11 then one sees that the flow velocity almost does not accelerate which points towards the conclusion that a breach flow slide is unlikely since the density current for a breach flow slide will accelerate fast.

Only in the last location the turbidity current can be 'steered' towards a flow with a maximal sand transport of 310 kg/sm, then the estimated volume also comes close to what is predicted for the Spijkerplaat. However, in this location the initial disturbances need to be extremely high which seems unlikely since a smaller initial disturbance would also create a breach flow slide, albeit of smaller magnitude (Section 4.4.2).

Location	Retrogression Velocity (mm/s)	s_{max} (kg/sm)	S_{mean} (kg/sm)	V (m^3)	f0
1	65.9	2296	1014	28 610 010	0.05
1	53.2	2650	1162	32 785 830	0.075
1	47.7	2600	1096	30 923 640	0.1
2	24.0	1931	542	15 292 530	0.05
2	17.4	2463	906	25 562 790	0.075
2	14.5	2817	1216	34 309 440	0.1
3	14.4	1374	746	21 048 390	0.05
3	9.6	1933	581	16 392 915	0.075
3	7.6	2413	950	26 804 250	0.1
4	27.0	728	291	8 210 565	0.05
4	19.4	1050	510	14 389 650	0.075
4	16.2	1354	459	12 950 685	0.1
5	109	310	132	3 696 165	0.05
5	90	310	117	3 301 155	0.075
5	89.5	310	104	2 934 360	0.1

Table 4.4-2: The maximal sand transport corresponding to the initial velocity.

It needs to be noted, however, that there is much uncertainty in these results since only a small amount of data was available about the slope. It might be, and most likely is, that the soil composition was very different from the ones that we used. Therefore these results need to be interpreted with reservation.

4.4.2 Proneness of the Slope to Breach Flow Slides

As mentioned in the previous section, the values for the location 1 through 4 in Table 4.4-2 are the minimal values for which a breach flow slide occurs. Investigation for the fifth location produces the table below.

Old Velocity (mm/s)	Retrogression Velocity (mm/s)	s_{max} (kg/sm)	S_{mean} (kg/sm)	V (m^3)	f0
109	29.8	51.1	17.7	356 703	0.05
90	21.5	51.2	14.9	301 435	0.075
89.5	18.0	53.9	13.5	273 165	0.1

Table 4.4-3: The minimal initial disturbance to create a breach flow slide.

Note that the values to actually create a breach flow slide are much lower than the initial disturbances that create a breach flow slide of the desired magnitude. Hence it is not very likely that the slope of the Spijkerplaat collapsed because of a breach flow slide, given the soil composition we used is correct since the slope would probably have (partly) collapsed sooner because of a smaller initial disturbance. It could be however that there was a huge liquefaction flow slide at the bottom of the slope which corresponds to this initial disturbance, this scenario can by no means be ruled out. Again it needs to be noted that the data for the slope composition was too poor to actually be able to conclude this with any certainty. We however have indication that a breach flow slide on a very shallow slope is note very likely to occur since the initial disturbances need to be fairly high.

4.5 CONCLUSION

We have considered four real world examples of slope failures and investigated whether or not a breach flow slide could have been involved in these collapses. For the first two cases, the Roompot and the Roggenplaat, a breach flow slide was most likely the cause of the collapse. It is very hard to conclude anything for the Plaat van de Oude Tonge since we have too little information about the geometry of the slope and collapse. Two breach flow slides may have occurred here where one initiated the other, but that is just speculation. The last case of the Spijkerplaat is also hard to analyze, again we miss a lot of valuable data. The main interest for this collapse was because of its magnitude (3.5 million m^3) and very shallow slope. The collapse could have been the result of a breach flow slide, but then there must have been a very high initial disturbance at the toe of the slope. This disturbance could have been caused by a large liquefaction flow slide, which is not very farfetched considering that the sand in the slope was mainly loosely packed.

One thing we see about all the slope failures is that it is probably never a pure breach flow slide. Most likely the collapse started with a sizable liquefaction flow slide which initiated the breach flow slide. This liquefaction flow slide will most likely have taken place at two thirds or lower of the slope.

There are two things that need to be noted however. Unlike liquefaction flow slides breach flow slides can also occur in densely packed sand (like rivers) and breach flow slides are observed, often during and due to dredging.

All the considered cases were in Zeeland. The steep slopes that we encountered are due to ebb and flood tides. Flows resulting from these tidal currents cause erosion in one place (creating the toe of the slope) and sedimentation in another place (which becomes the top of the slope) which cause large masses of loosely packed sand. This process will create steep and high slopes which ultimately collapse. A nice example of this is the Spijkerplaat, every 3-4 years the process is repeated, see Figure 4.4-1.

5 APPENDIX: FIGURES

5.1 SENSITIVITY ANALYSIS

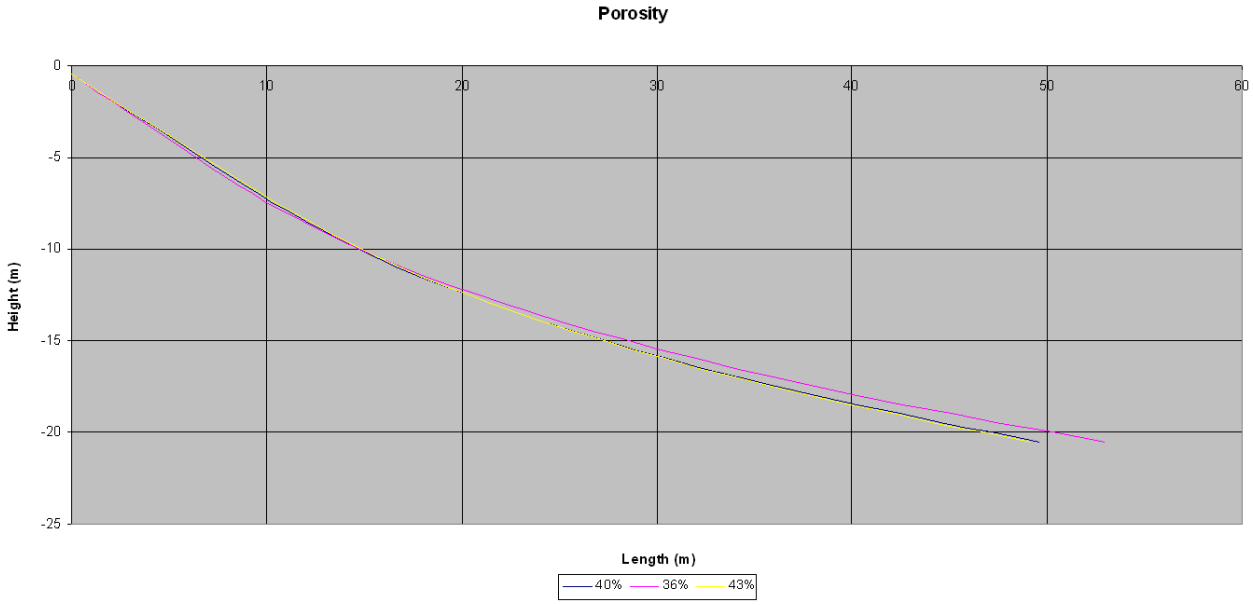

Figure 5.1-1: Sensitivity analysis porosity.

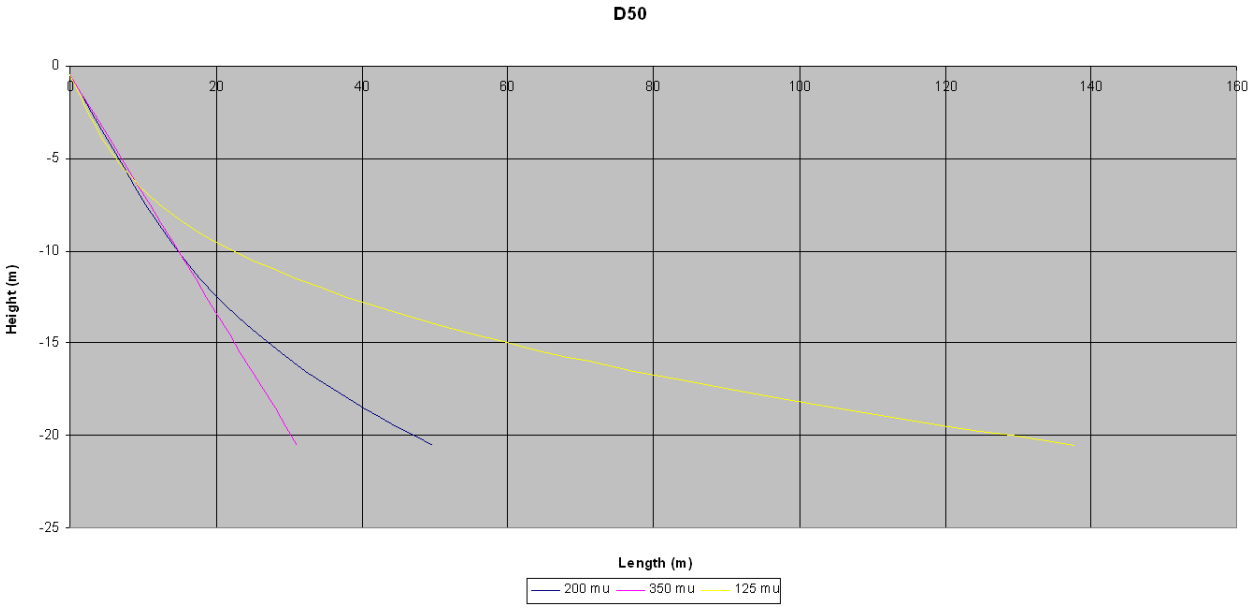

Figure 5.1-2: Sensitivity analysis D_{50}.

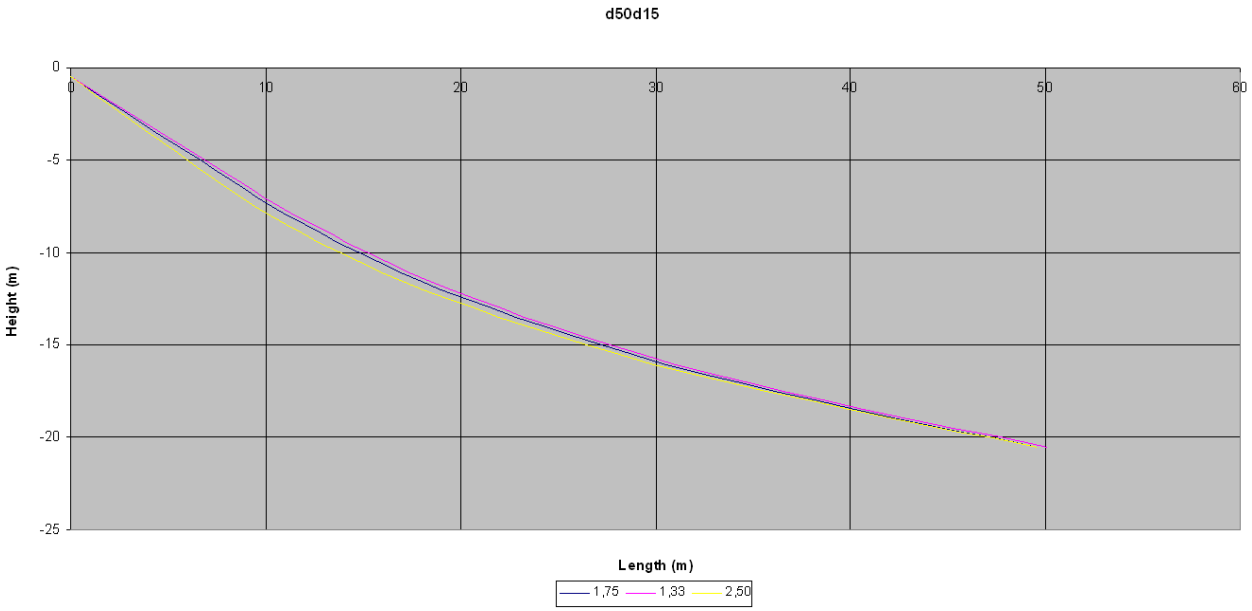

Figure 5.1-3: Sensitivity analysis $D_{50}D_{15}$.

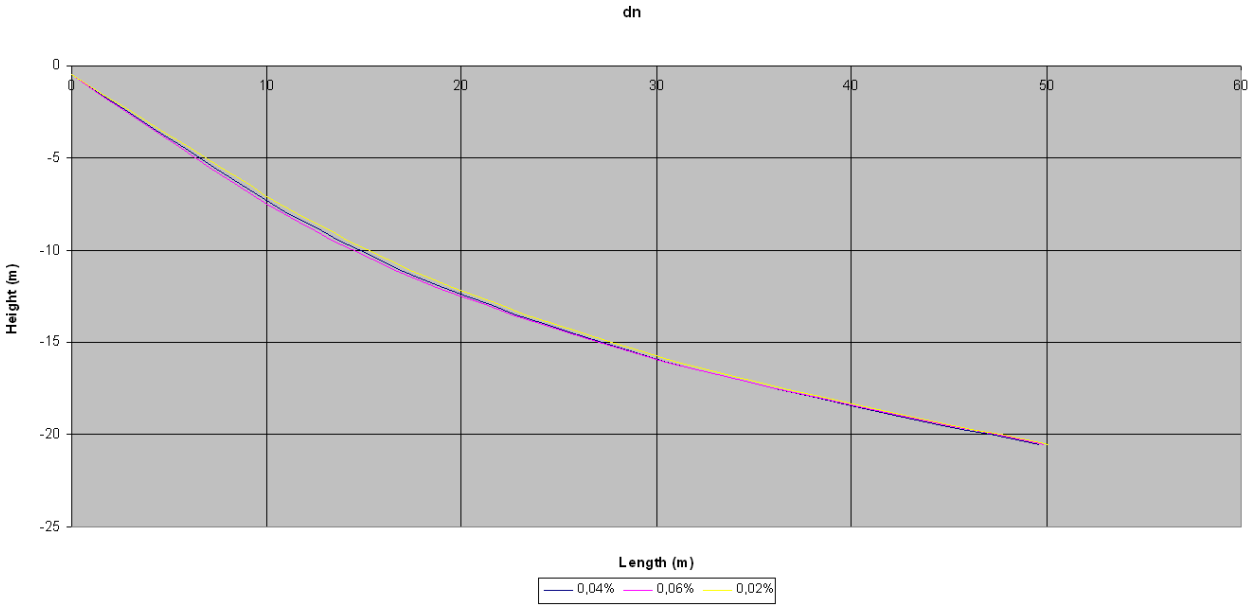

Figure 5.1-4: Sensitivity analysis Δn.

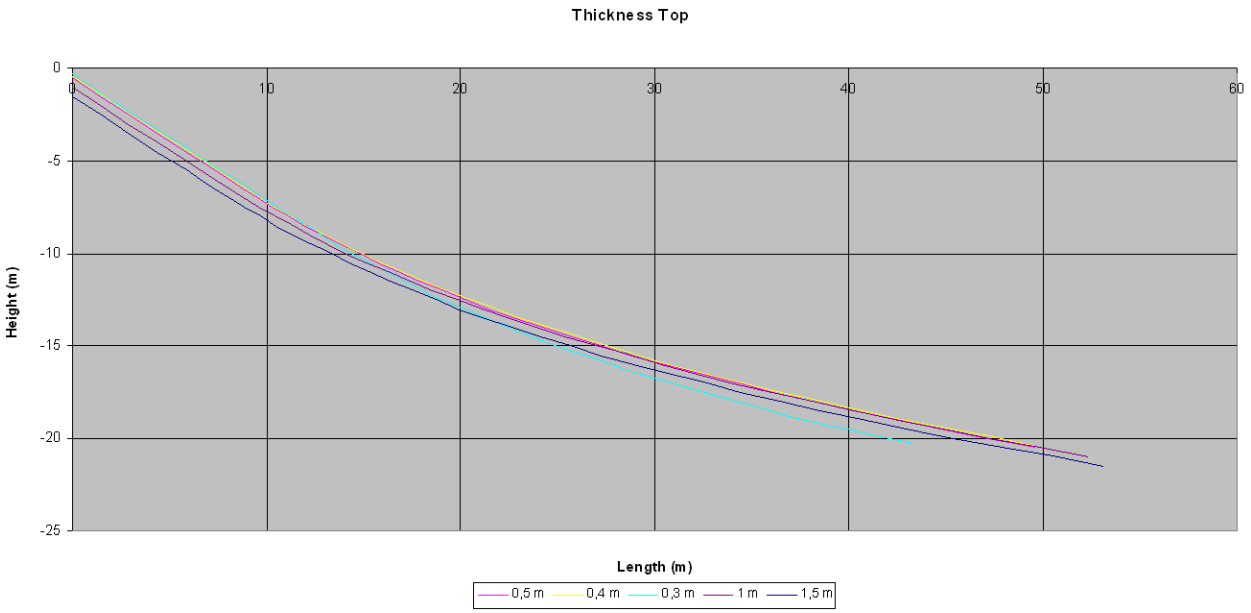

Figure 5.1-5: Sensitivity analysis thickness top.

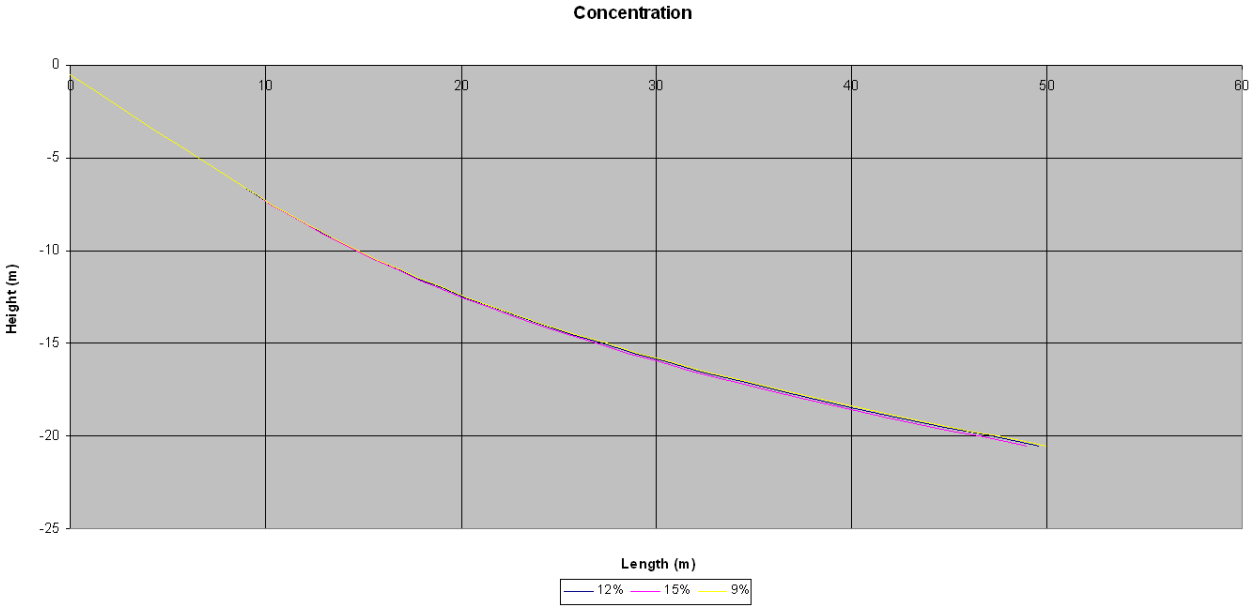

Figure 5.1-6: Sensitivity analysis concentration.

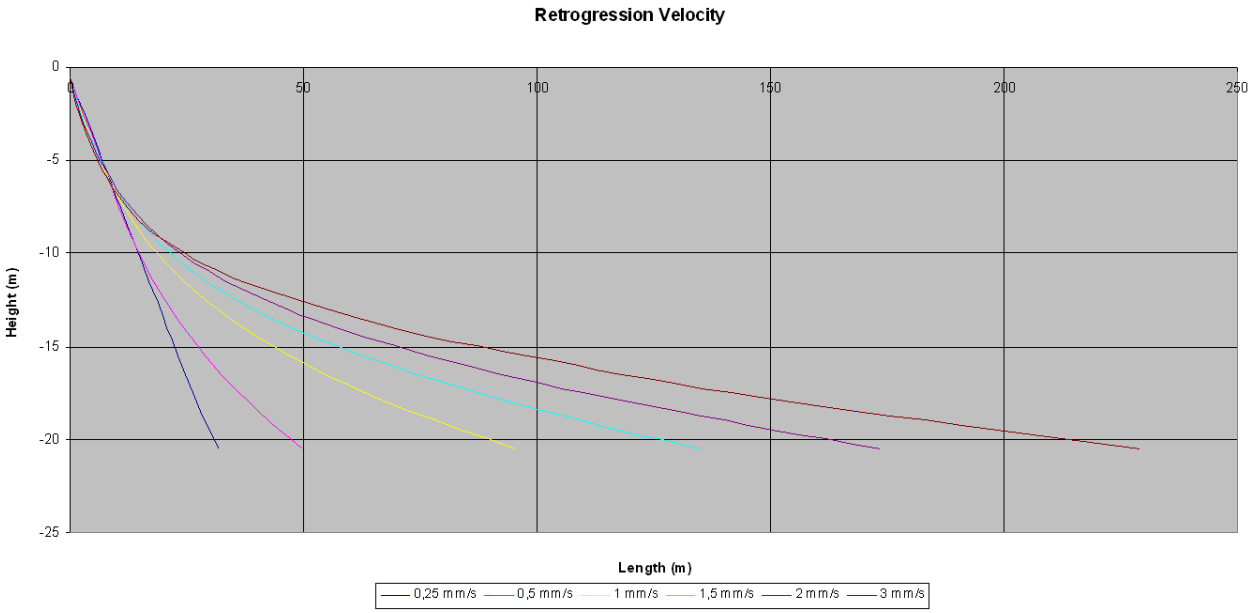

Figure 5.1-7: Sensitivity analysis retrogression velocity.

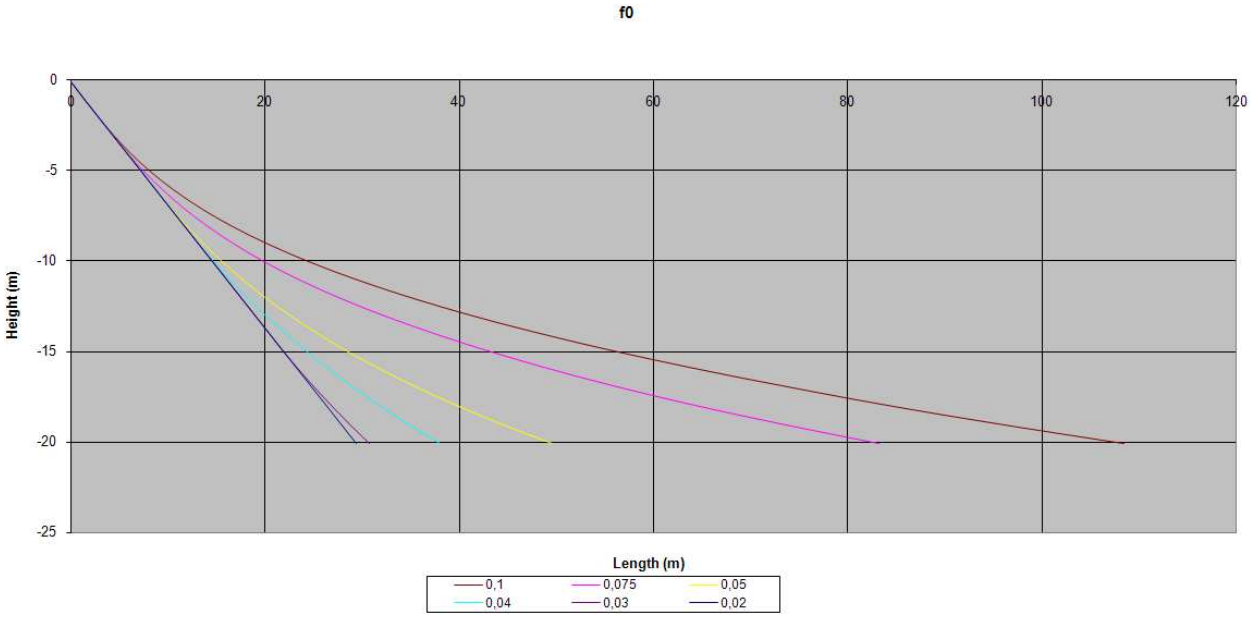

Figure 5.1-8: Sensitivity analysis f_0.

5.2 ROOMPOT

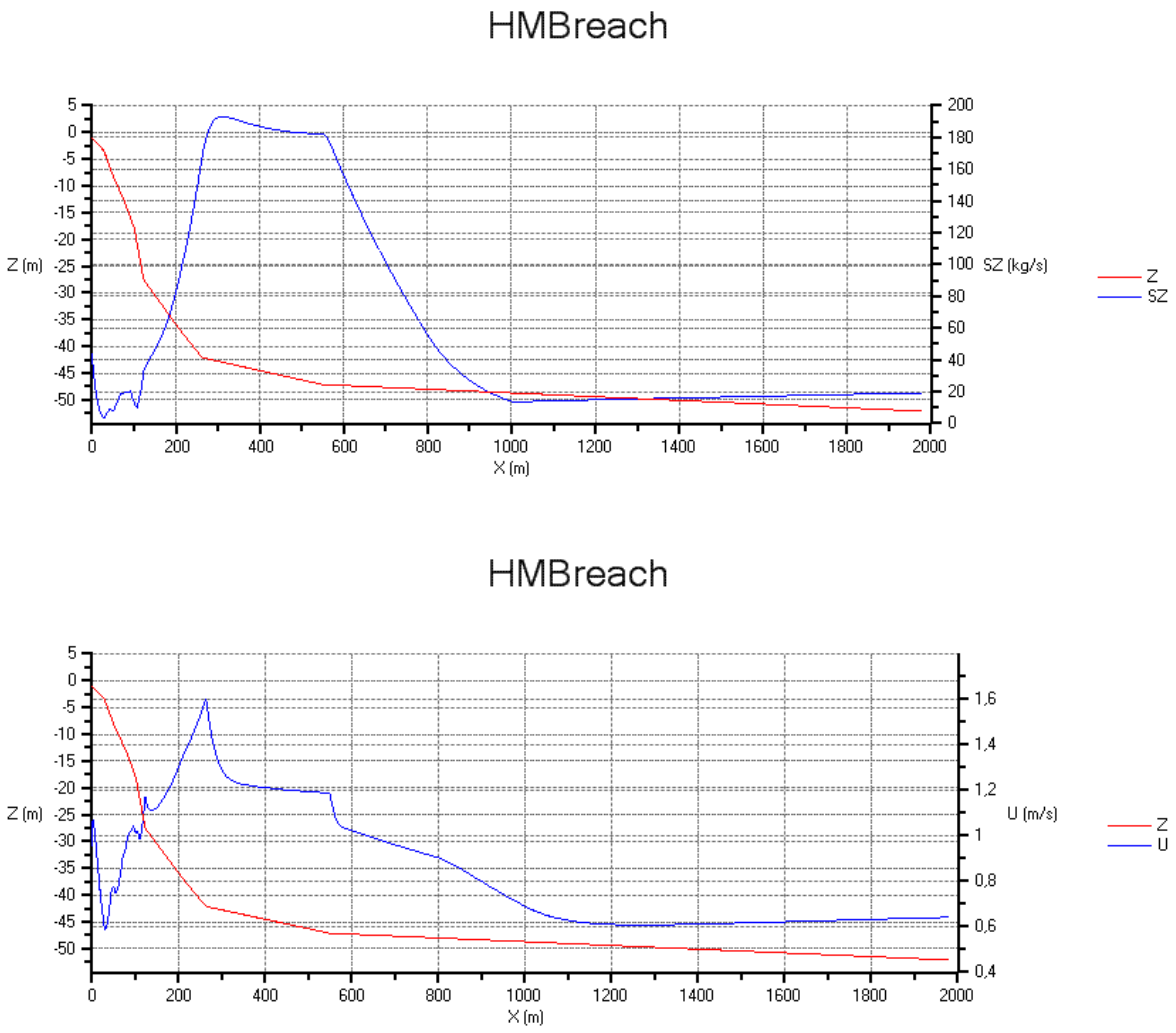

Figure 5.2-1: Sand transport and speed for location 1 and f_0 = 0.05.

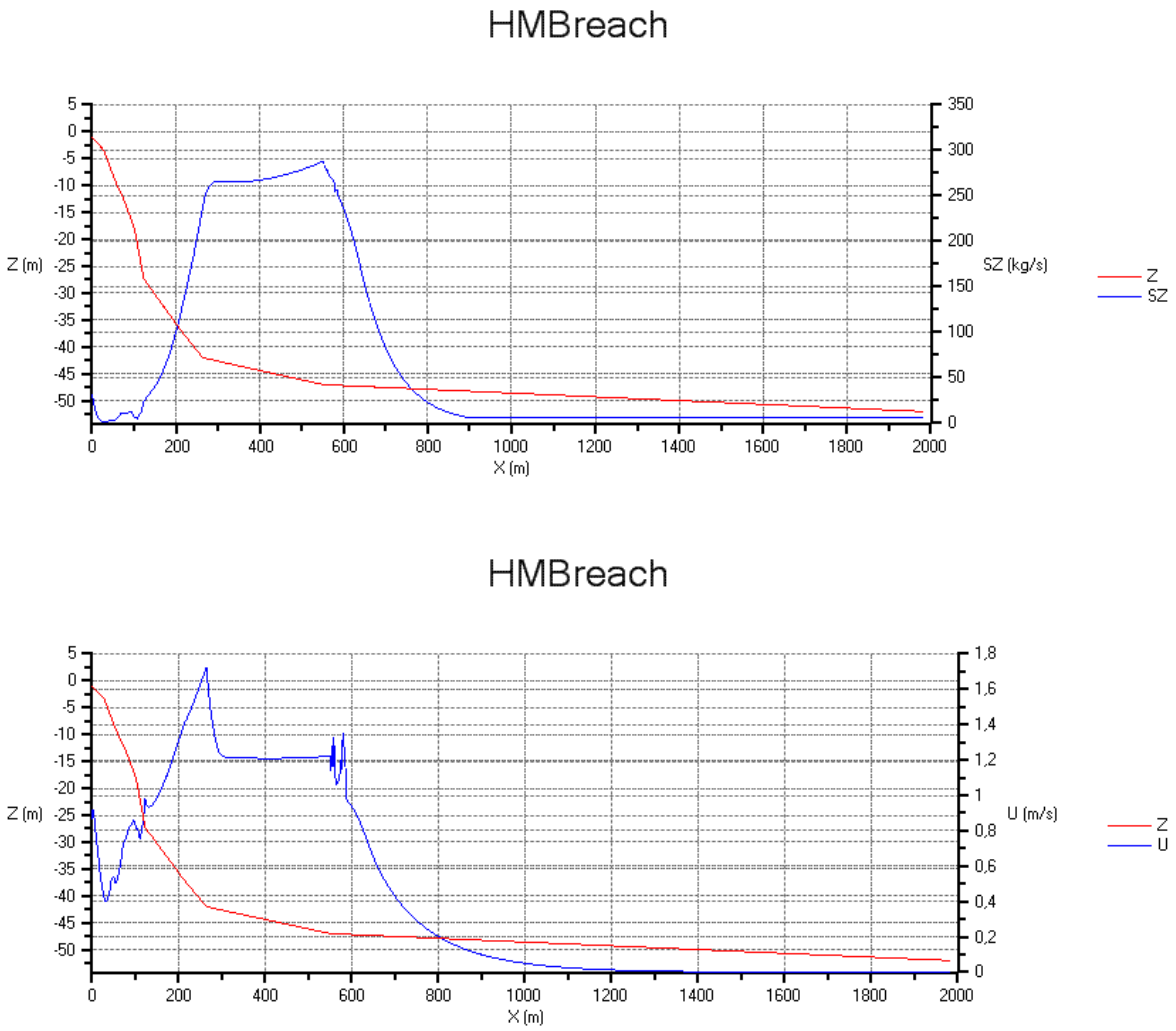

Figure 5.2-2: Sand transport and speed for location 1 and f_0 = 0.075.

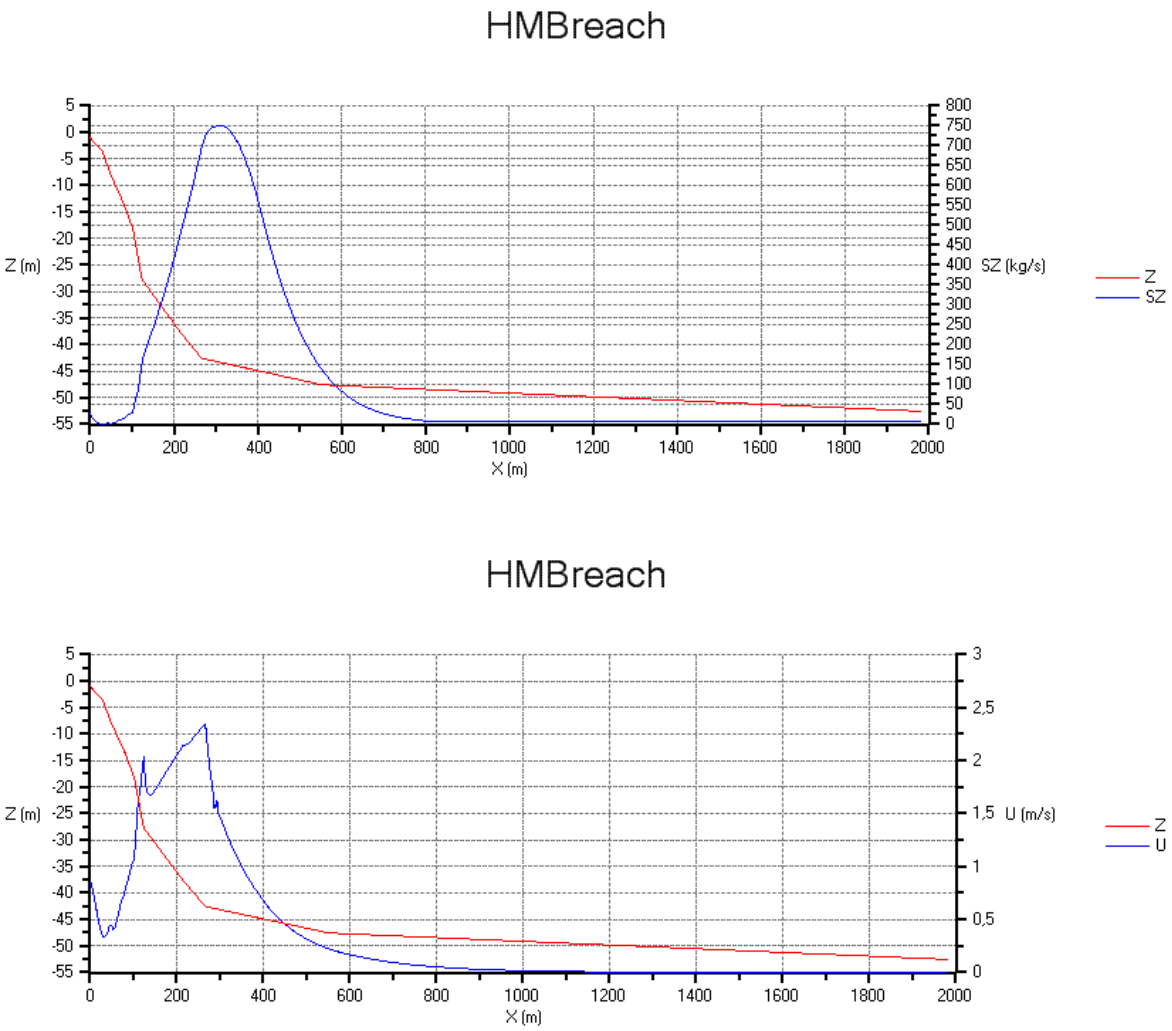

Figure 5.2-3: Sand transport and speed for location 1 and f_0 = 0.1.

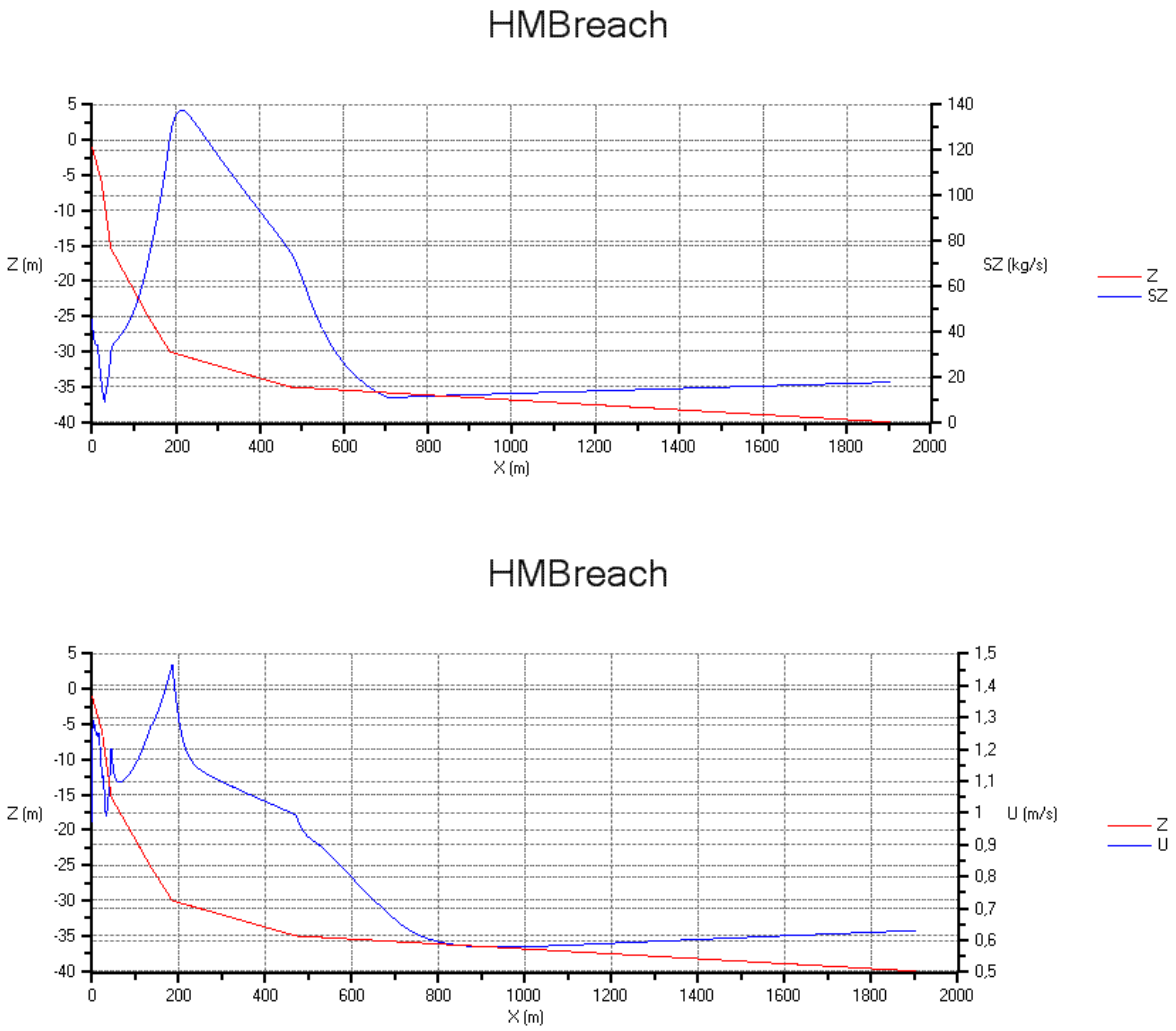

Figure 5.2-4: Sand transport and speed for location 2 and f_0 = 0.05.

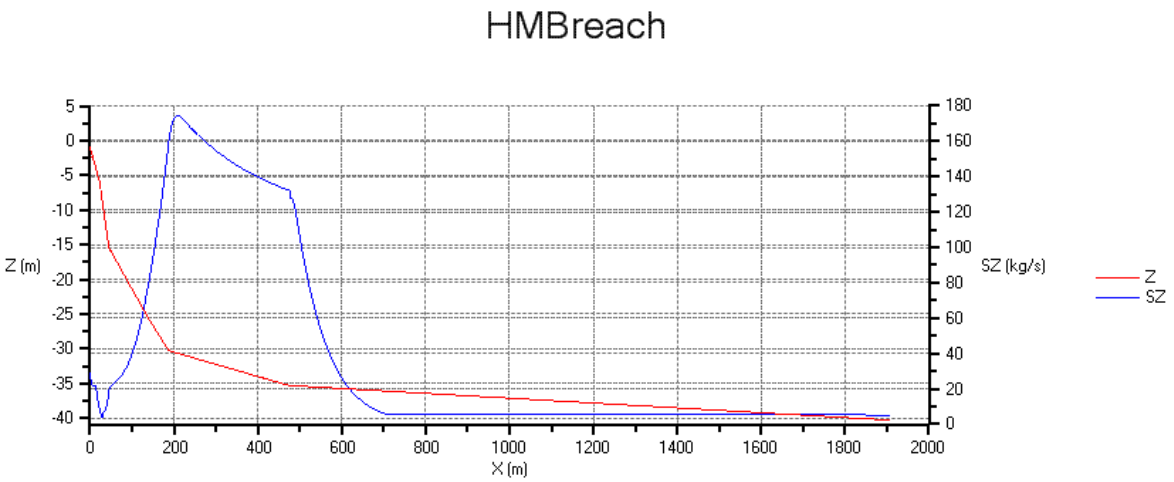

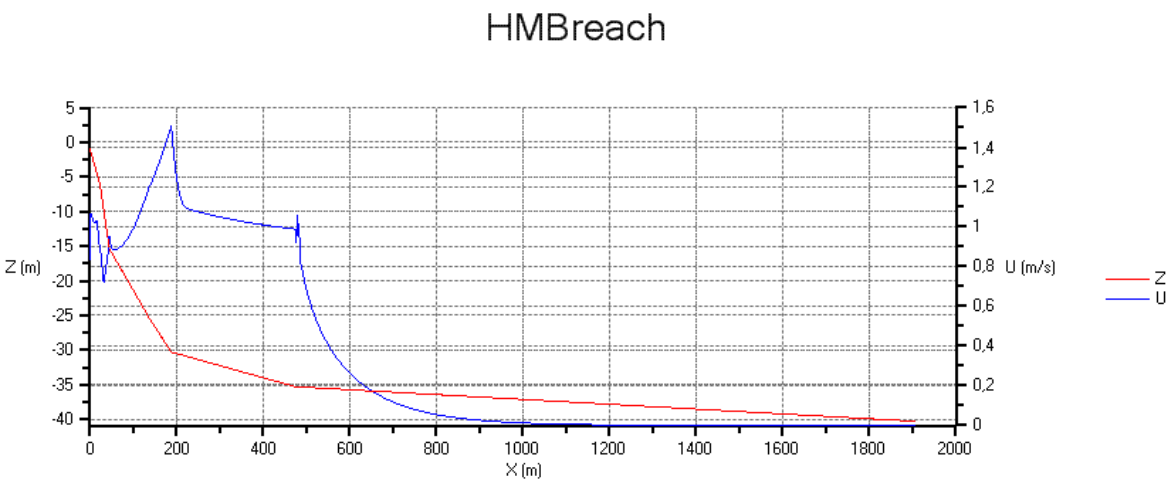

Figure 5.2-5: Sand transport and speed for location 2 and f_0 = 0.075.

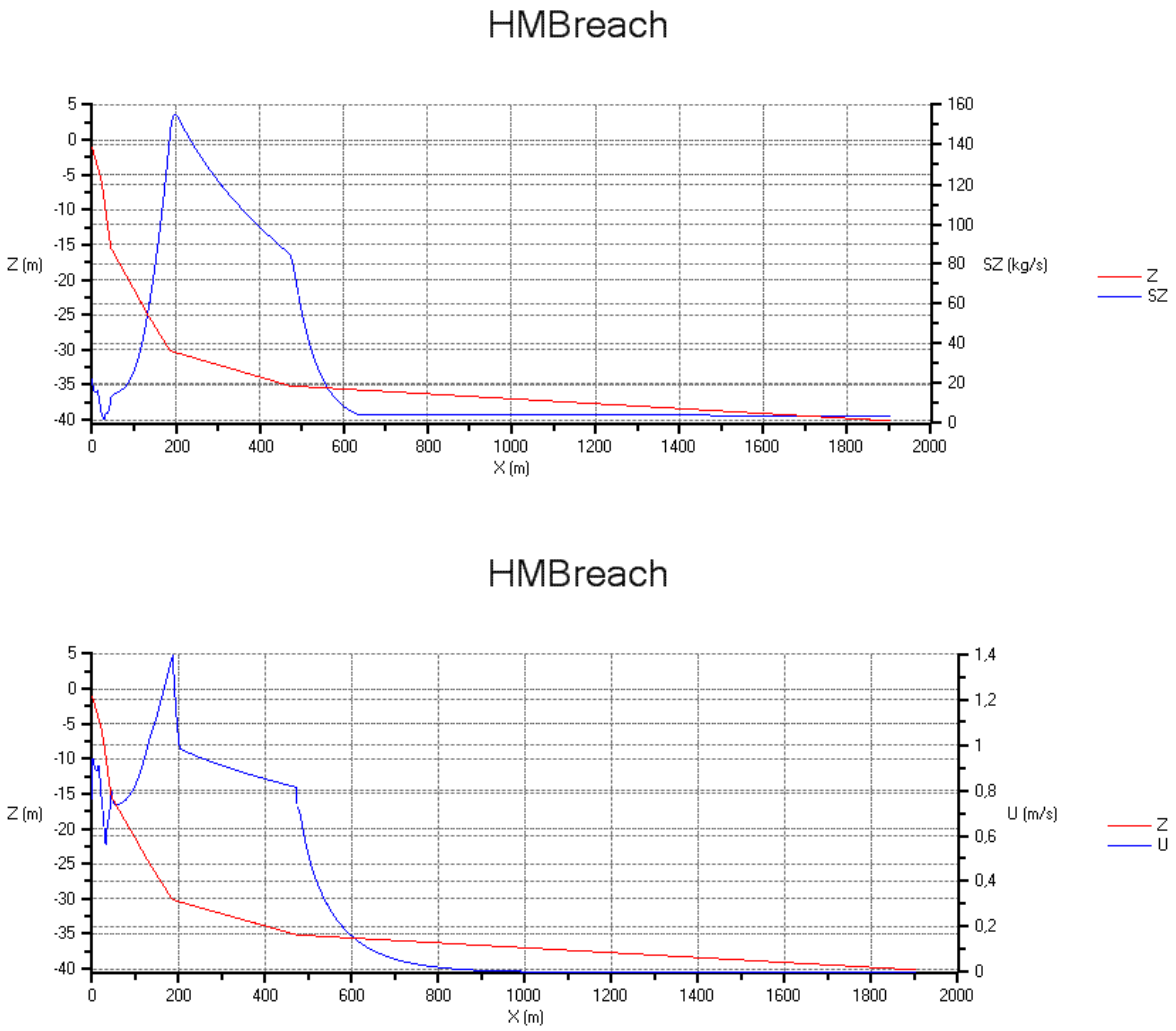

Figure 5.2-6: Sand transport and speed for location 2 and f_0 = 0.1.

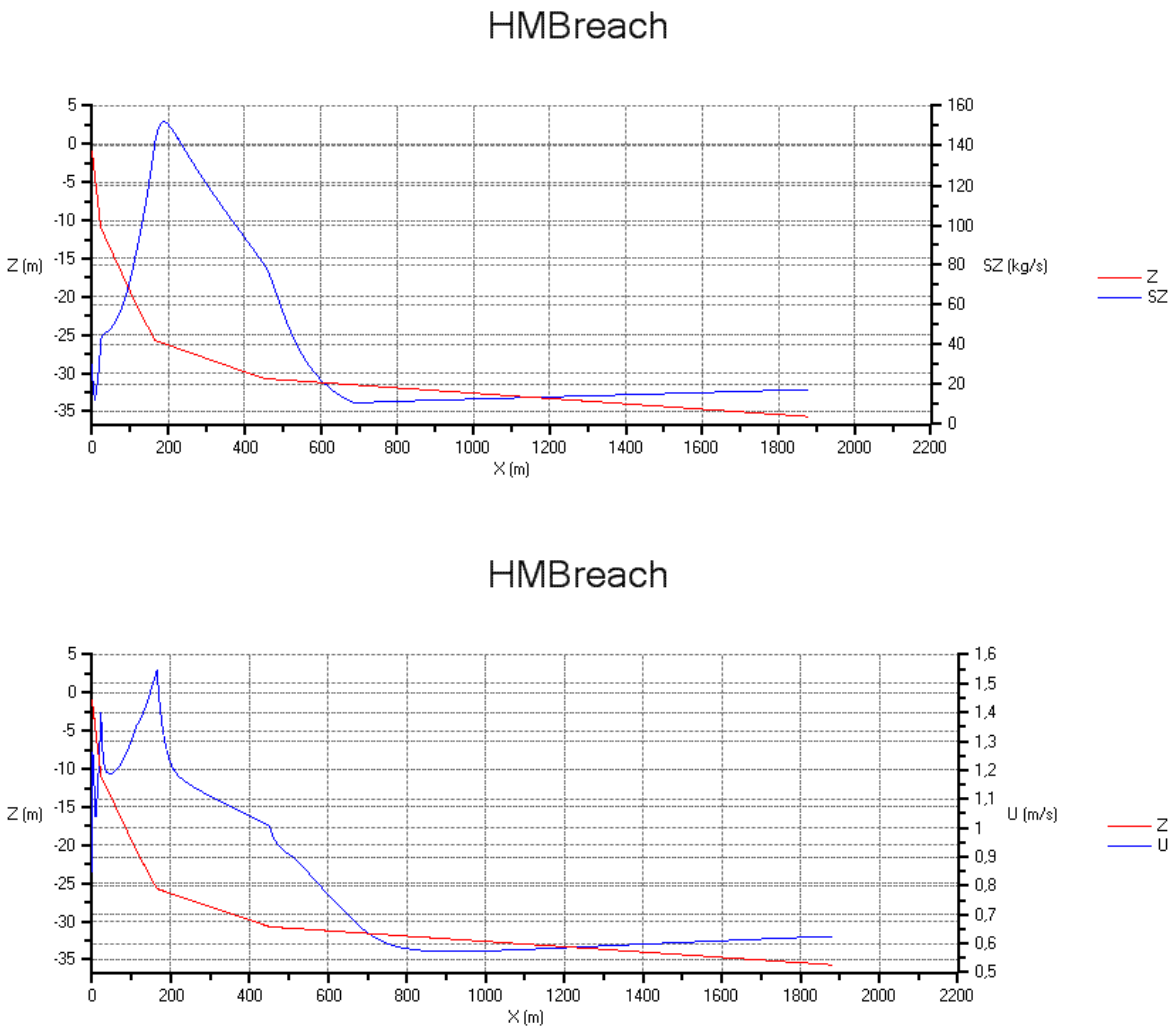

Figure 5.2-7: Sand transport and speed for location 3 and f_0 = 0.05.

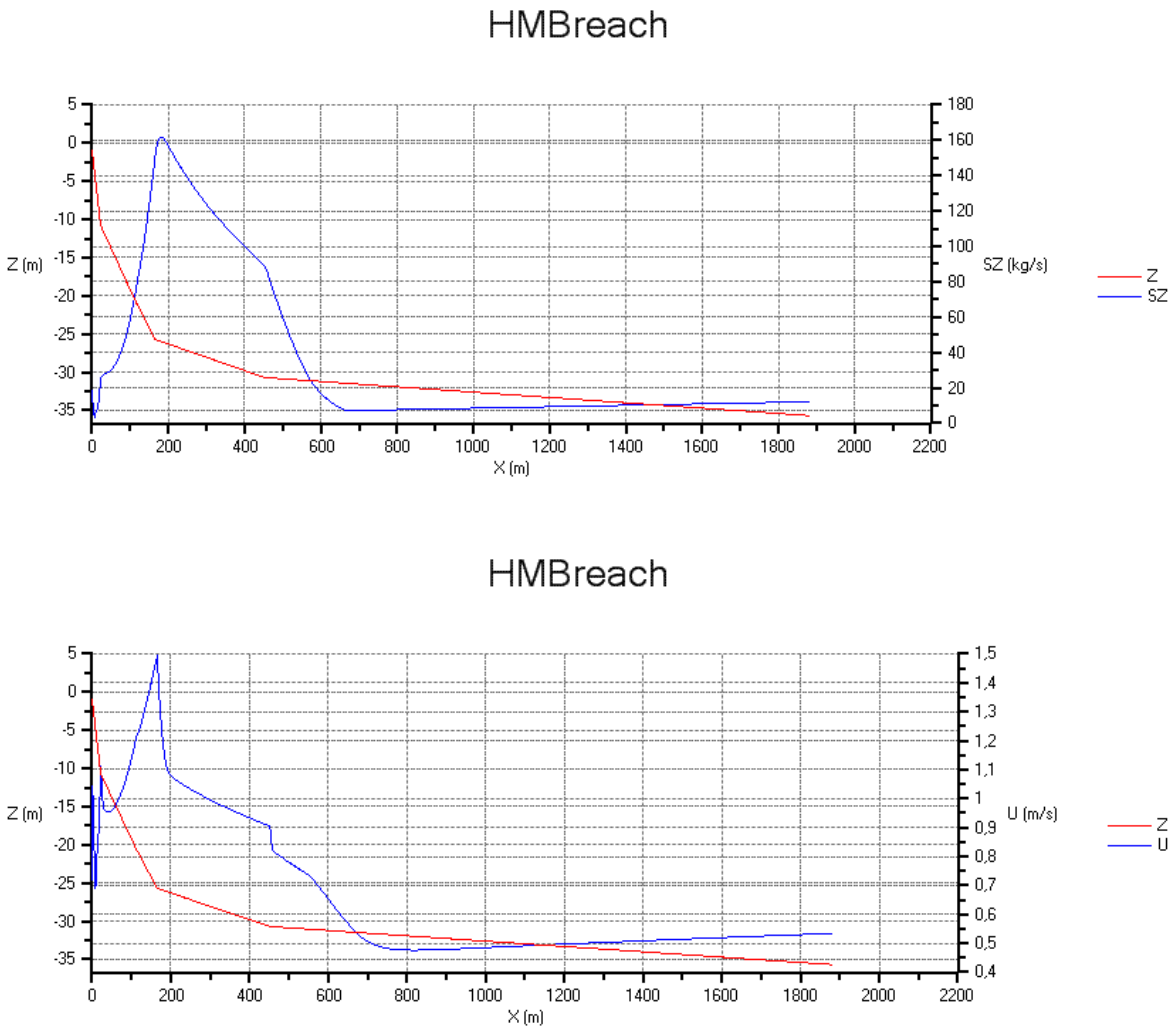

Figure 5.2-8: Sand transport and speed for location 3 and f_0 = 0.075.

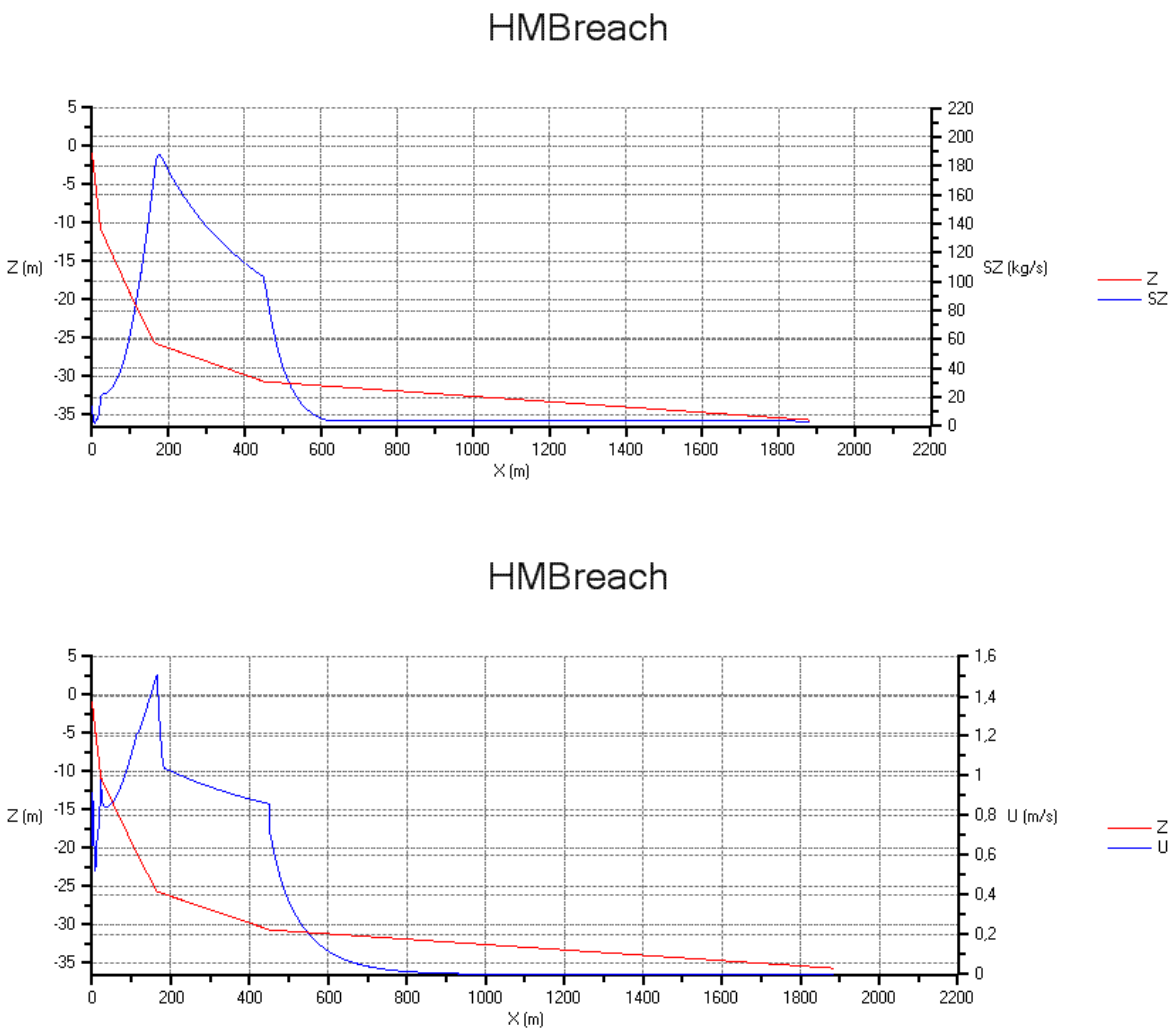

Figure 5.2-9: Sand transport and speed for location 3 and f_0 = 0.1.

5.3 ROGGENPLAAT

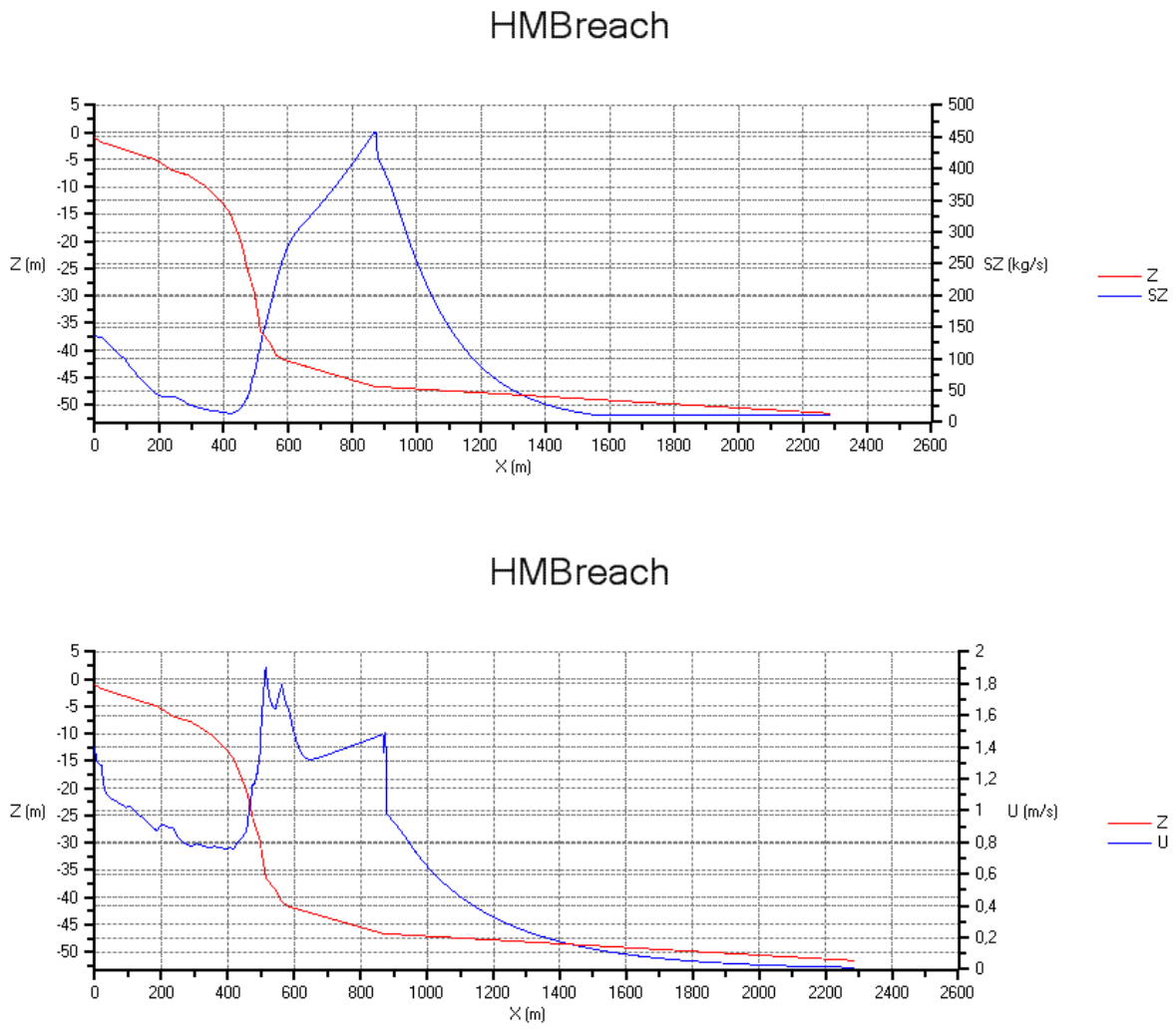

Figure 5.3-1: Sand transport and speed for location 1 and f_0 = 0.05.

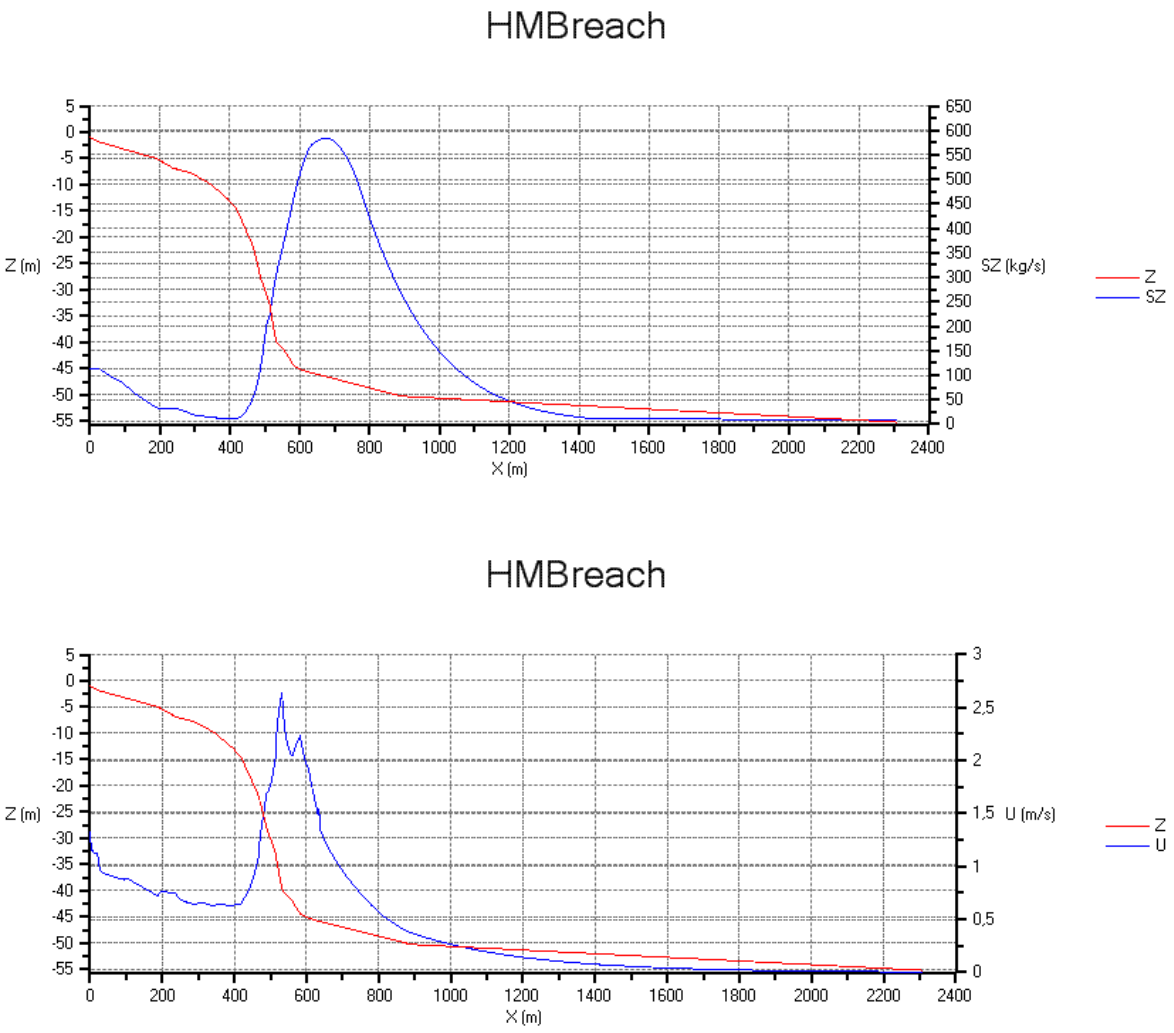

Figure 5.3-2: Sand transport and speed for location 1 and $f_0 = 0.075$.

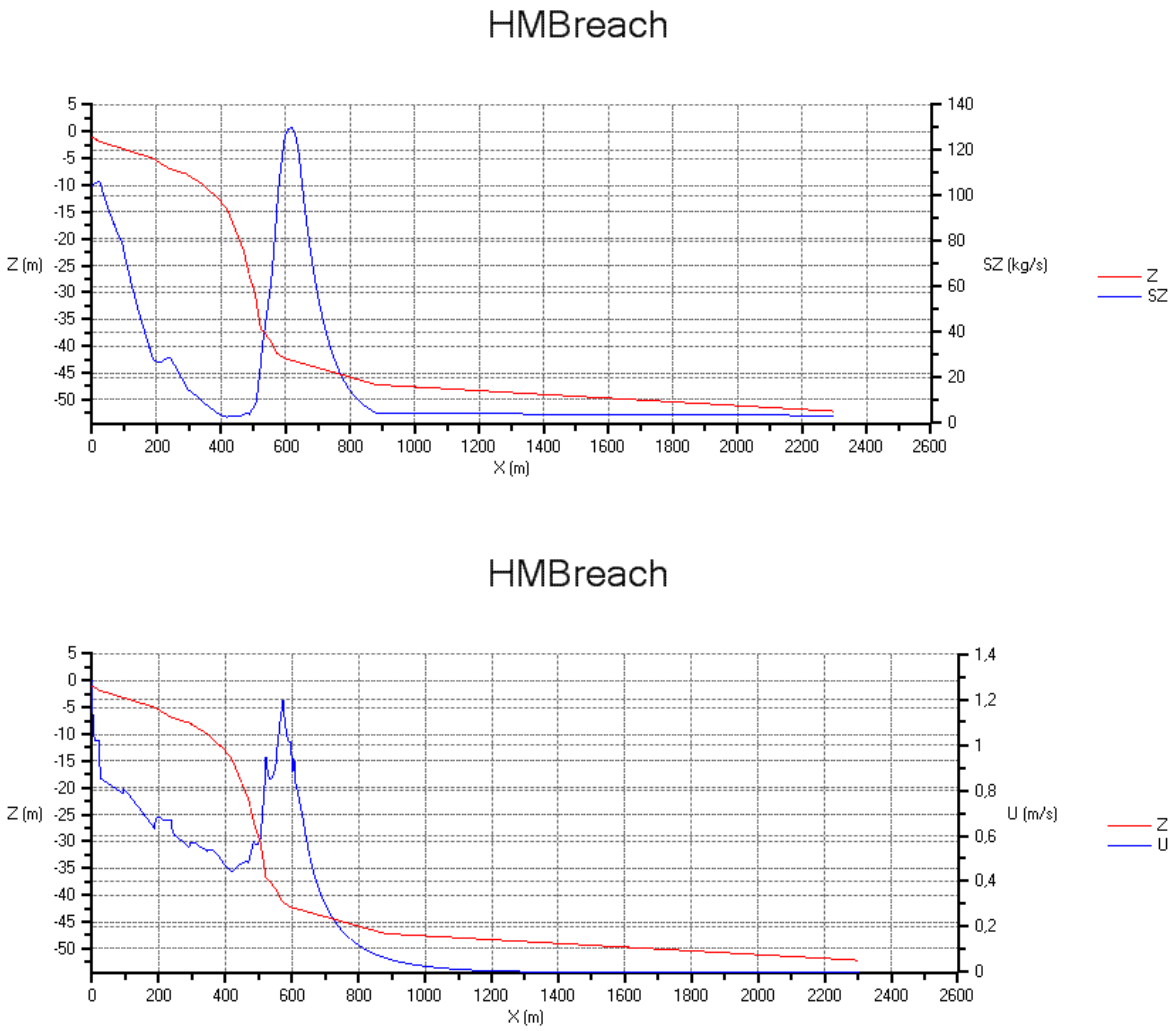

Figure 5.3-3: Sand transport and speed for location 1 and f_0 = 0.1.

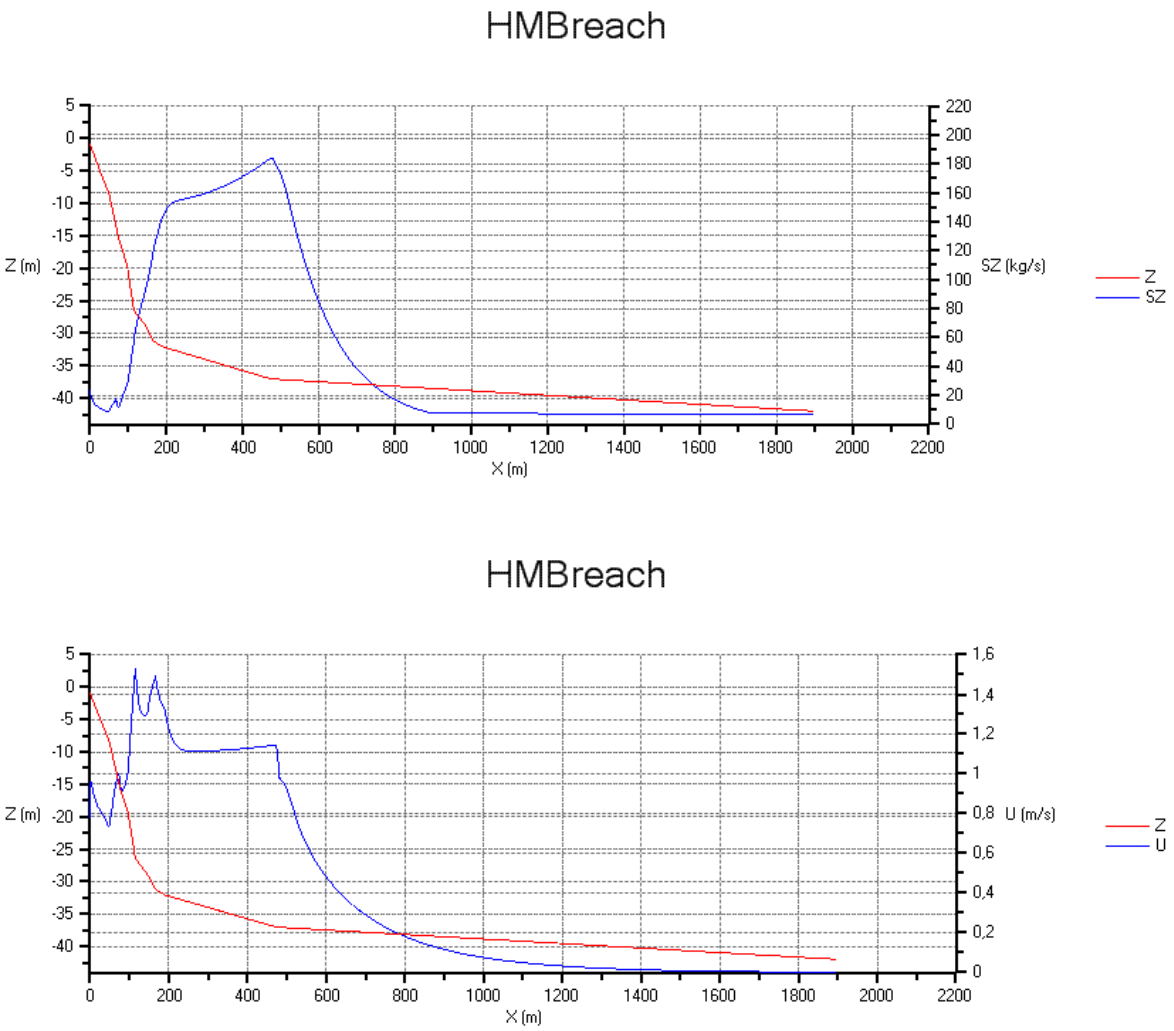

Figure 5.3-4: Sand transport and speed for location 2 and f_0 = 0.05.

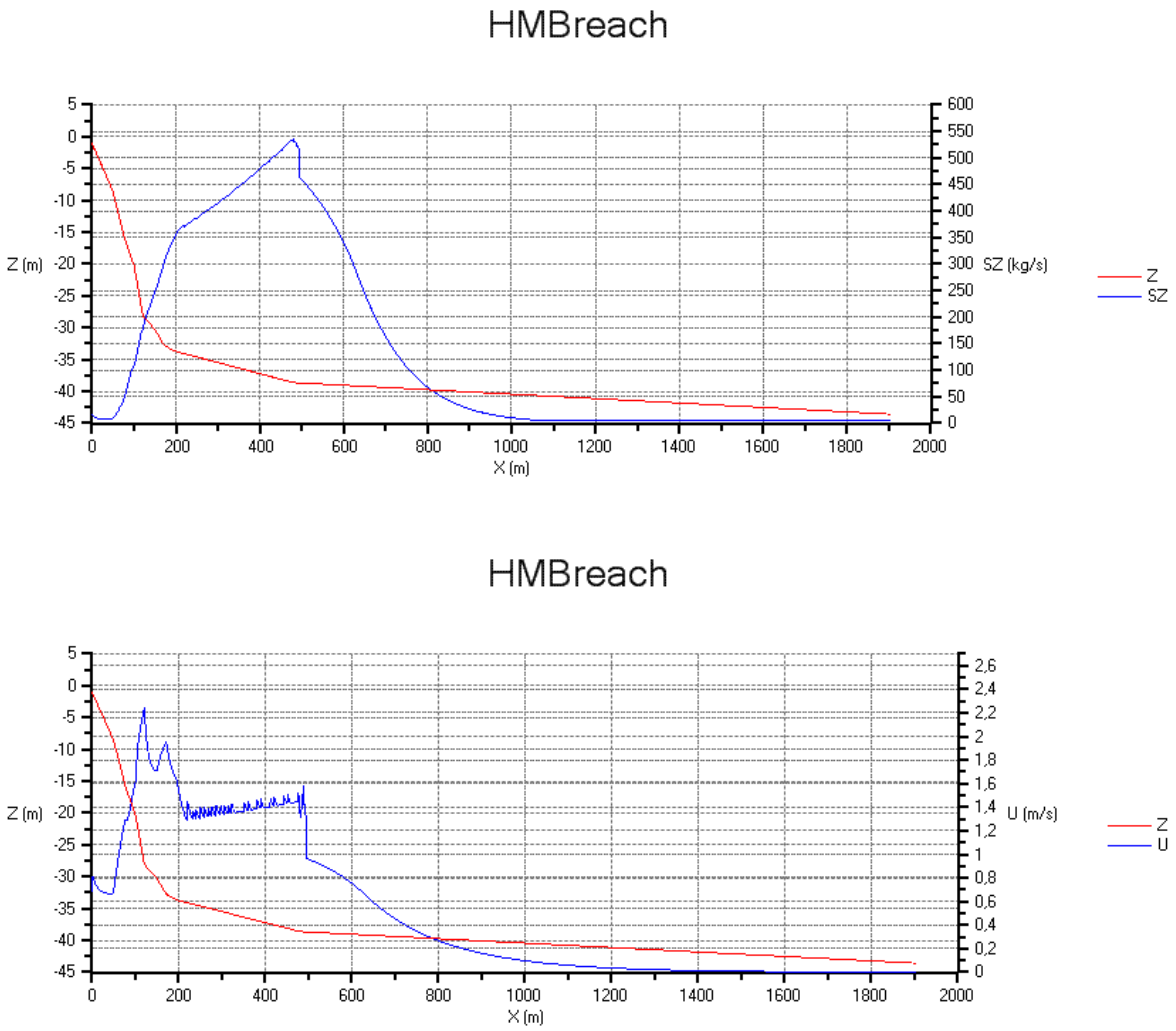

Figure 5.3-5: Sand transport and speed for location 2 and f_0 = 0.075.

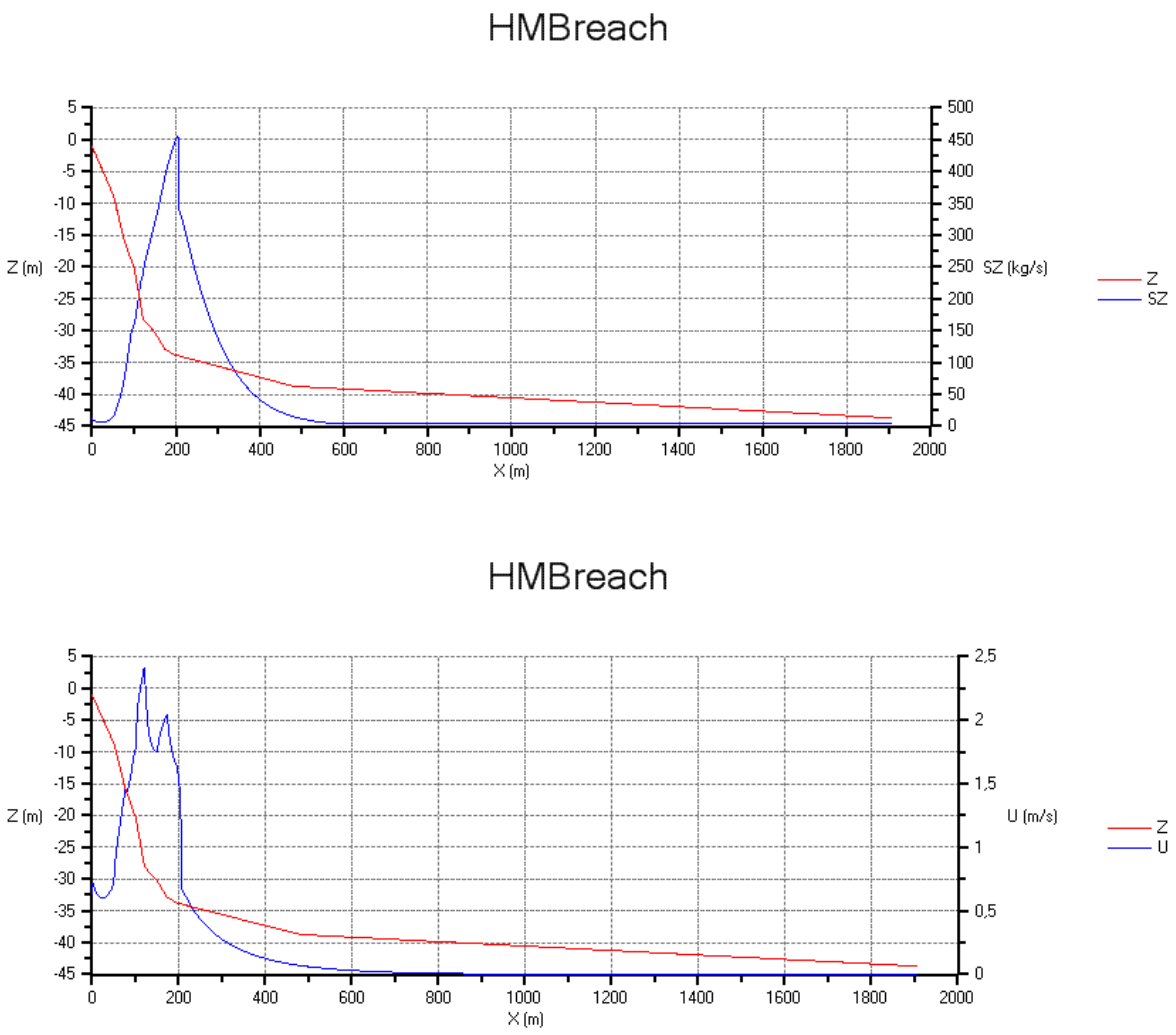

Figure 5.3-6: Sand transport and speed for location 2 and f_0 = 0.1.

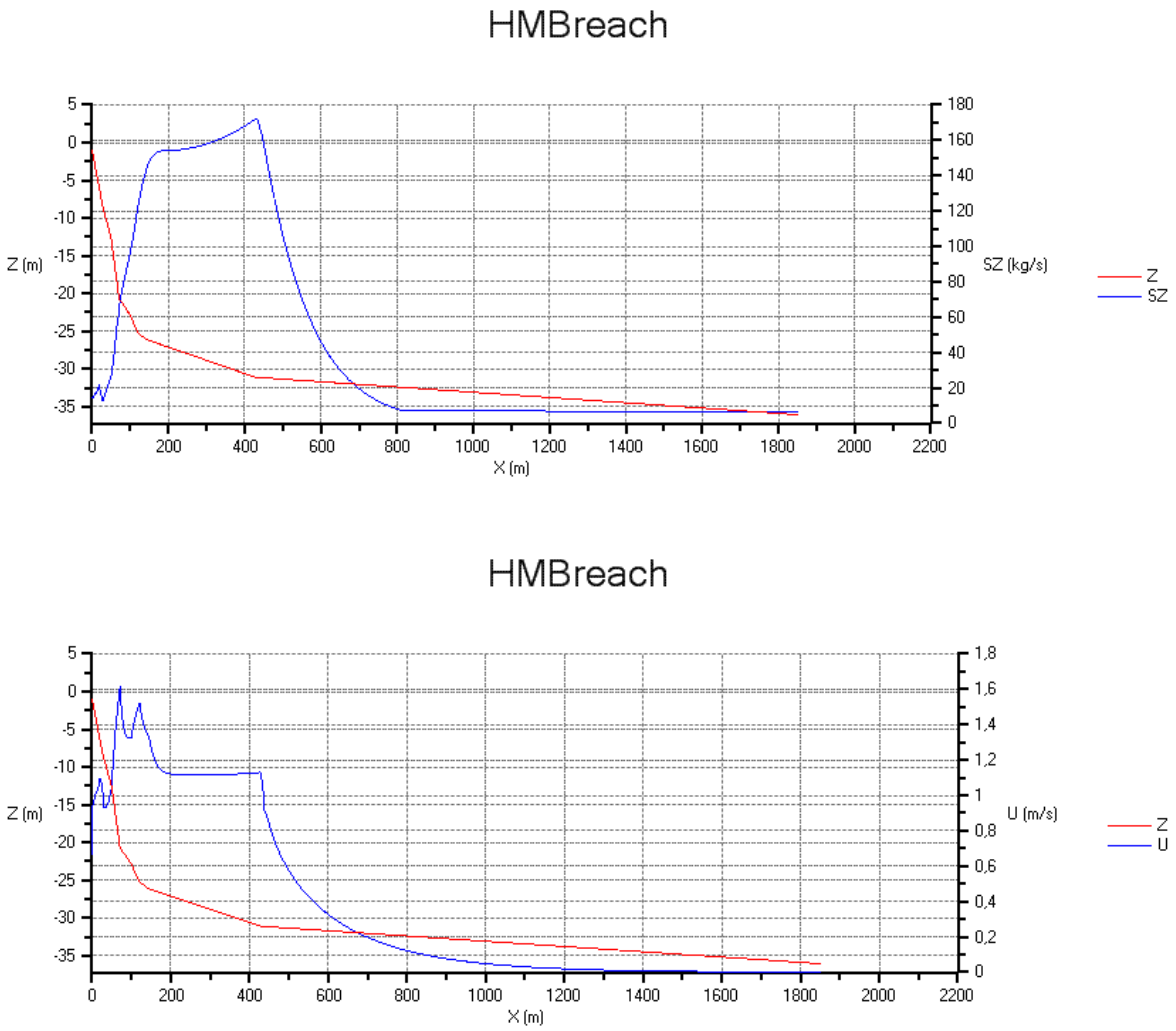

Figure 5.3-7: Sand transport and speed for location 3 and f_0 = 0.05.

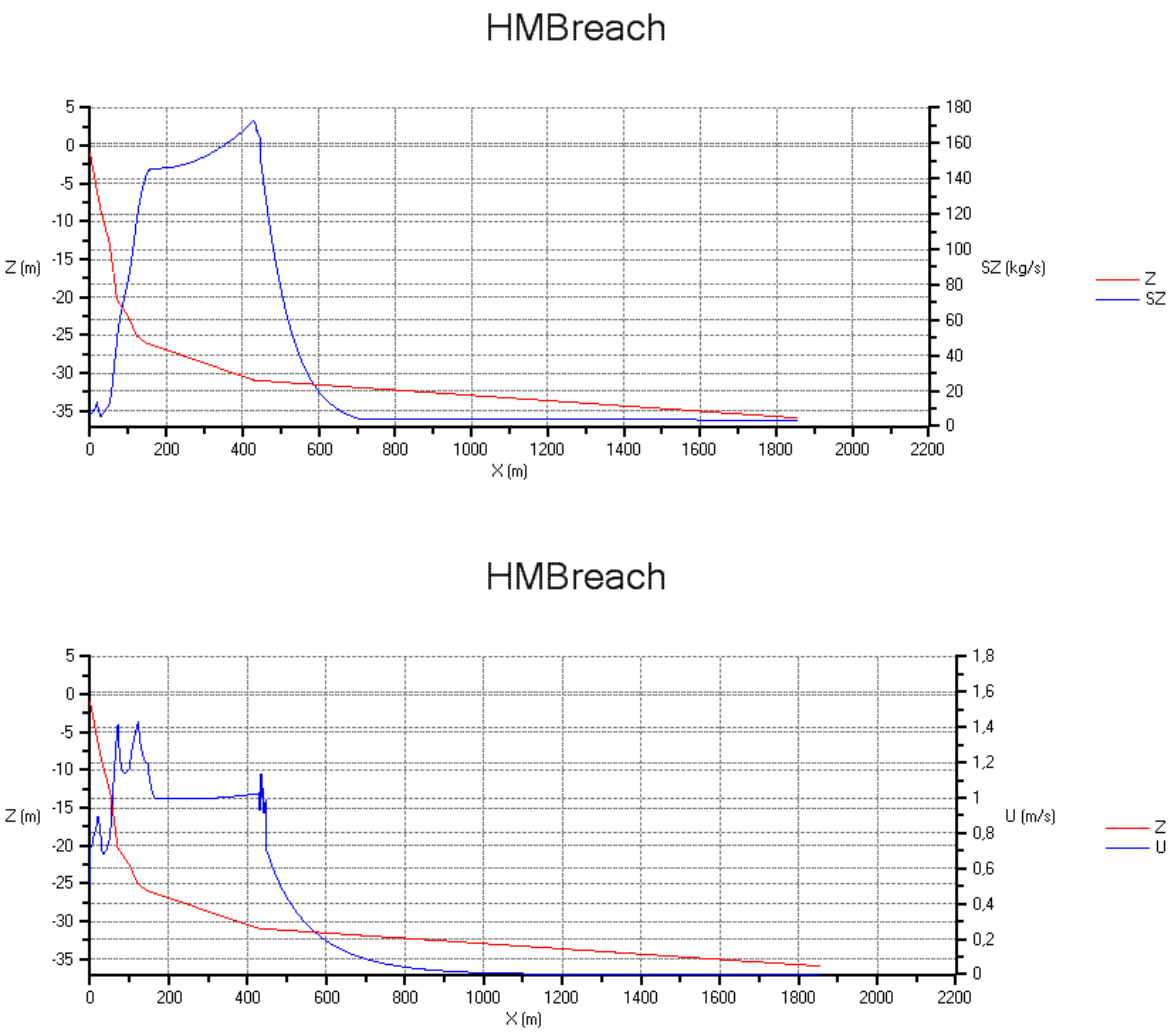

Figure 5.3-8: Sand transport and speed for location 3 and f_0 = 0.075.

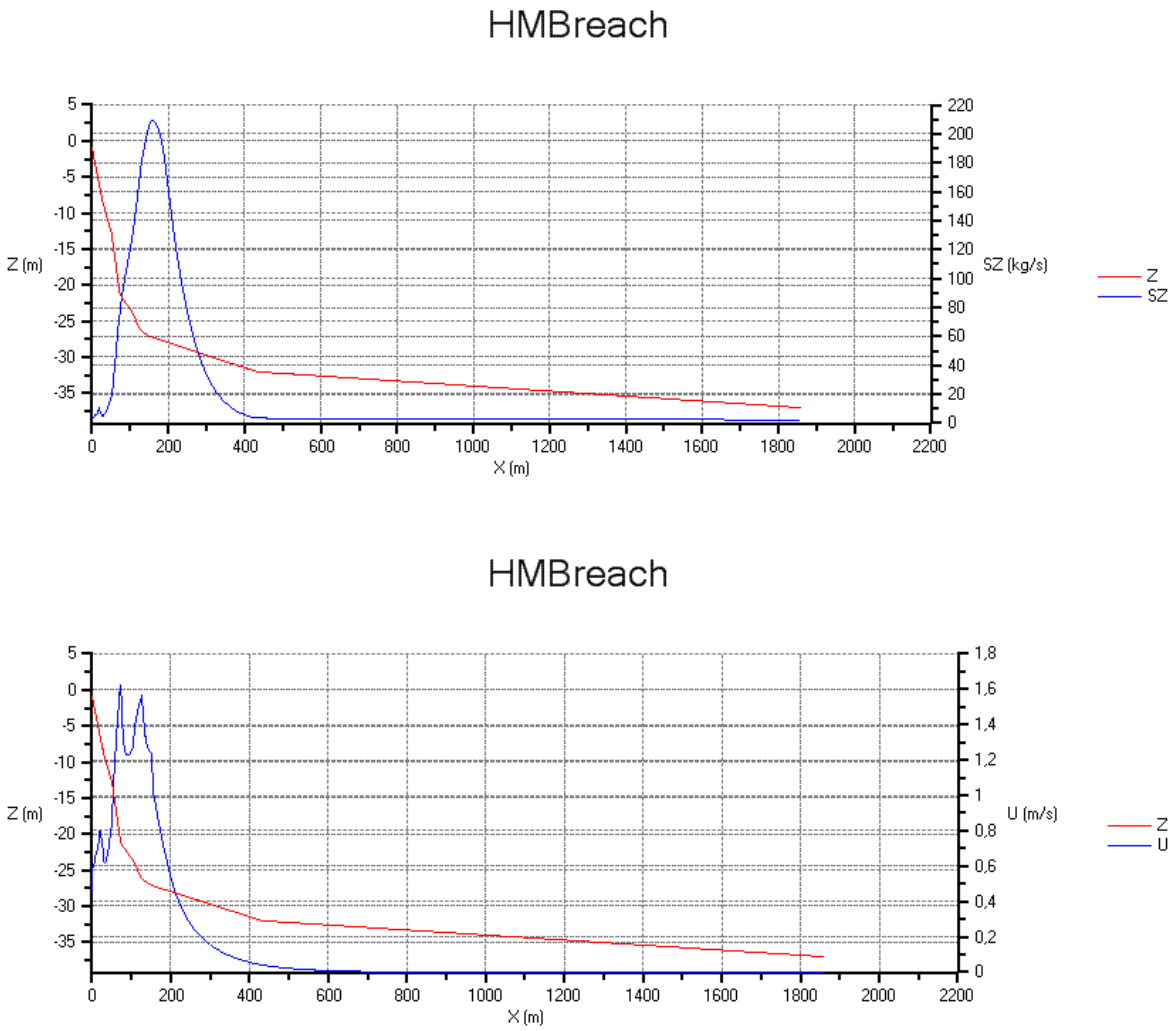

Figure 5.3-9: Sand transport and speed for location 3 and f_0 = 0.1.

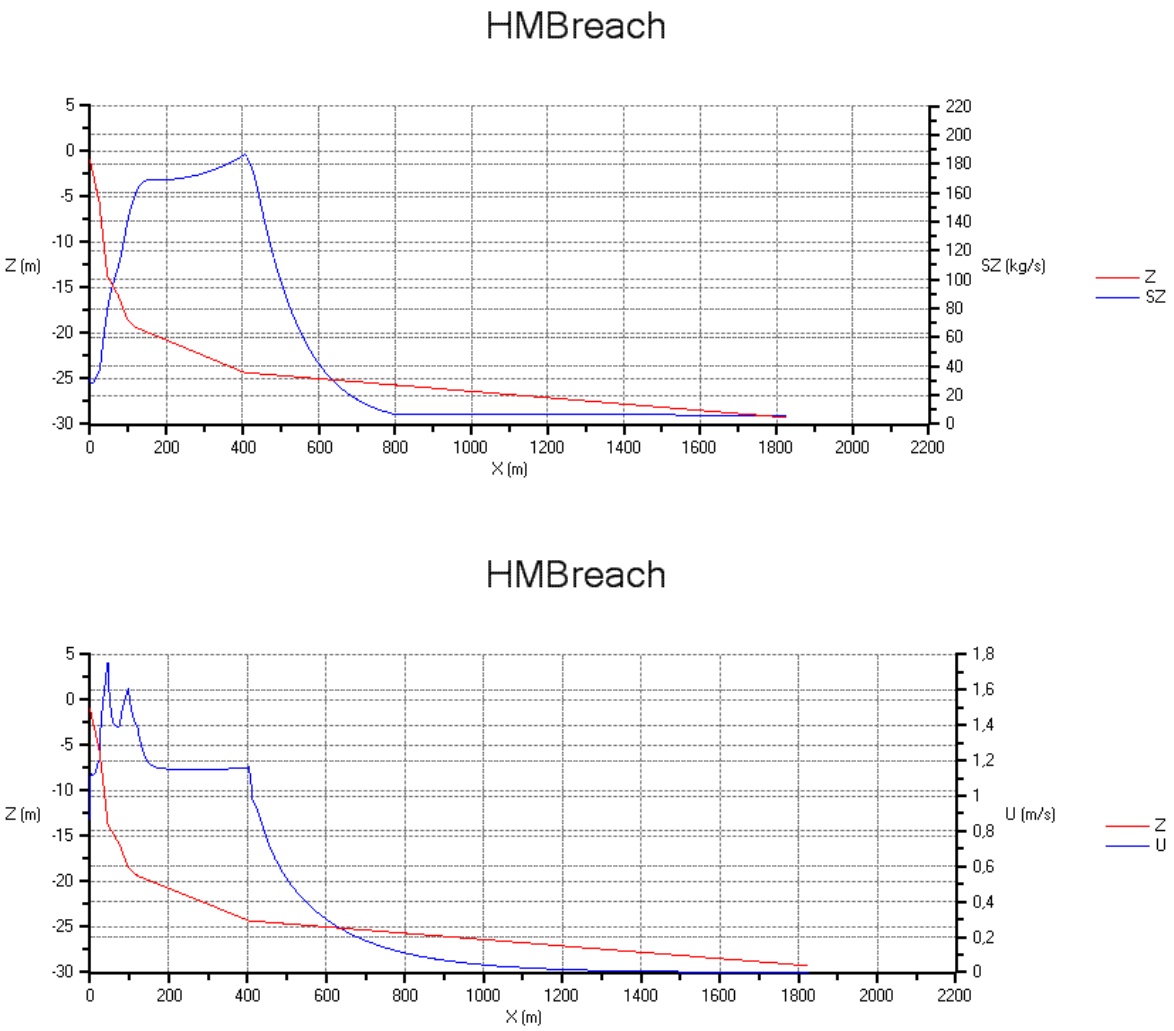

Figure 5.3-10: Sand transport and speed for location 4 and f_0 = 0.05.

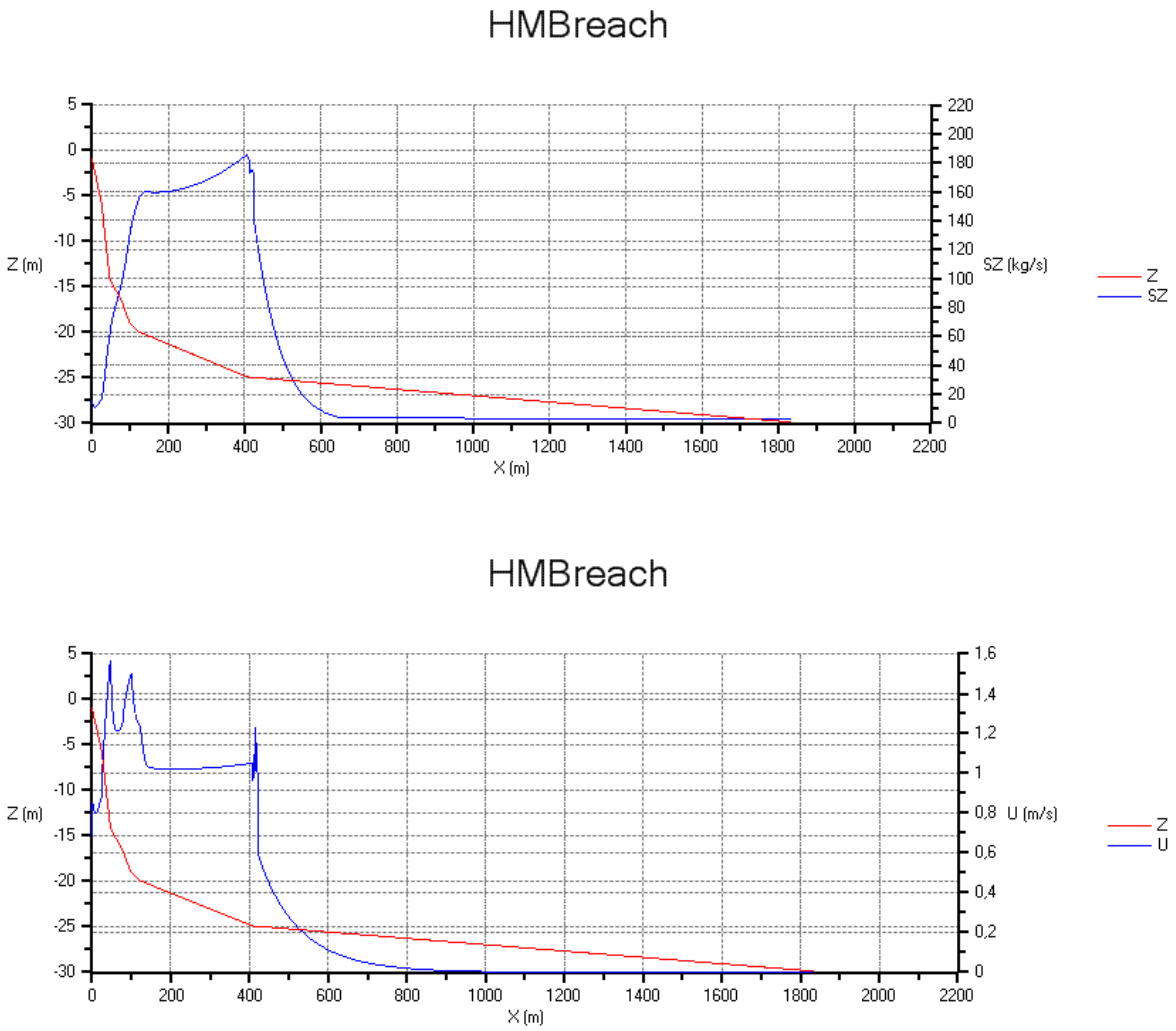

Figure 5.3-11: Sand transport and speed for location 4 and f_0 = 0.075.

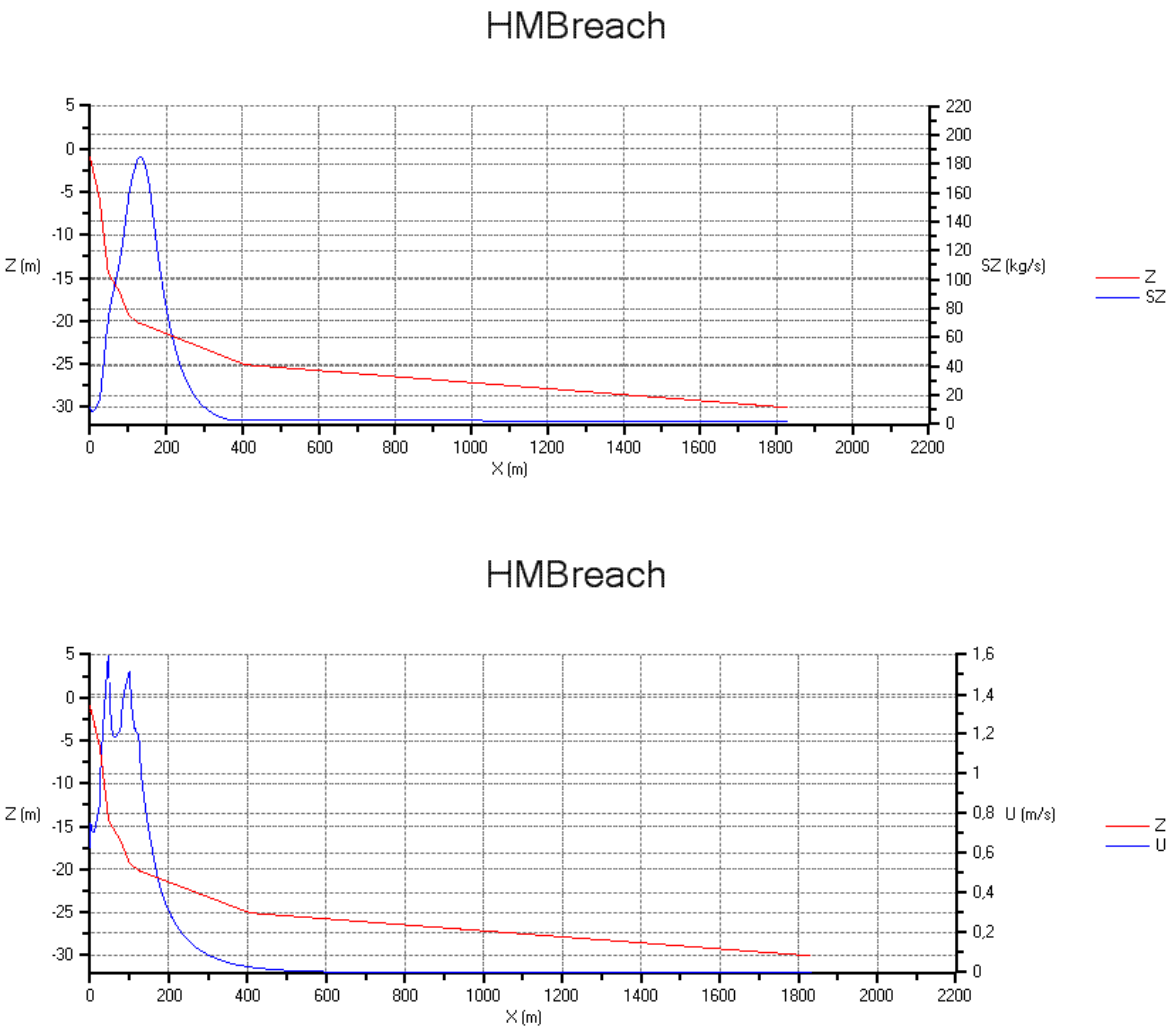

Figure 5.3-12: Sand transport and speed for location 4 and f_0 = 0.1.

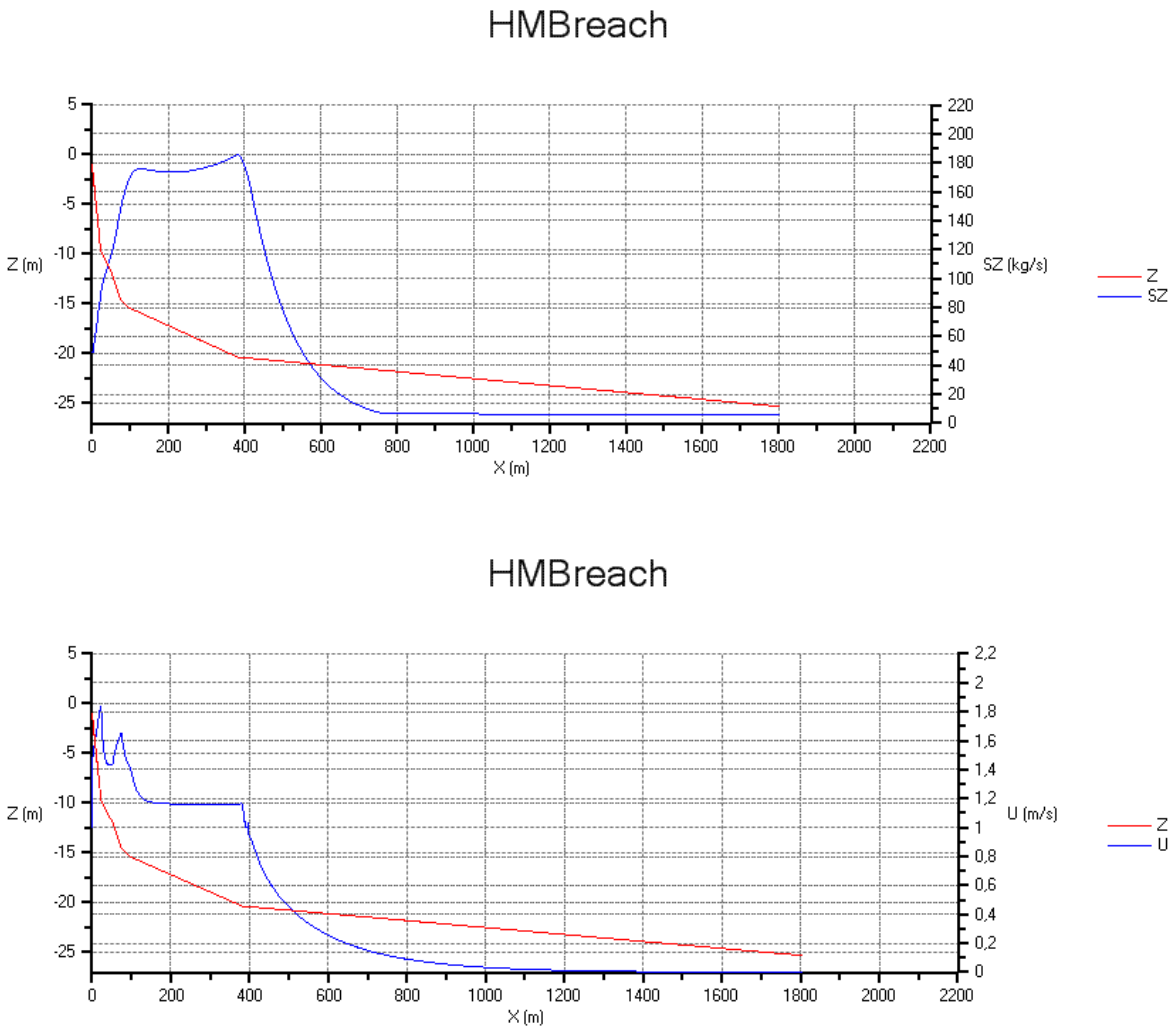

Figure 5.3-13: Sand transport and speed for location 5 and f_0 = 0.05.

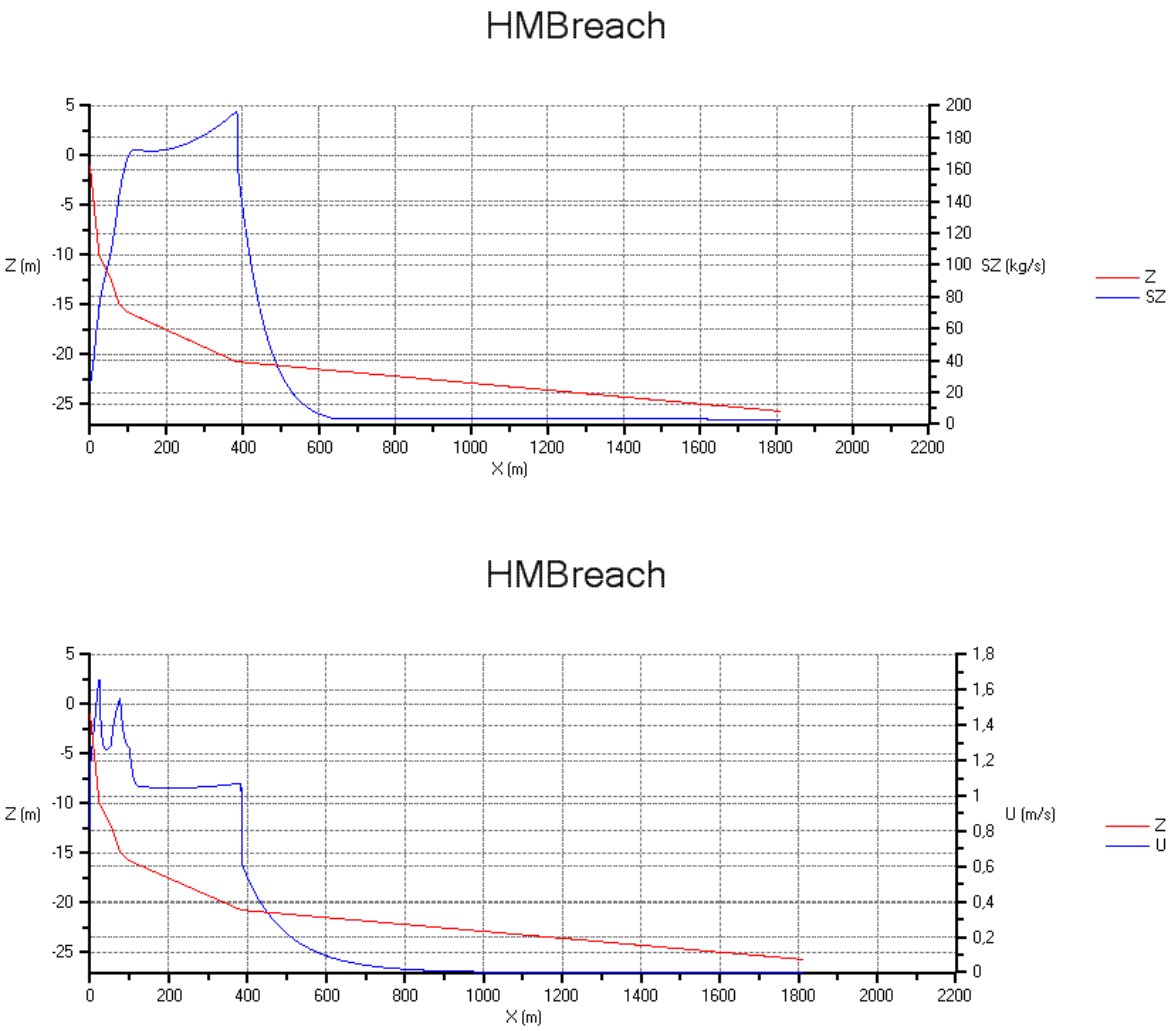

Figure 5.3-14: Sand transport and speed for location 5 and f_0 = 0.075.

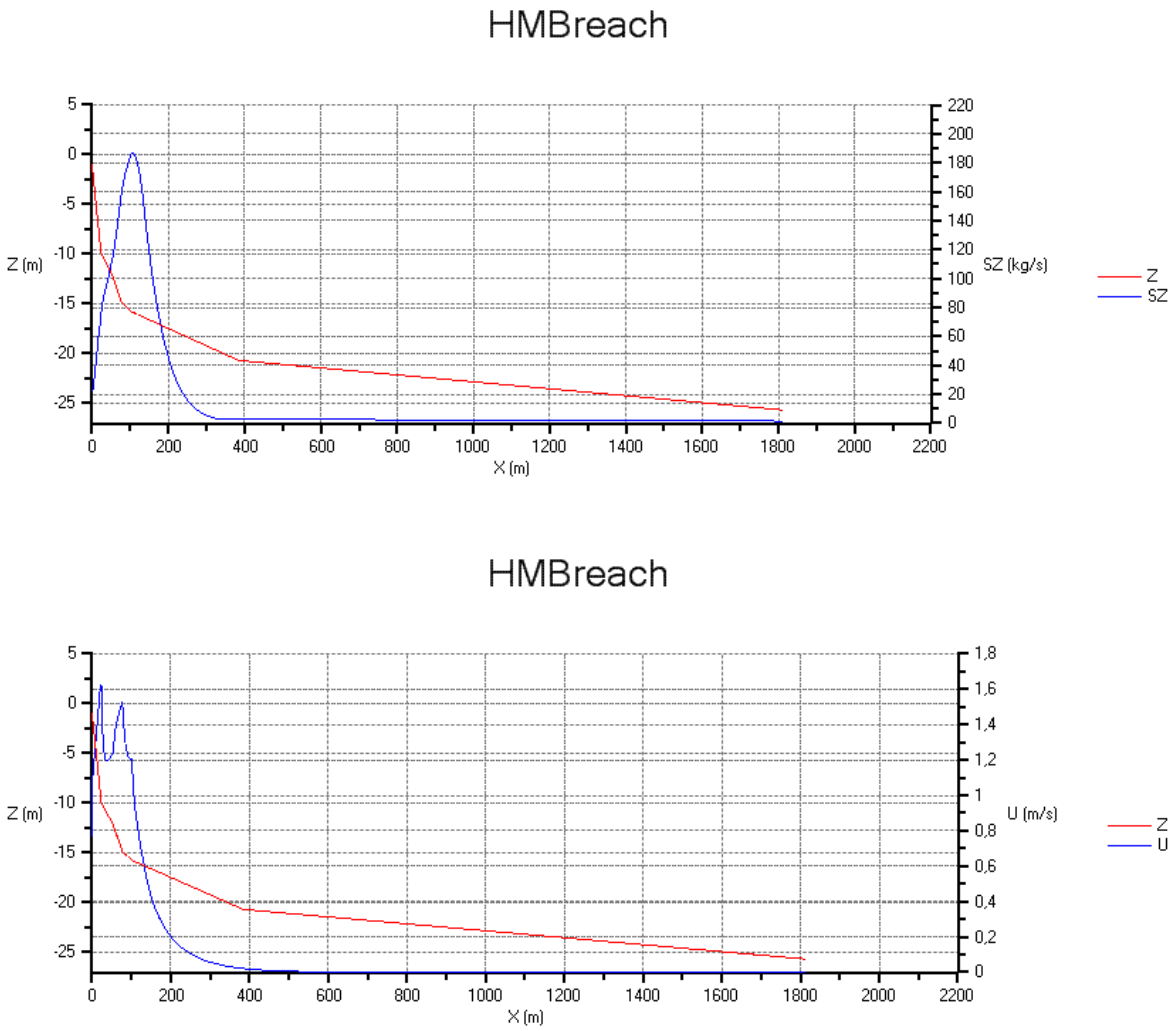

Figure 5.3-15: Sand transport and speed for location 5 and f_0 = 0.1.

5.4 PLAAT VAN OUDE TONGE

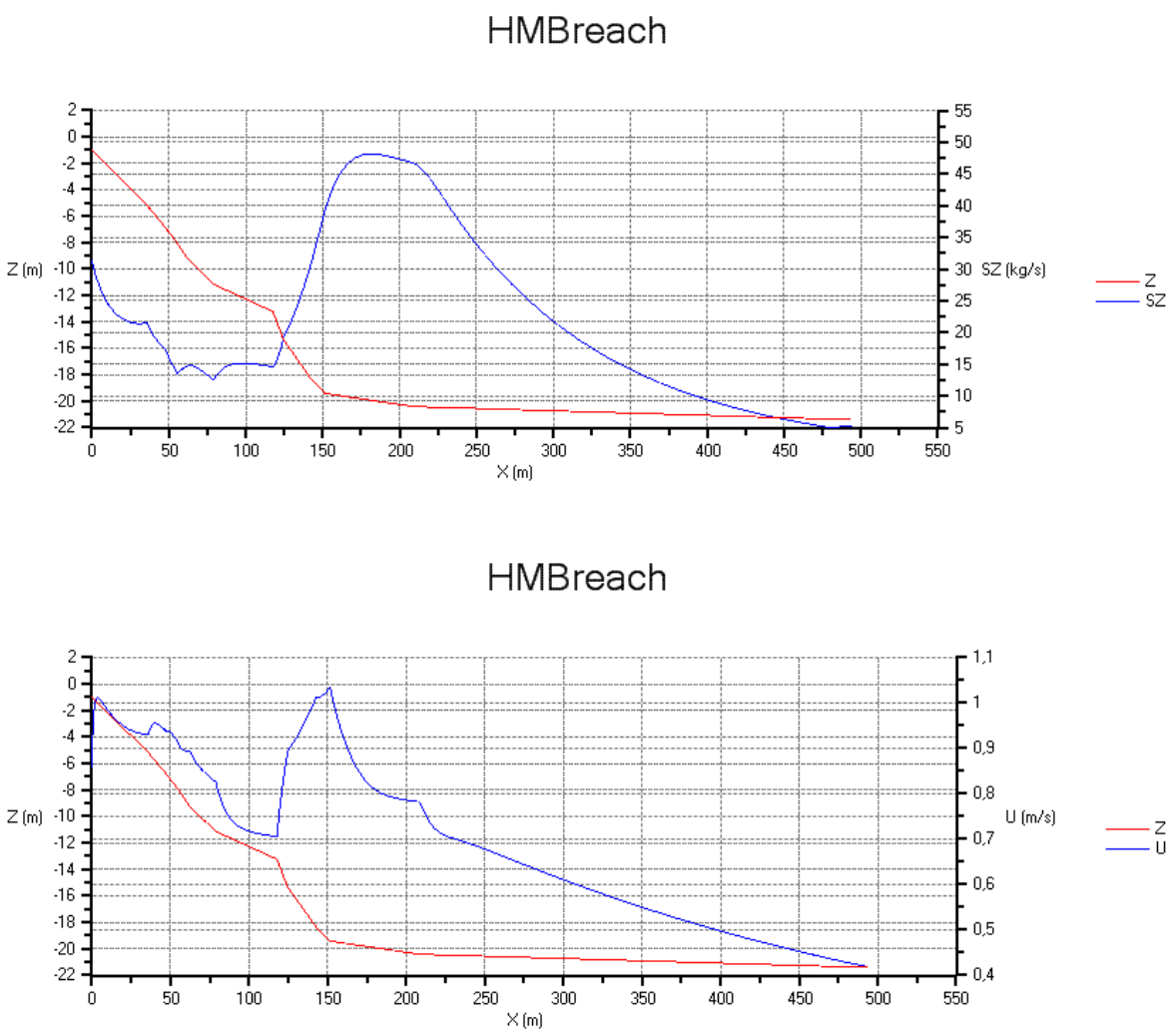

Figure 5.4-1: Sand transport and speed for location 1 and f_0 = 0.05.

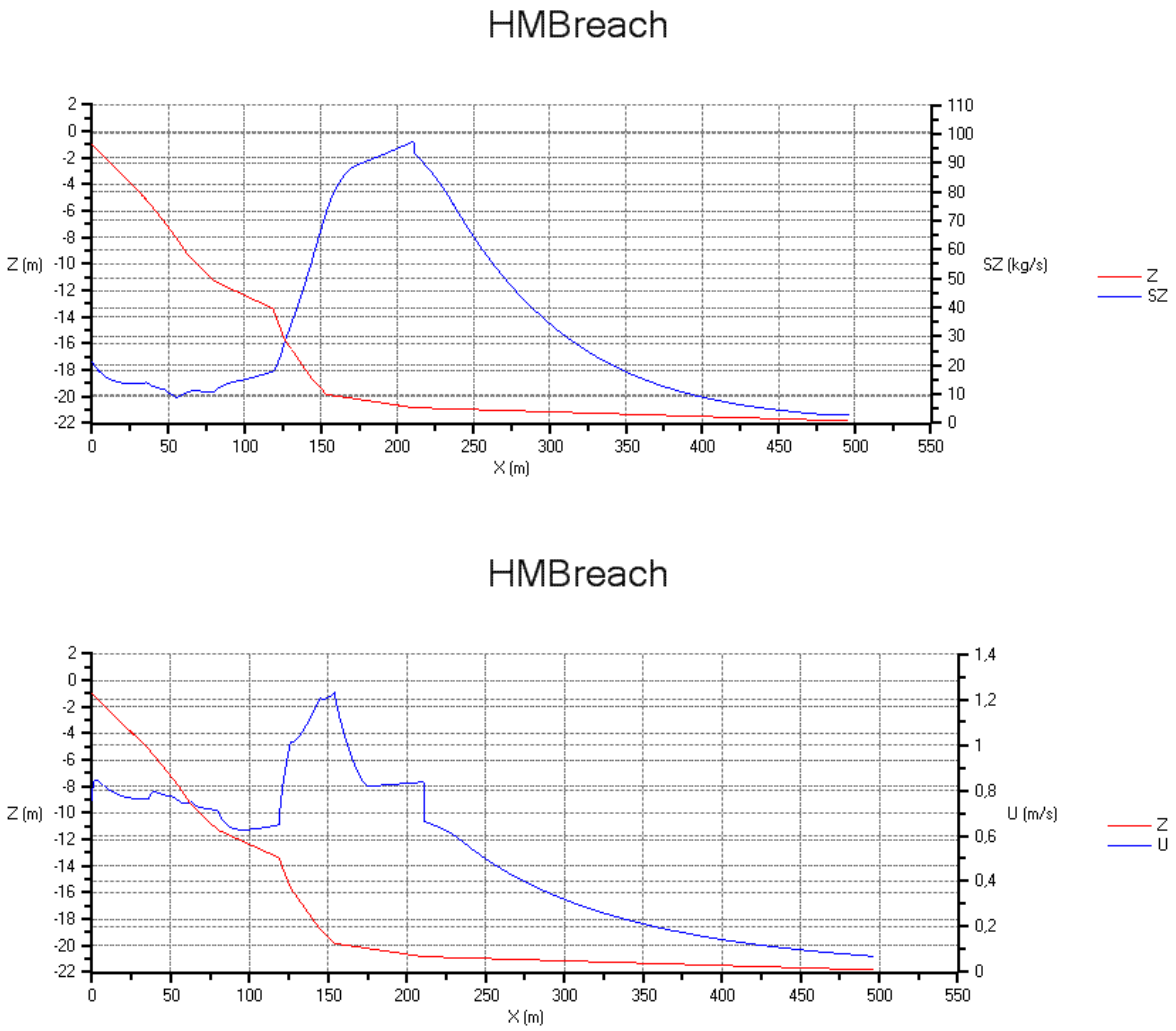

Figure 5.4-2: Sand transport and speed for location 1 and f_0 = 0.075.

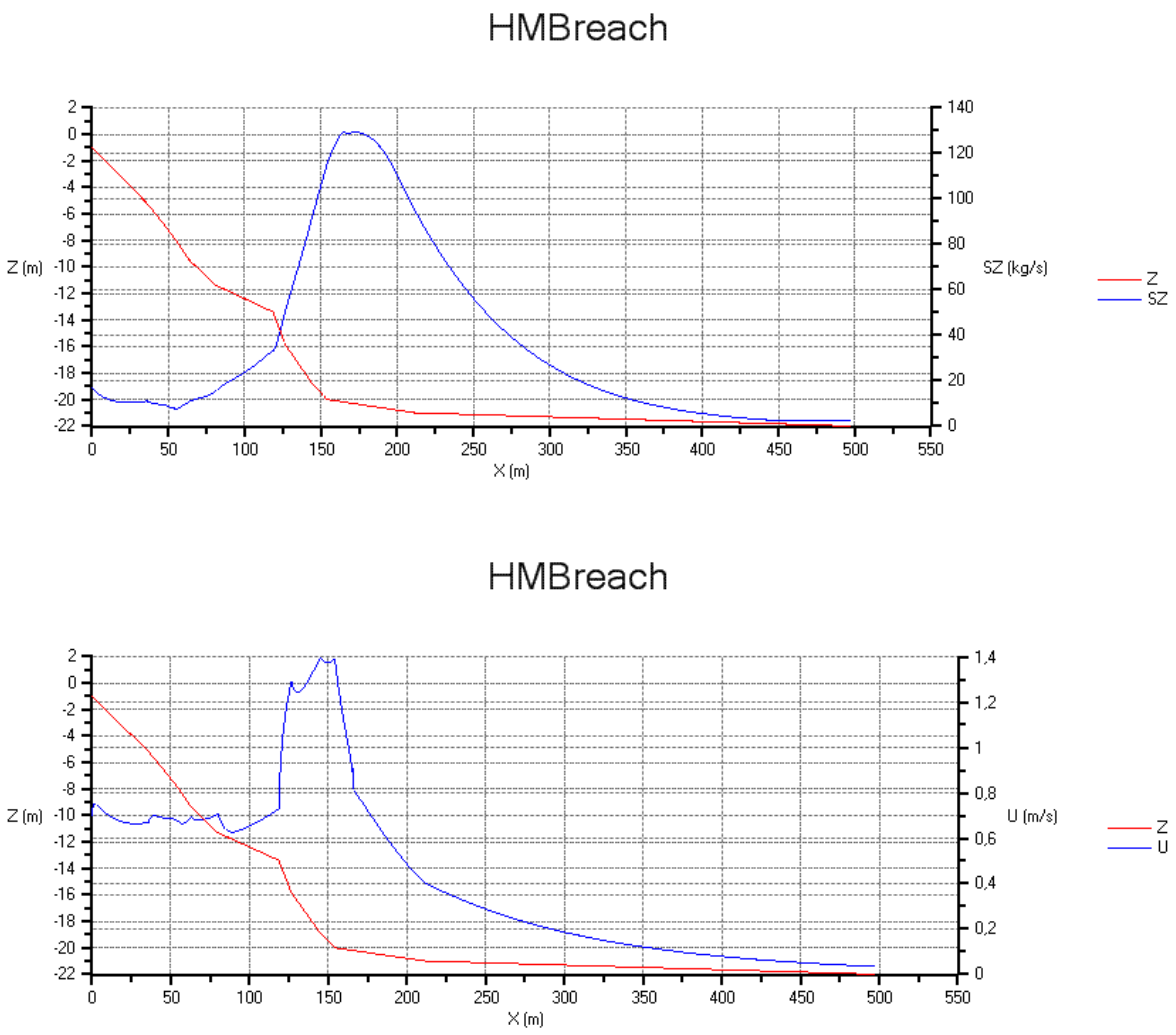

Figure 5.4-3: Sand transport and speed for location 1 and f_0 = 0.1.

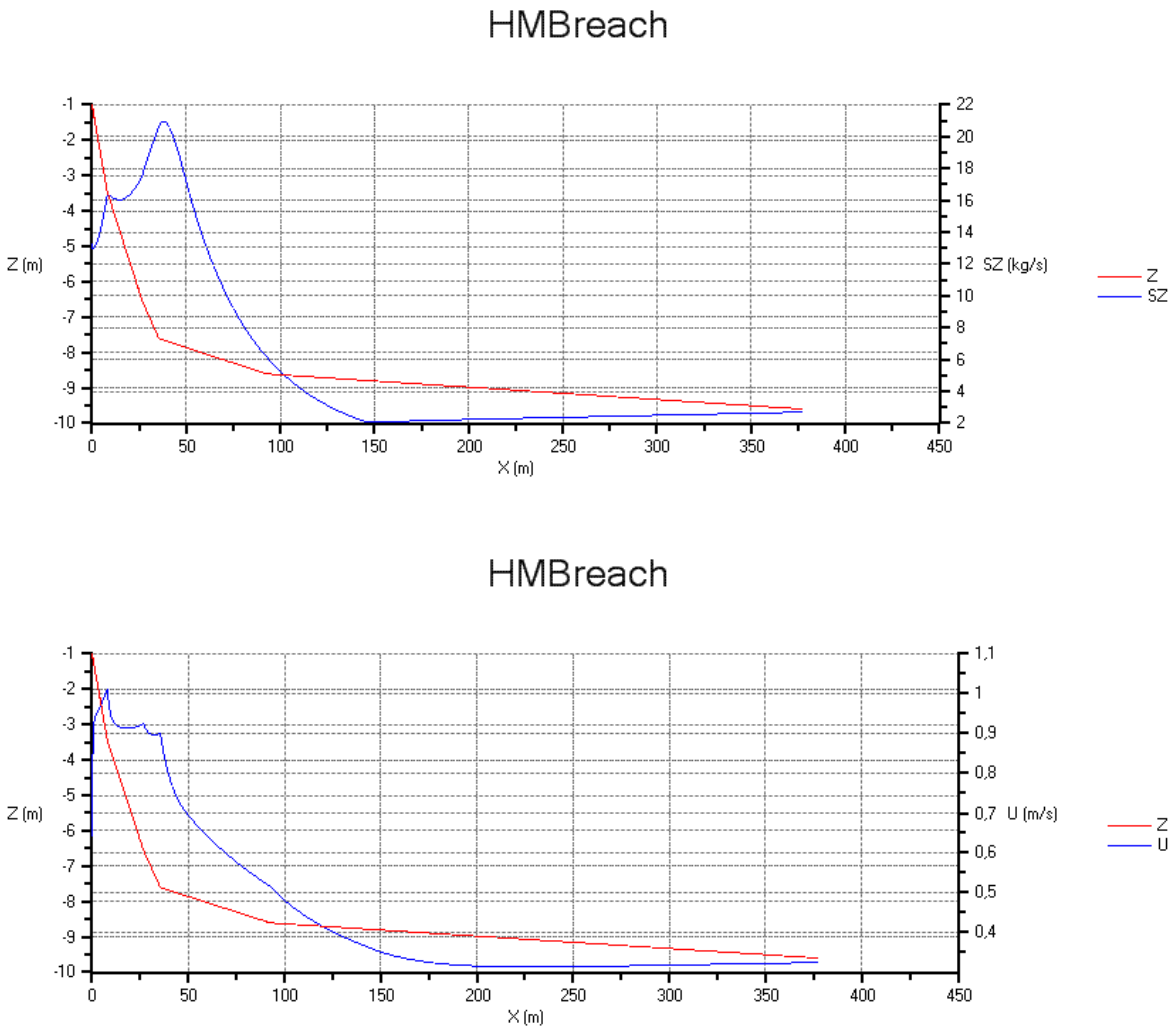

Figure 5.4-4: Sand transport and speed for location 2 and f_0 = 0.05.

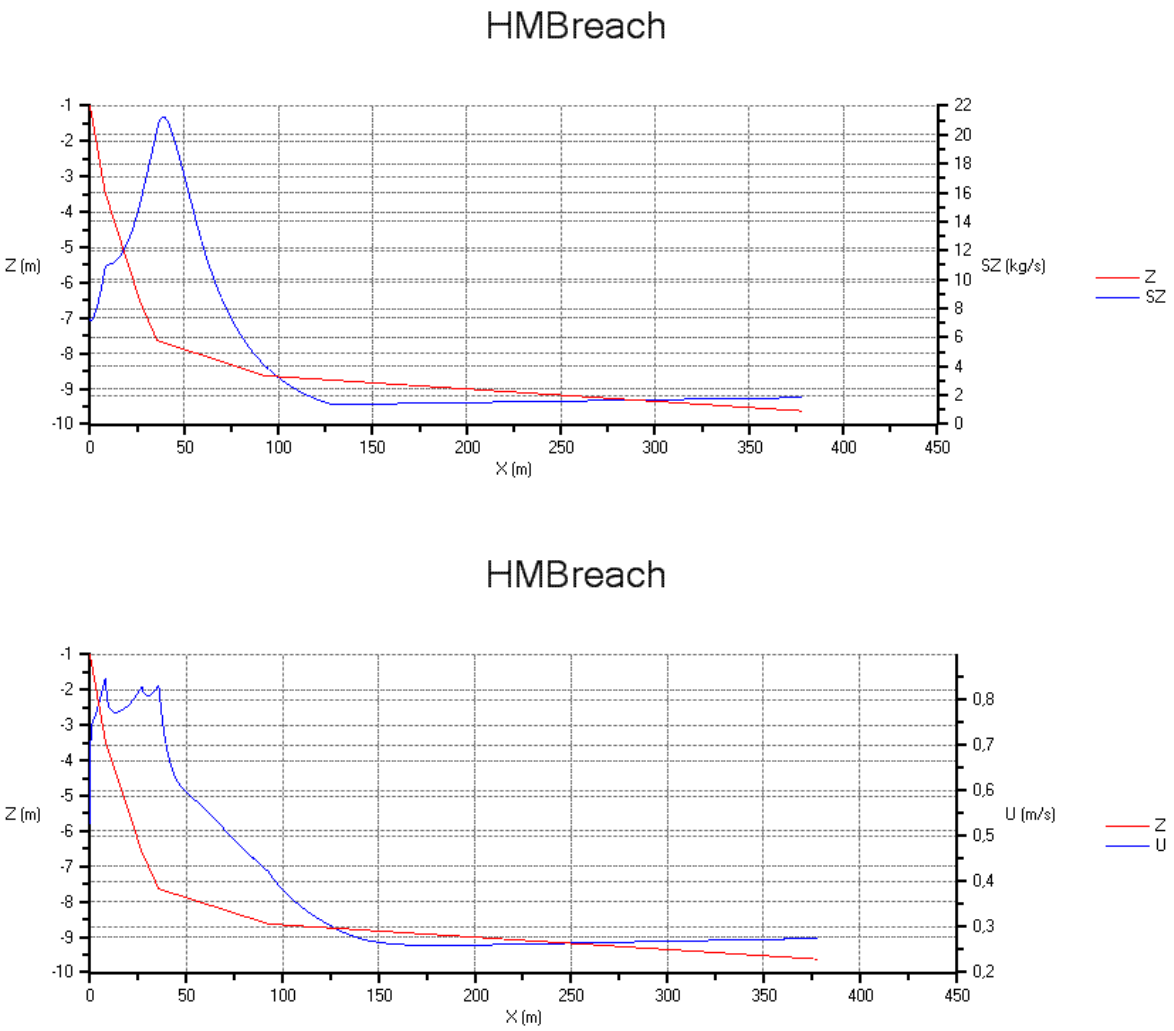

Figure 5.4-5: Sand transport and speed for location 2 and f_0 = 0.075.

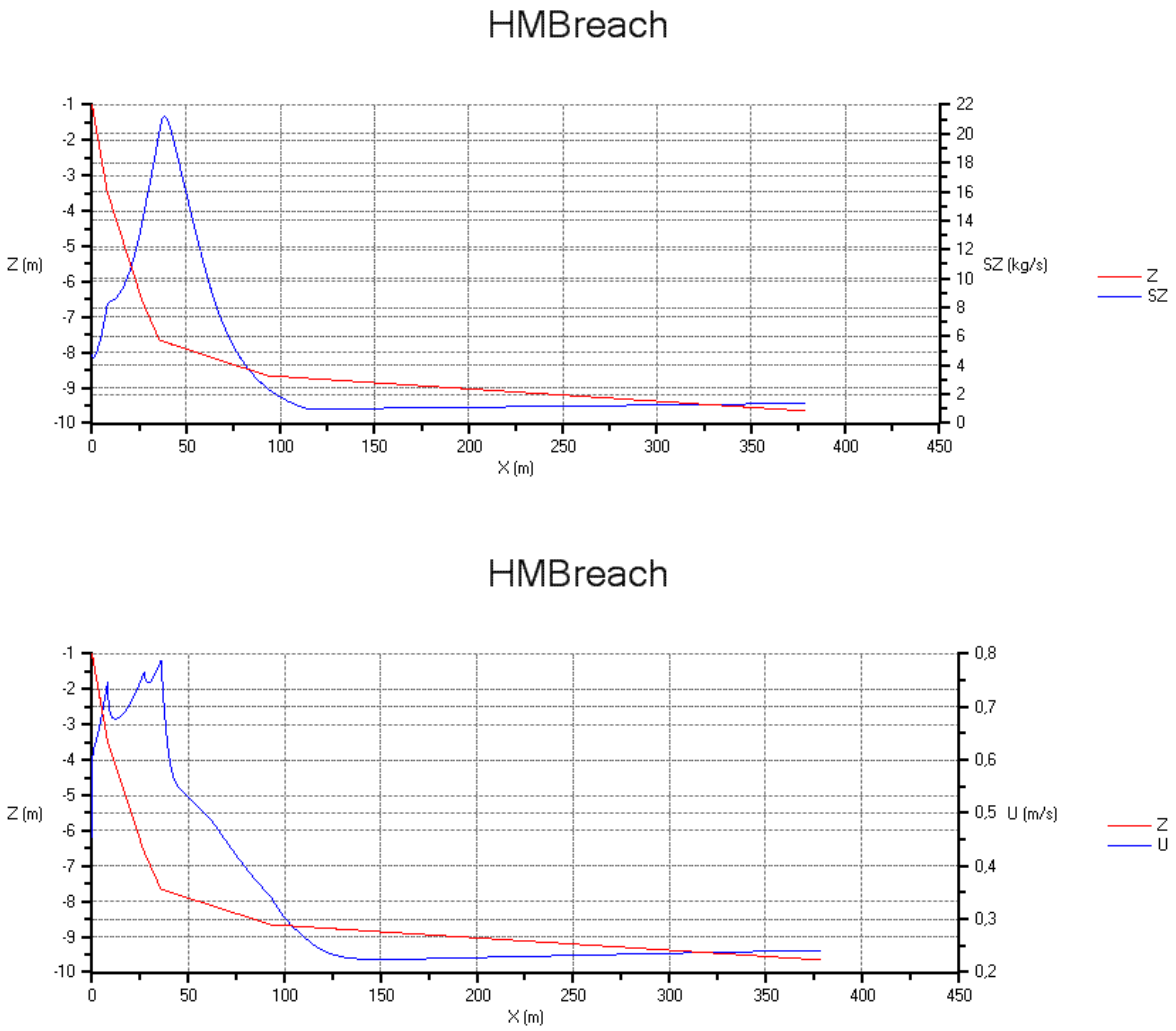

Figure 5.4-6: Sand transport and speed for location 2 and f_0 = 0.1.

5.5 SPIJKERPLAAT

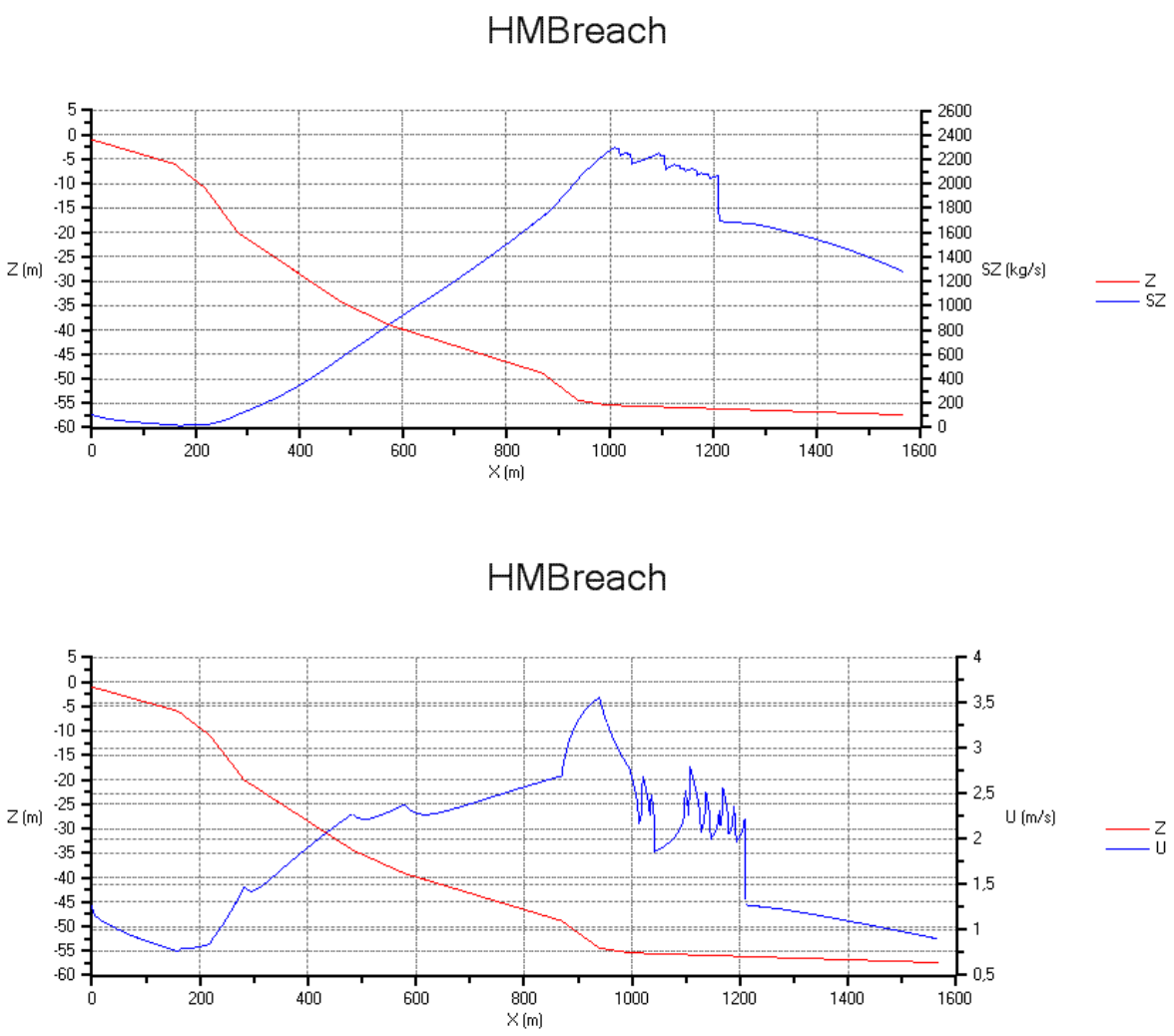

Figure 5.5-1: Sand transport and speed for location 1 and f_0 = 0.05.

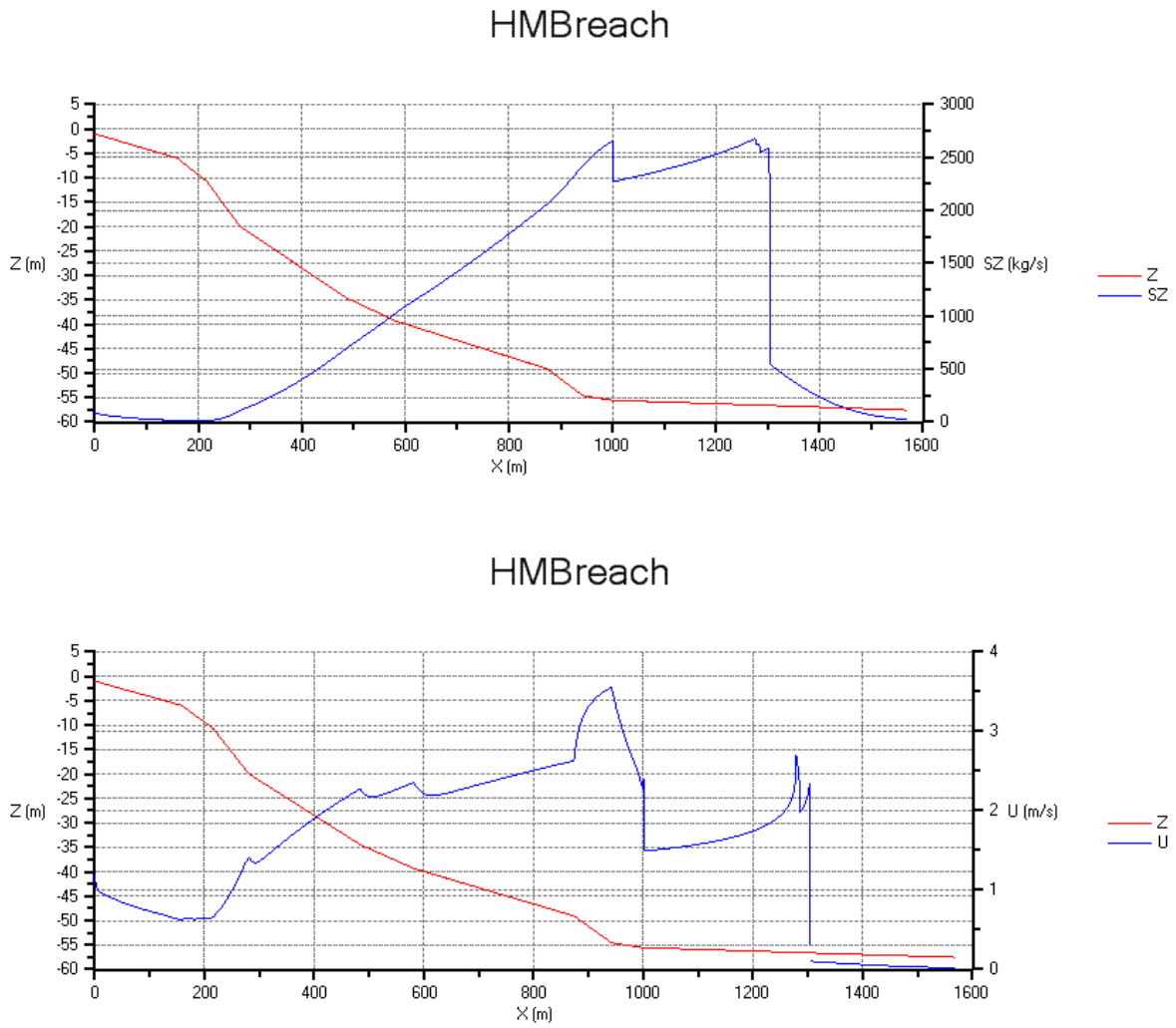

Figure 5.5-2: Sand transport and speed for location 1 and f_0 = 0.075.

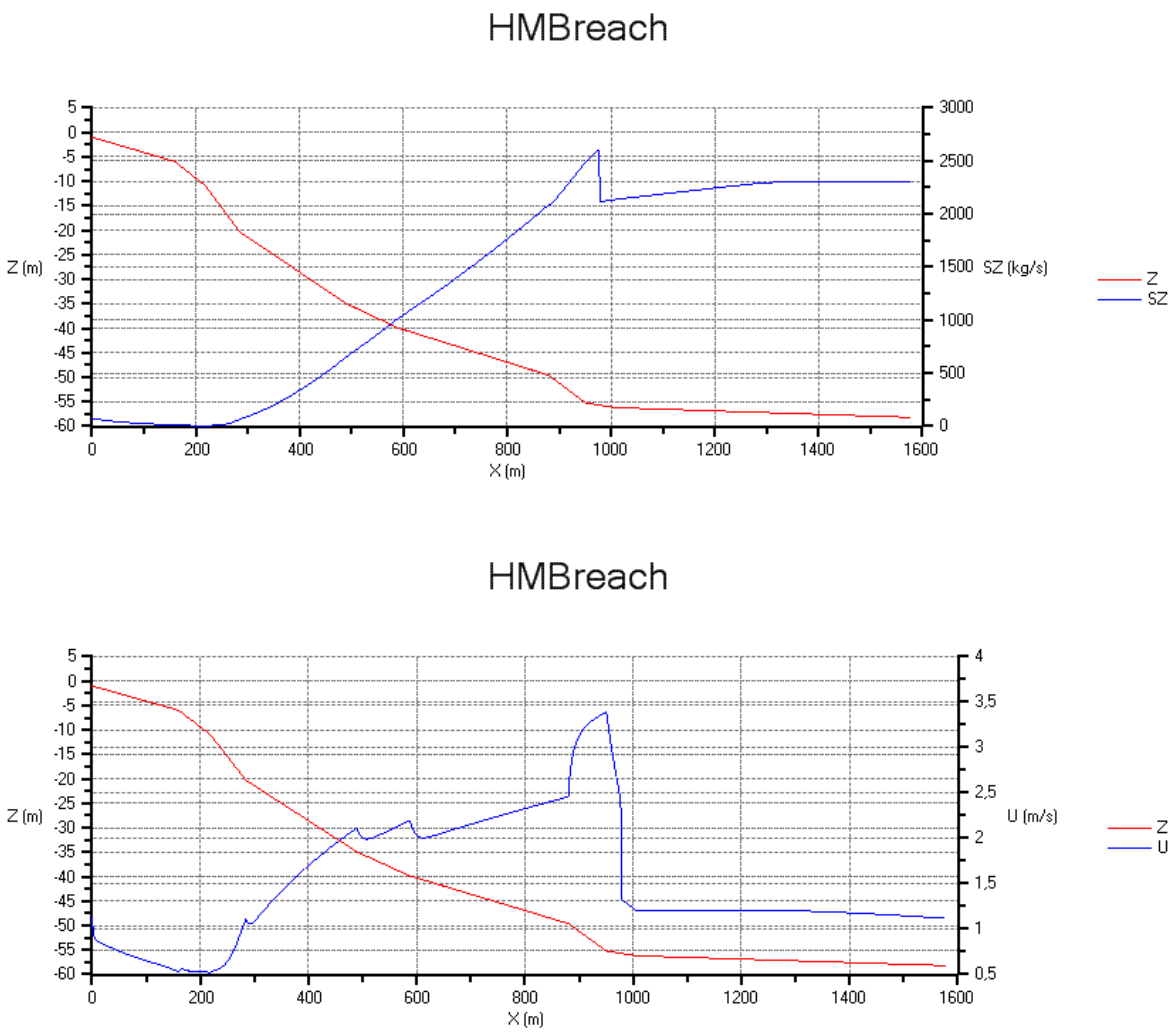

Figure 5.5-3: Sand transport and speed for location 1 and f_0 = 0.1.

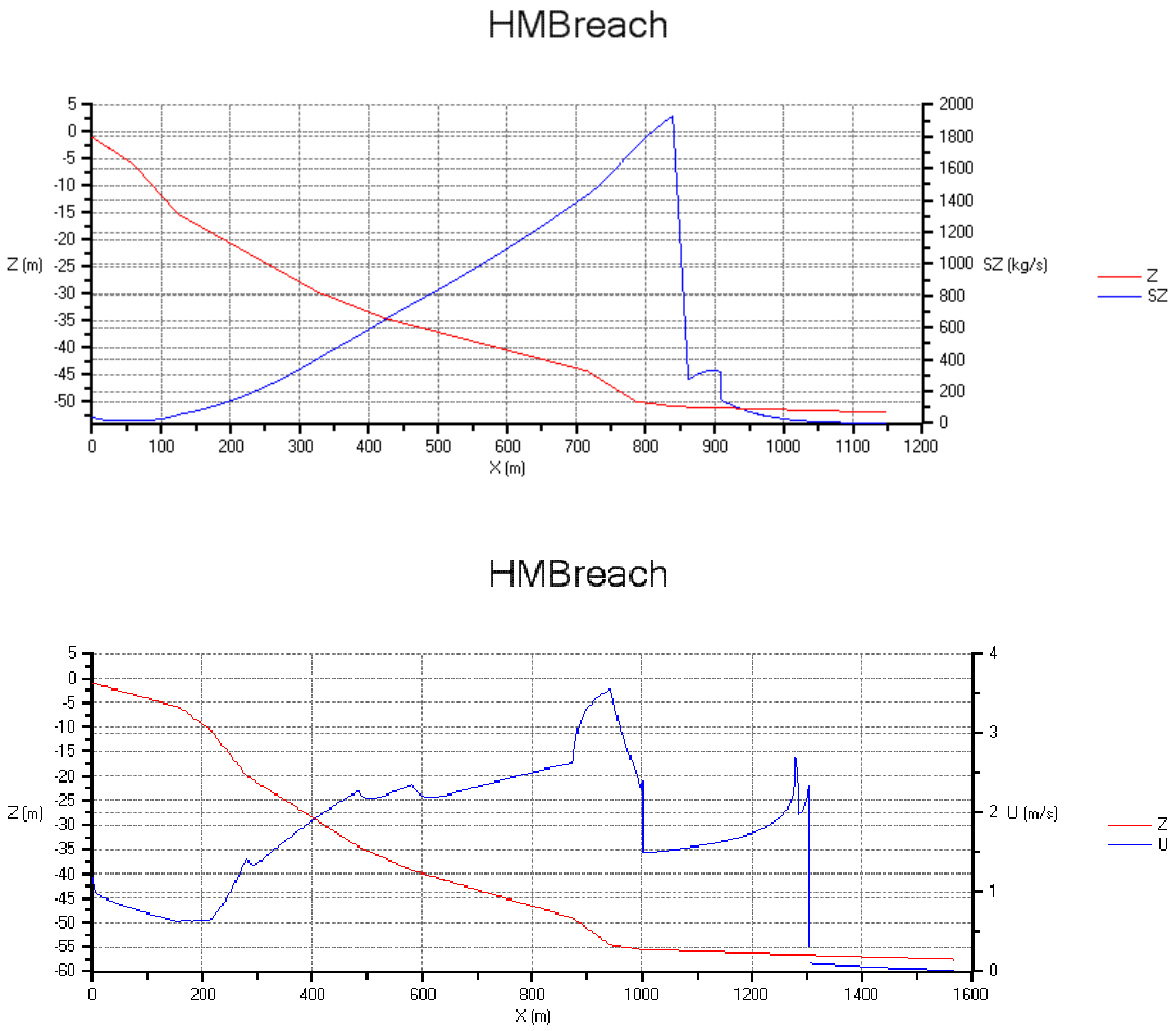

Figure 5.5-4: Sand transport and speed for location 2 and f_0 = 0.05.

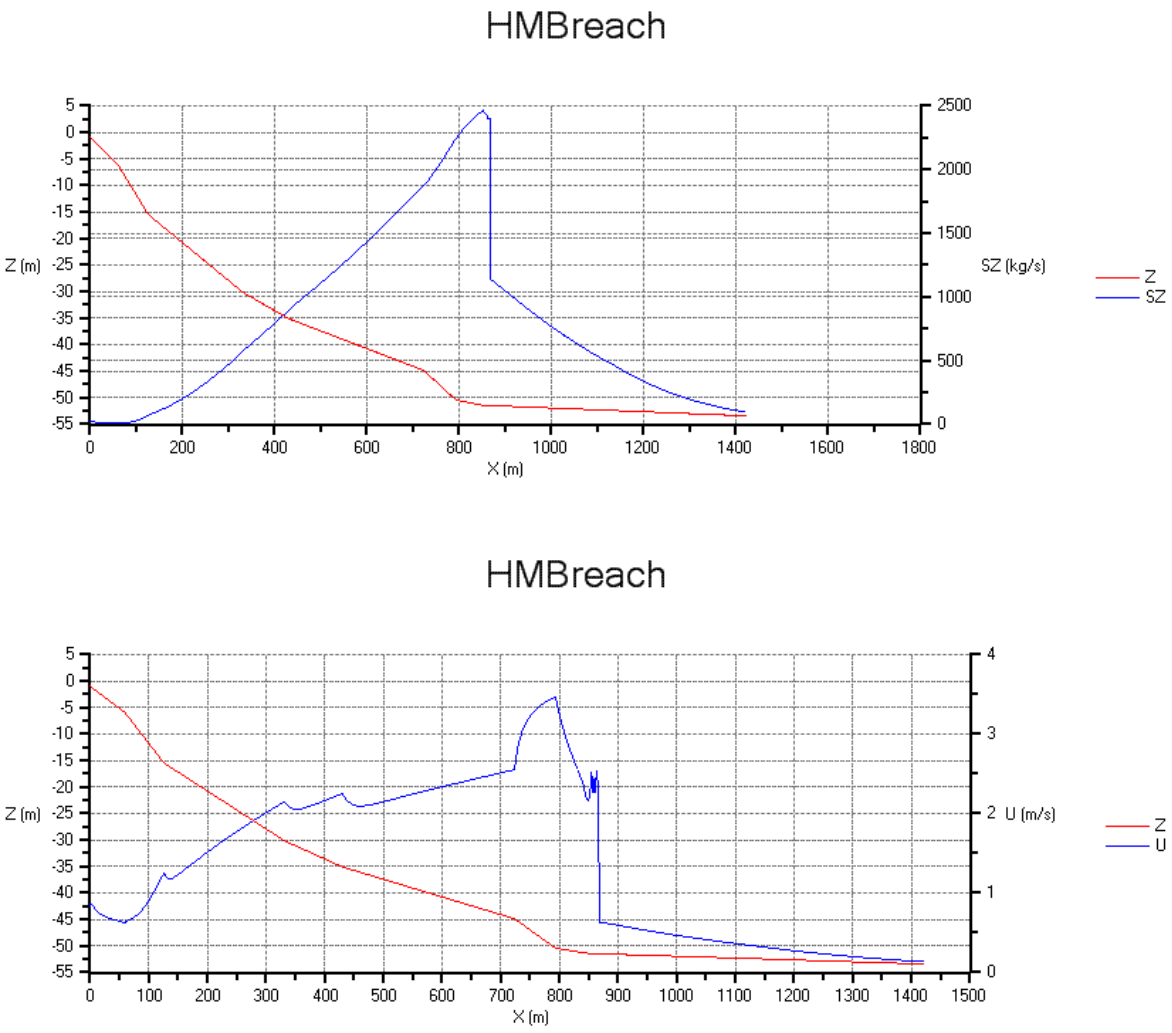

Figure 5.5-5: Sand transport and speed for location 2 and f_0 = 0.075.

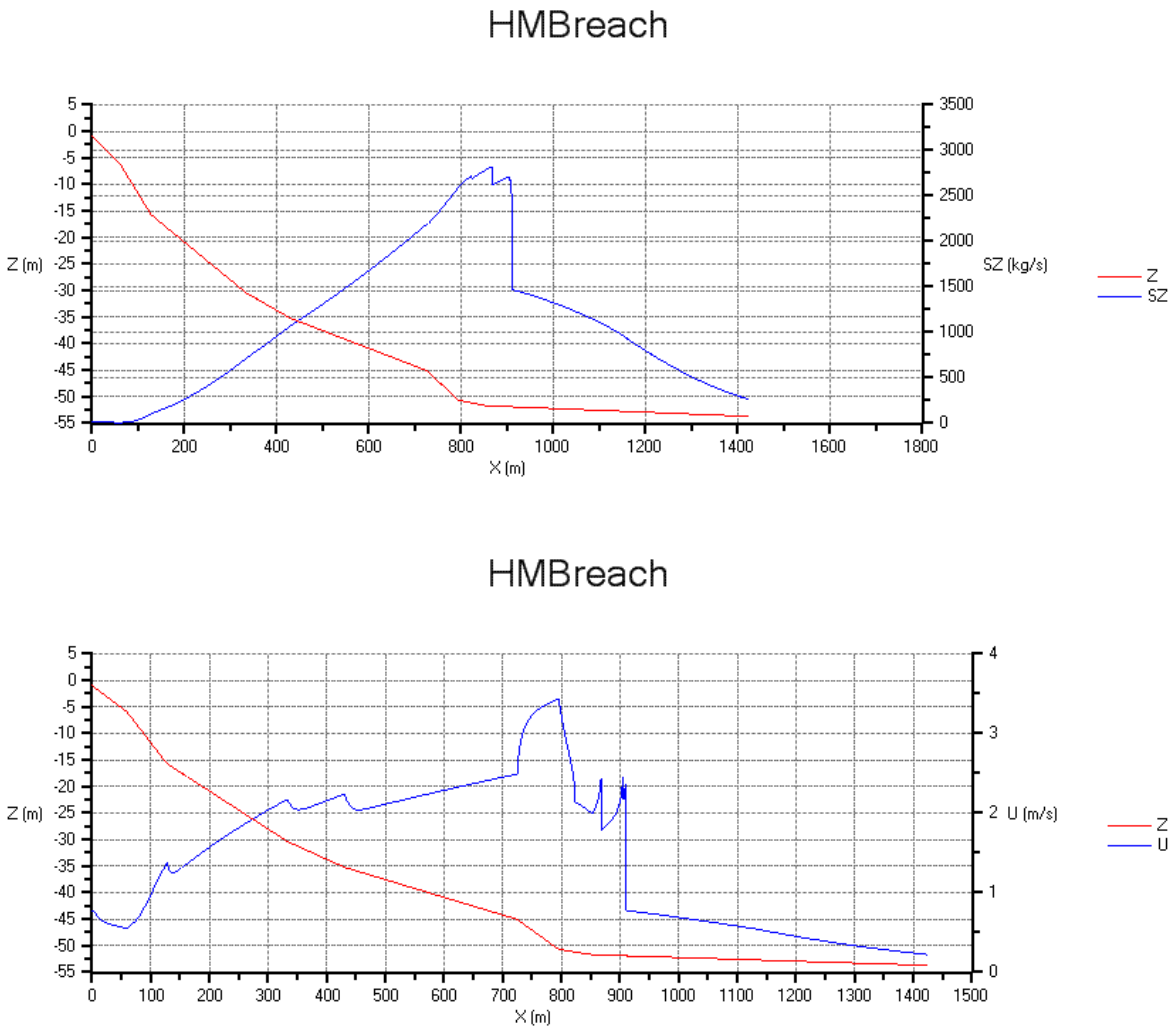

Figure 5.5-6: Sand transport and speed for location 2 and f_0 = 0.1.

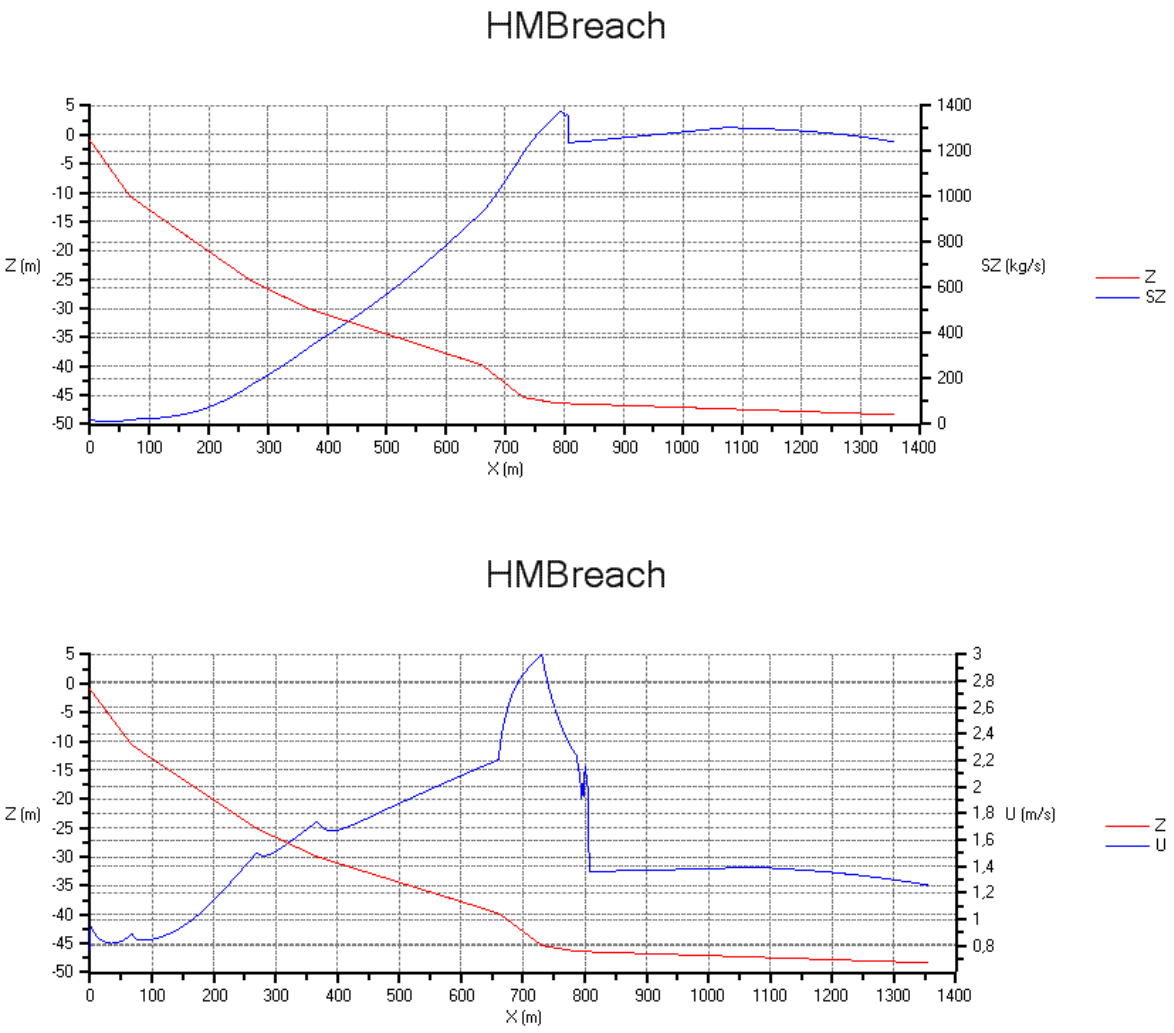

Figure 5.5-7: Sand transport and speed for location 3 and f_0 = 0.05.

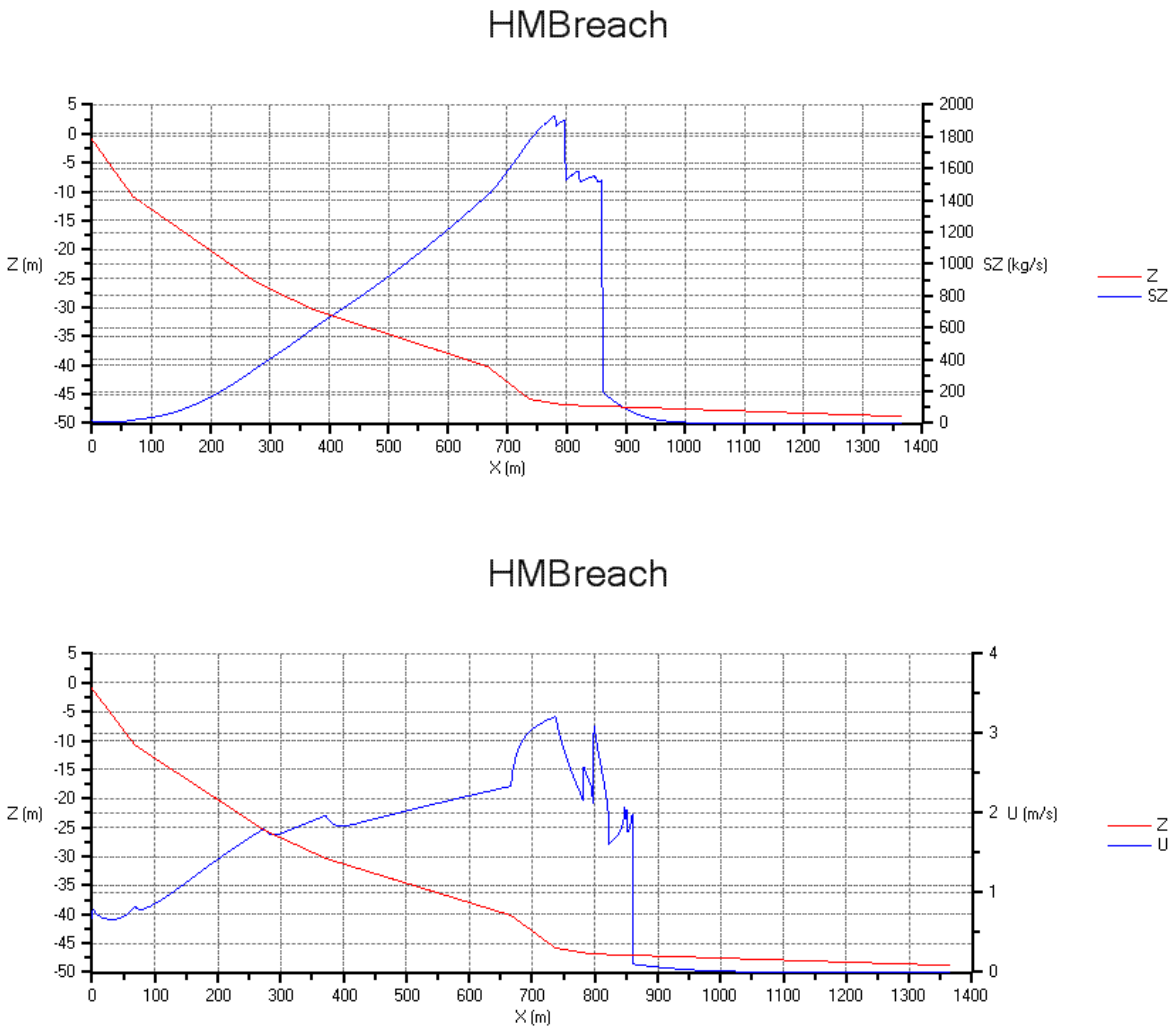

Figure 5.5-8: Sand transport and speed for location 3 and f_0 = 0.075.

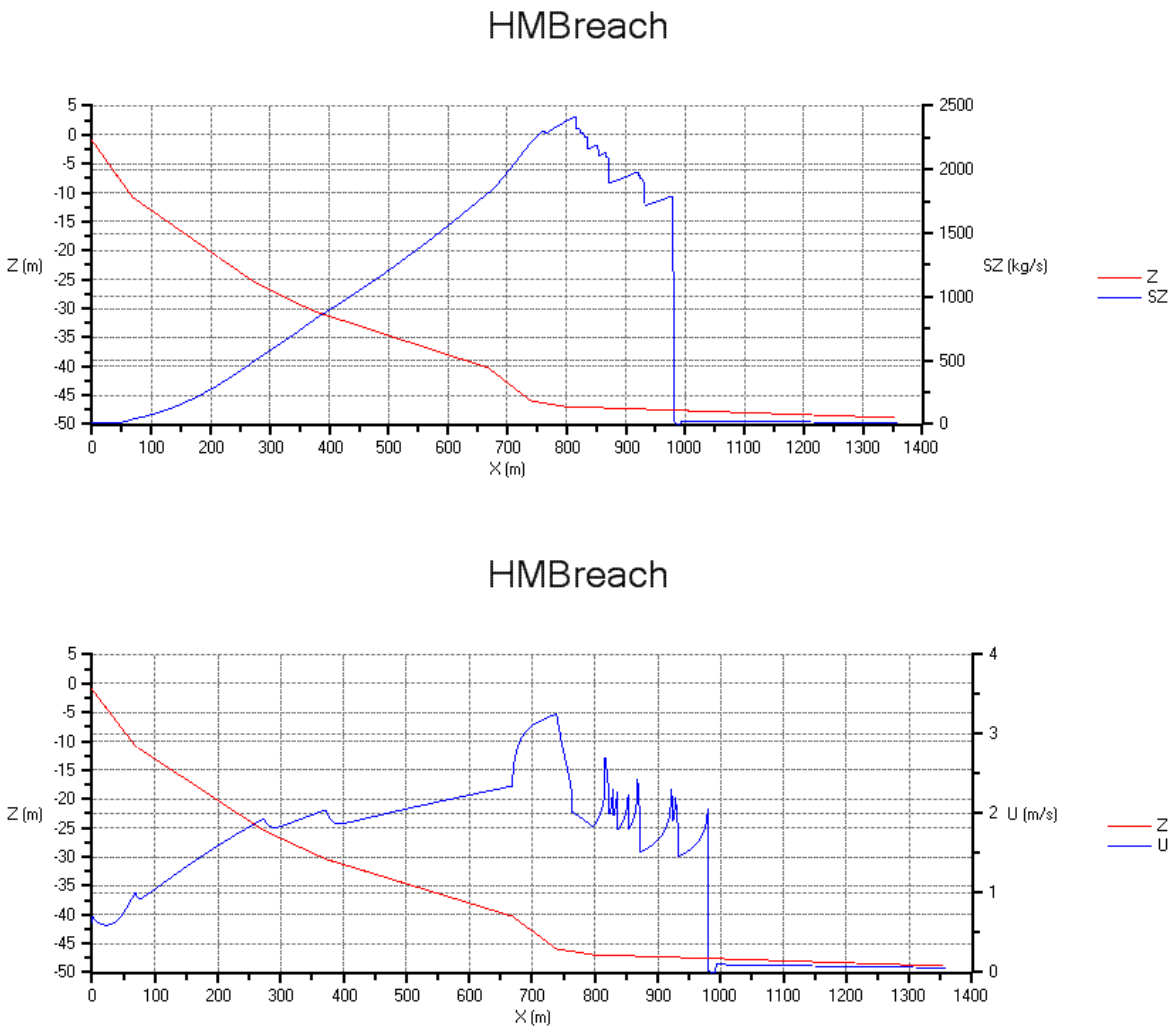

Figure 5.5-9: Sand transport and speed for location 3 and $f_0 = 0.1$.

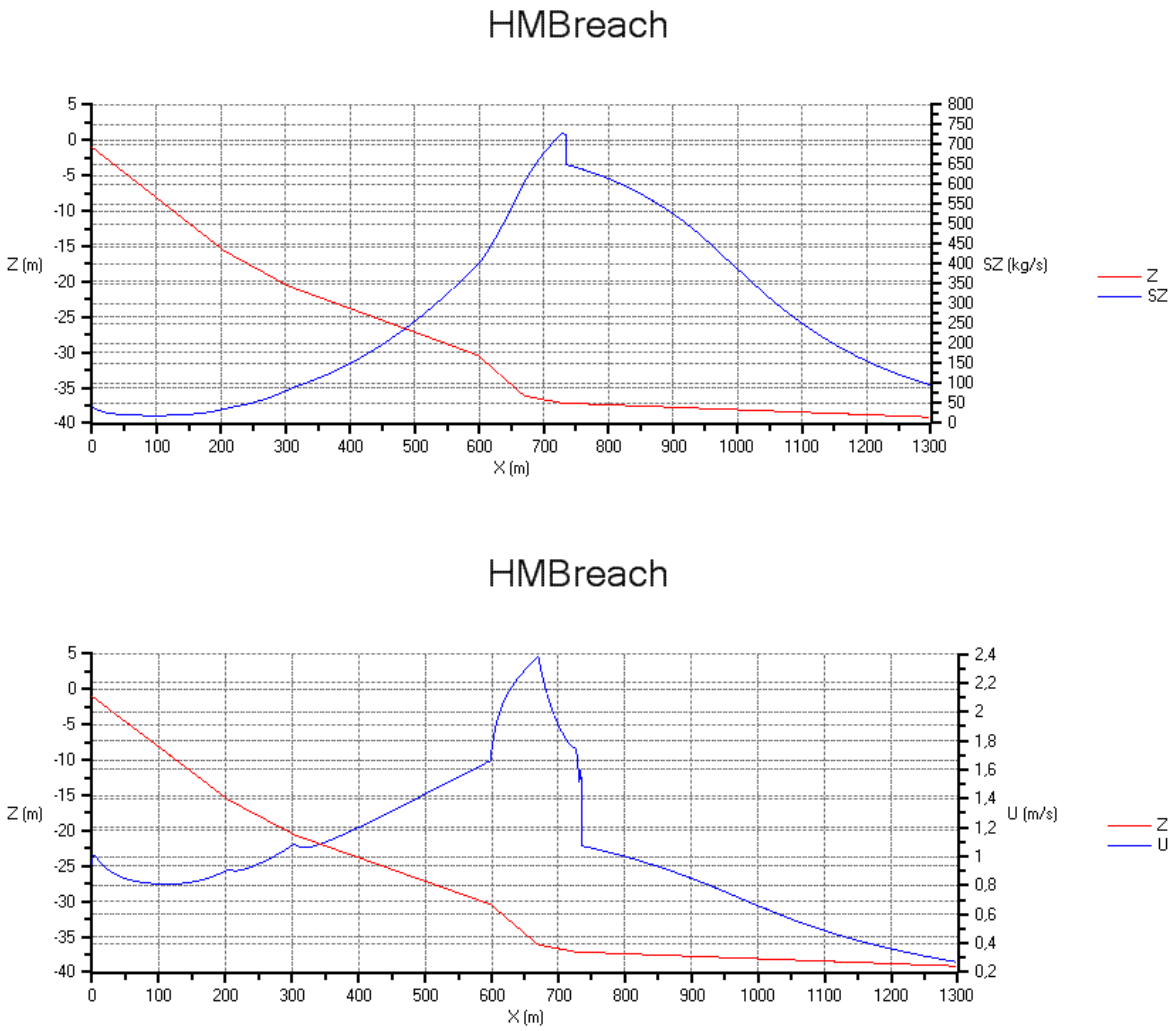

Figure 5.5-10: Sand transport and speed for location 4 and f_0 = 0.05.

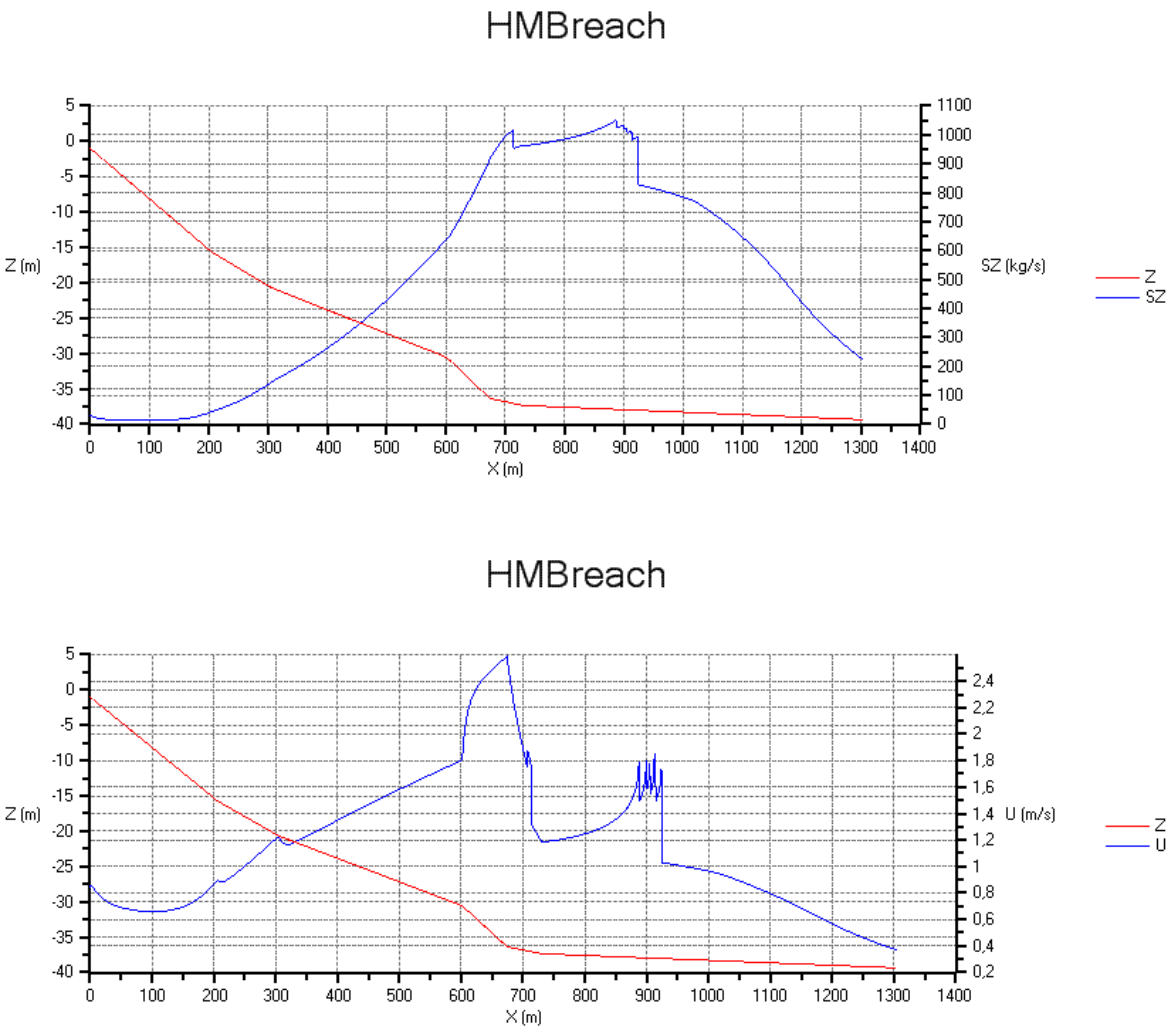

Figure 5.5-11: Sand transport and speed for location 4 and f_0 = 0.075.

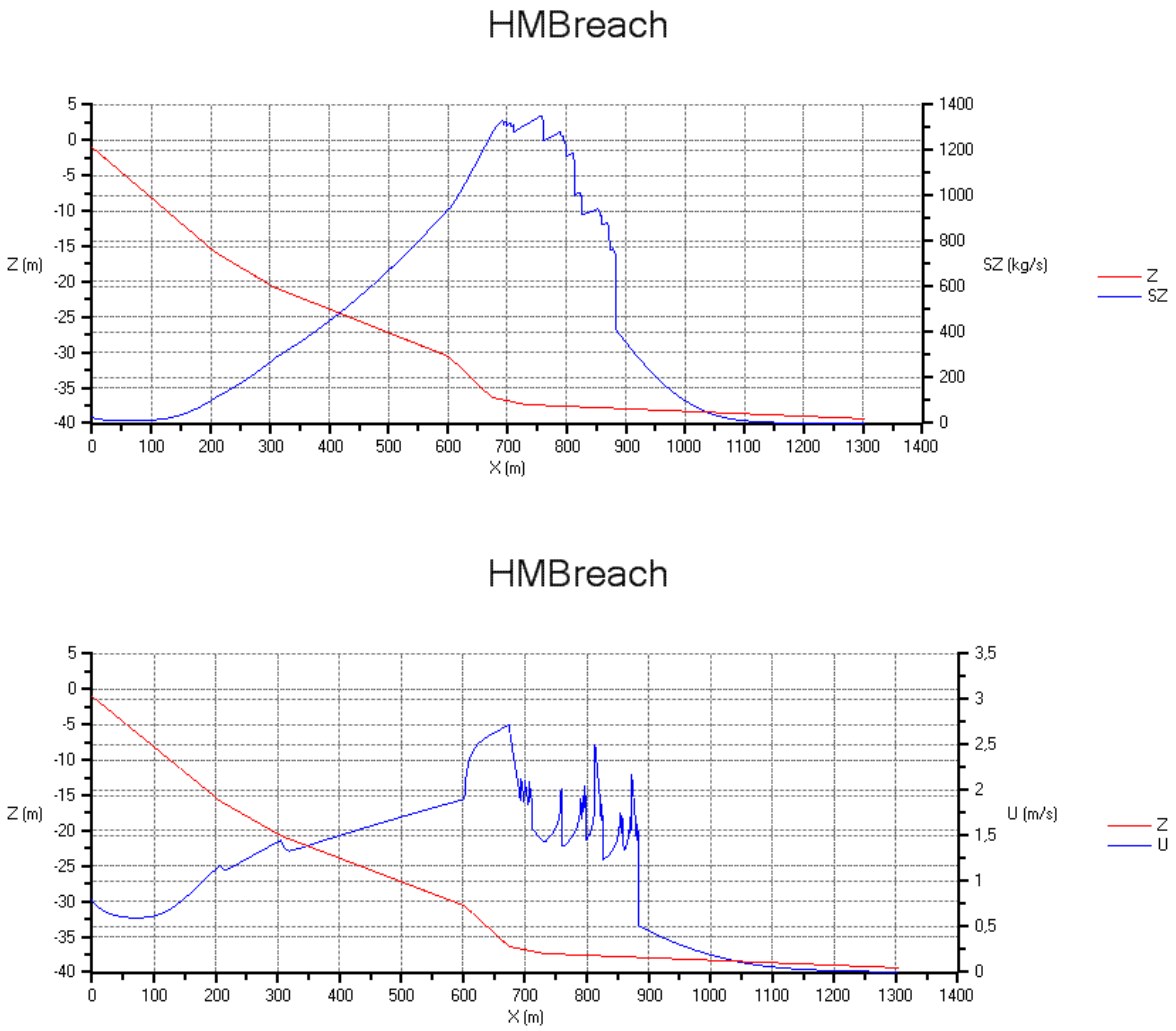

Figure 5.5-12: Sand transport and speed for location 4 and f_0 = 0.1.

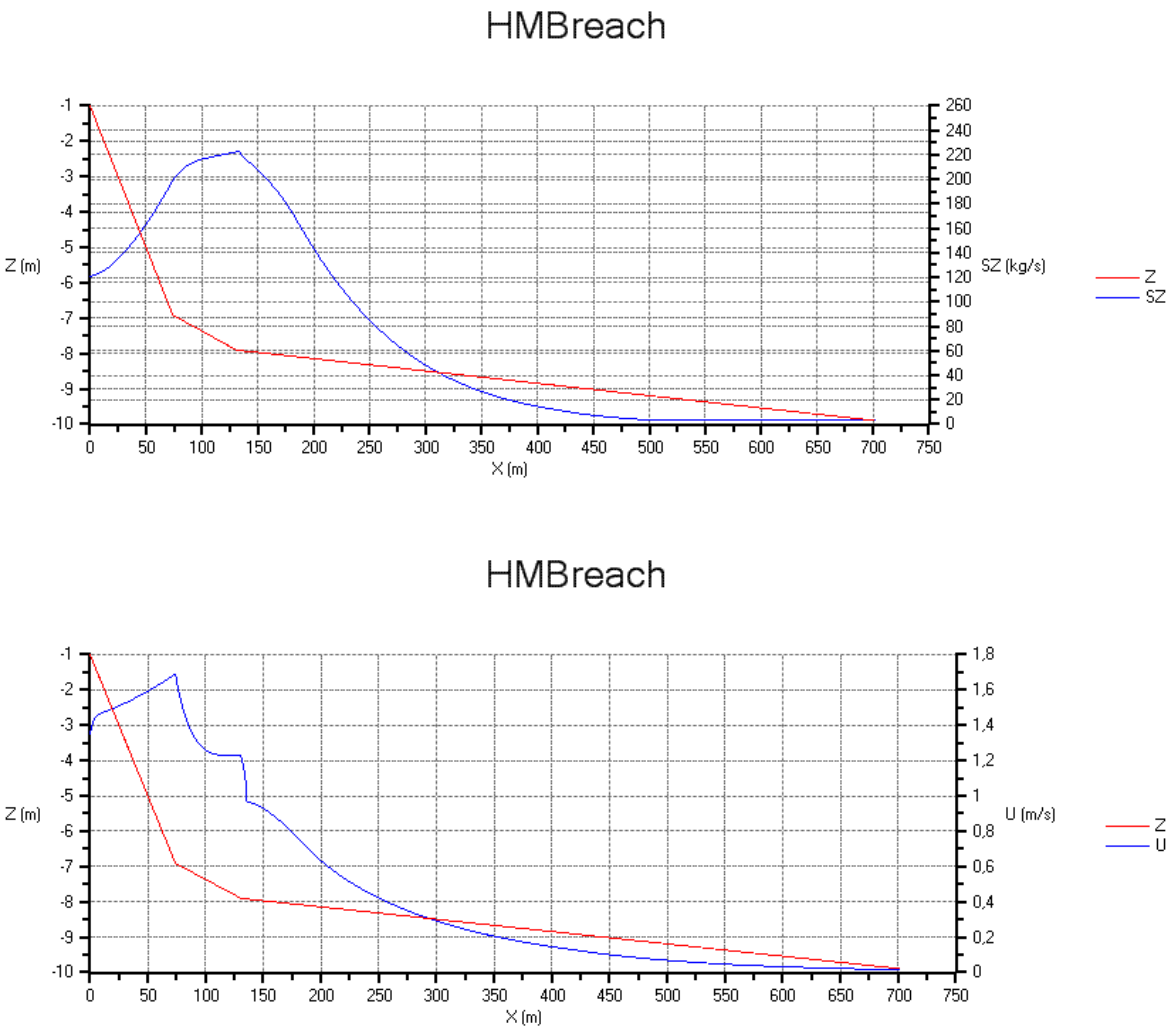

Figure 5.5-13: Sand transport and speed for location 5 and f_0 = 0.05.

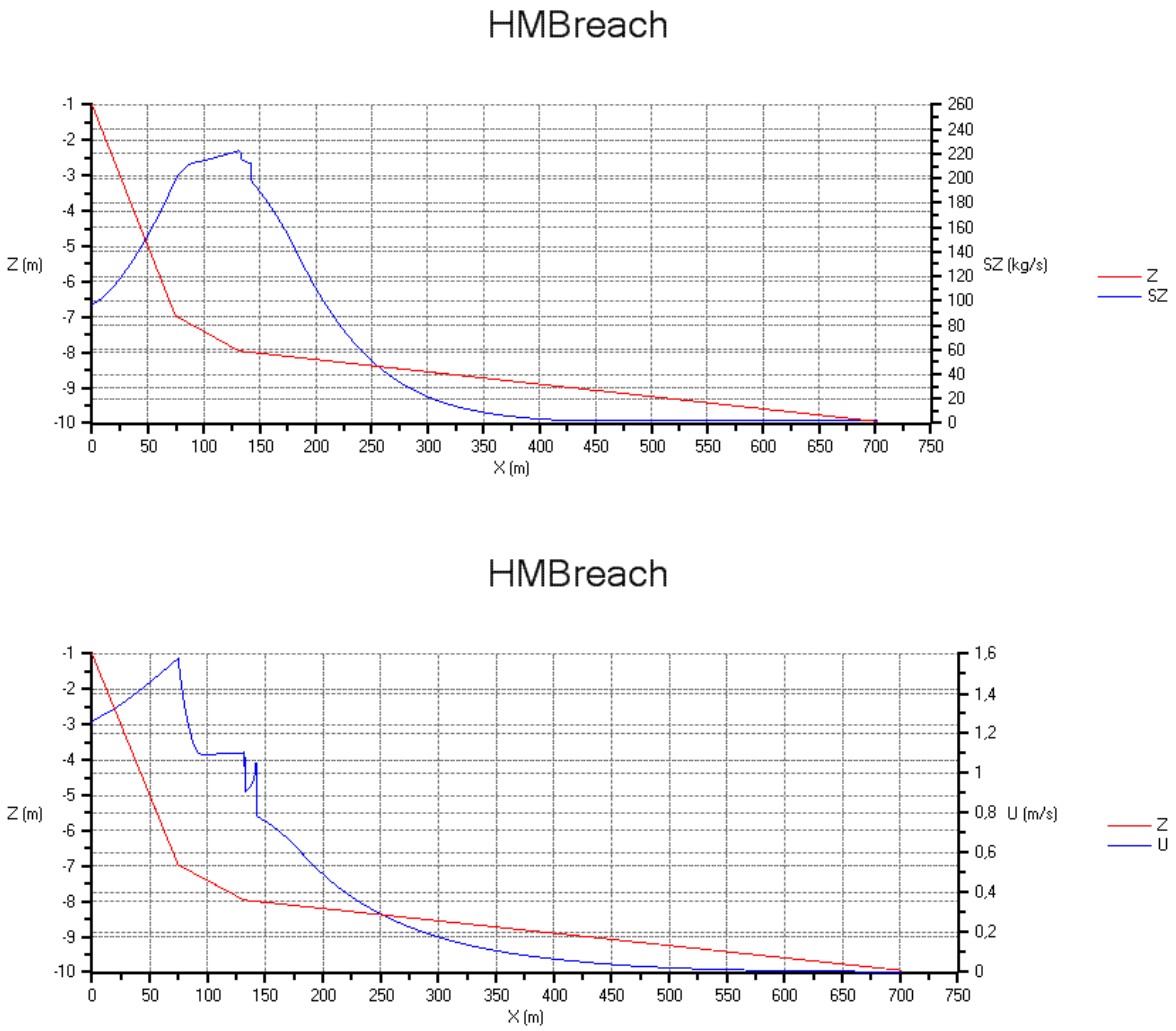

Figure 5.5-14: Sand transport and speed for location 5 and f_0 = 0.075.

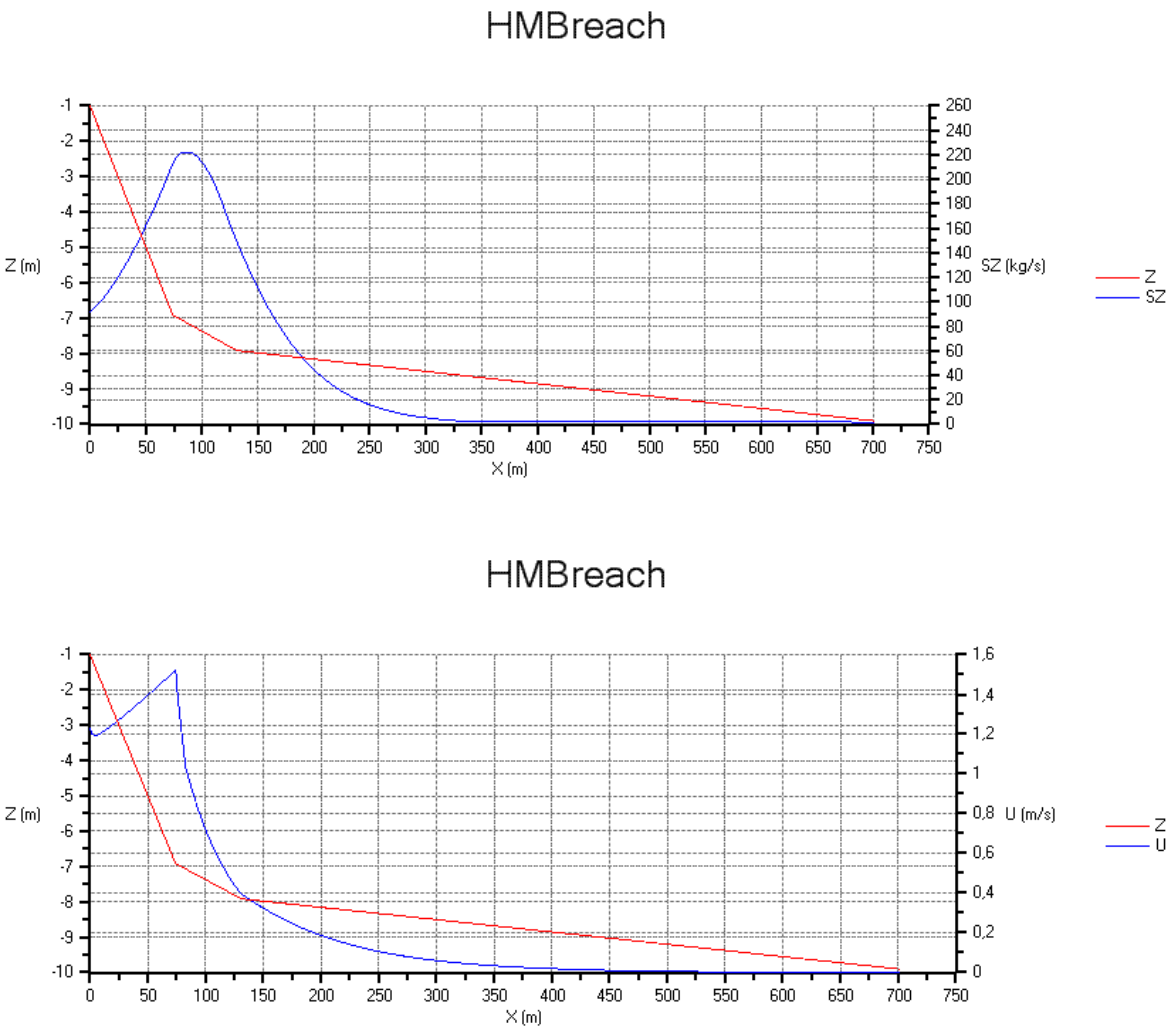

Figure 5.5-15: Sand transport and speed for location 5 and f_0 = 0.1.

6 APPENDIX: TABLES

6.1 SENSITIVITY ANALYSIS HMBREACH

Input:	Thickness (m)	Porosity (%)	D_{50} (µu)
Layer 1	1	40	200
Layer 2	1	40	200
Layer 3	1	40	200
Layer 4	1	40	200
Layer 5	1	40	200
Layer 6	1	40	200
Layer 7	1	40	200
Layer 8	1	40	200
Layer 9	1	40	200
Layer 10	1	40	200
Layer 11	1	40	200
Layer 12	1	40	200
Layer 13	1	40	200
Layer 14	1	40	200
Layer 15	1	40	200
Layer 16	1	40	200
Layer 17	1	40	200
Layer 18	1	40	200
Layer 19	1	40	200
Layer 20	1	40	200

Table 6.1-1: Input HMBreach for the sensitivity analysis HMBreach.

6.2 SENSITIVITY ANALYSIS HMTURB

Input:	Thickness (m)	Porosity (%)	D_{50} (µu)	Angle (deg)
Layer 1	1	40	200	10
Layer 2	1	40	200	13
Layer 3	1	40	200	16,5
Layer 4	1	40	200	20
Layer 5	1	40	200	16,5
Layer 6	1	40	200	13
Layer 7	1	40	200	10
Layer 8	1	40	200	8
Layer 9	1	40	200	6
Layer 10	1	40	200	4
Layer 11	1	40	200	2
Layer 12	1	40	200	1
Layer 13	1	40	200	0,5
Layer 14	1	40	200	0,25
Layer 15	1	40	200	10
Layer 16	1	40	200	13
Layer 17	1	40	200	16,5
Layer 18	1	40	200	20
Layer 19	1	40	200	16,5
Layer 20	1	40	200	13

Table 6.2-1: Input HMBreach for the sensitivity analysis HMTurb.

6.3 ROGGENPLAAT

Input:	Thickness (m)	Porosity (%)	D_{50} (µu)	Δn	Angle (deg)	Input:	Thickness (m)	Porosity (%)	D_{50} (µu)	Δn	Angle (deg)
Layer 1	0,8	43	165	0,084	2,181641404	Layer 35	0,85	49	170	0,015	10,7843
Layer 2	0,7	43	165	0,084	1,091216225	Layer 36	0,9	39,6	175	0,155	10,7843
Layer 3	0,7	43	165	0,084	1,091216225	Layer 37	0,8	39,6	175	0,155	10,7843
Layer 4	0,95	41,4	190	0,089	1,091216225	Layer 38	0,7	40	180	0,124	20,85446
Layer 5	0,85	41,4	190	0,089	1,091216225	Layer 39	0,6	40	180	0,124	20,85446
Layer 6	0,85	41,4	190	0,089	2,181641404	Layer 40	0,1	41	180	0,115	20,85446
Layer 7	1,05	40,4	175	0,125	2,181641404	Layer 41	0,4	45	185	0,03	20,85446
Layer 8	1,05	40,4	175	0,125	1,091216225	Layer 42	0,7	41,4	180	0,095	20,85446
Layer 9	1,05	40,4	175	0,125	2,181641404	Layer 43	0,65	41,4	180	0,095	20,85446
Layer 10	1	44,6	170	0,034	2,181641404	Layer 44	0,85	42,6	200	0,13	20,85446
Layer 11	1	44,6	170	0,034	3,270487923	Layer 45	0,85	42,6	200	0,13	20,85446
Layer 12	1	44,6	170	0,034	3,270487923	Layer 46	0,85	42,6	200	0,13	20,85446
Layer 13	1	44,6	170	0,034	3,270487923	Layer 47	0,85	42,6	200	0,13	20,85446
Layer 14	1	44,6	170	0,034	4,356975006	Layer 48	0,85	42,6	200	0,13	20,85446
Layer 15	1	44,6	170	0,034	4,356975006	Layer 49	0,65	35,8	65	0,476	20,85446
Layer 16	1	44,6	170	0,034	8,664135433	Layer 50	0,6	35,8	65	0,476	20,85446
Layer 17	1	44,6	170	0,034	8,664135433	Layer 51	0,8	41,6	200	0,1	20,85446
Layer 18	1	44,6	170	0,034	8,664135433	Layer 52	0,7	41,6	200	0,1	4,356975
Layer 19	1	44,6	170	0,034	8,664135433	Layer 53	0,7	41,6	200	0,1	4,356975
Layer 20	1	44,6	170	0,034	8,664135433	Layer 54	0,95	42	200	0,078	4,356975
Layer 21	1	44,6	170	0,034	8,664135433	Layer 55	0,9	42	200	0,078	6,519802
Layer 22	0,75	44,6	170	0,034	8,664135433	Layer 56	0,9	42	200	0,078	6,519802
Layer 23	1,05	43,4	135	0,068	8,664135433	Layer 57	0,9	42	200	0,078	6,519802
Layer 24	1,05	43,4	135	0,068	14,93141718	Layer 58	0,9	42	200	0,078	2,181641
Layer 25	1,05	43,4	135	0,068	14,93141718	*Layer 59*	*1*	*42*	*200*	*0,078*	*1*
Layer 26	1,05	42,8	185	0,065	14,93141718	*Layer 60*	*1*	*42*	*200*	*0,078*	*1*
Layer 27	1,05	42,8	185	0,065	14,93141718	*Layer 61*	*1*	*42*	*200*	*0,078*	*1*
Layer 28	0,8	44	155	0,065	14,93141718	*Layer 62*	*1*	*42*	*200*	*0,078*	*1*
Layer 29	0,9	42,4	310	0,051	14,93141718	*Layer 63*	*1*	*42*	*200*	*0,078*	*1*
Layer 30	0,9	42,4	310	0,051	14,93141718	*Layer 64*	*1*	*42*	*200*	*0,078*	*0,2*
Layer 31	0,9	42,4	310	0,051	14,93141718	*Layer 65*	*1*	*42*	*200*	*0,078*	*0,2*
Layer 32	0,8	45,6	175	0,015	10,78429787	*Layer 66*	*1*	*42*	*200*	*0,078*	*0,2*
Layer 33	0,7	45,6	175	0,015	10,78429787	*Layer 67*	*1*	*42*	*200*	*0,078*	*0,2*
Layer 34	0,7	45,6	175	0,015	10,78429787	*Layer 68*	*1*	*42*	*200*	*0,078*	*0,2*

Table 6.3-1: Input HMTurb for the Roggenplaat before collapse, the italic layers were added.

6.4 SPIJKERPLAAT

Input:	Thickness (m)	Porosity (%)	D_{50} (µu)	D_{15} (µu)	Angle (deg)	Input:	Thickness (m)	Porosity (%)	D_{50} ɹ)	D_{15} (µu)	Angle (deg)
Layer 1	1	42	175	125	1,79	Layer 28	1	41,5	160	112	4,09
Layer 2	1	42	175	125	1,79	Layer 29	1	41,5	160	112	4,09
Layer 3	1	41	175	125	1,79	Layer 30	1	41,5	160	112	4,09
Layer 4	1	41	175	125	1,79	Layer 31	1	41,5	160	112	4,09
Layer 5	1	41	175	125	1,79	Layer 32	1	41,5	160	112	4,09
Layer 6	1	40	175	125	4,76	Layer 33	1	41,5	160	112	4,09
Layer 7	1	41	160	112	4,76	Layer 34	1	41,5	160	112	4,09
Layer 8	1	41,5	160	112	4,76	Layer 35	1	41,5	160	112	4,09
Layer 9	1	41,5	160	112	4,76	Layer 36	1	41,5	160	112	2,86
Layer 10	1	43	160	112	4,76	Layer 37	1	41,5	160	112	2,86
Layer 11	1	41	160	112	8,13	Layer 38	1	41,5	160	112	2,86
Layer 12		41	160	112	8,13	Layer 39	1	41,5	160	112	2,86
Layer 13	1	41,5	160	112	8,13	Layer 40	1	41,5	160	112	2,86
Layer 14	1	40	160	112	8,13	Layer 41	1	41,5	160	112	1,91
Layer 15	1	41	160	112	8,13	Layer 42	1	41,5	160	112	1,91
Layer 16	1	41,5	160	112	8,13	Layer 43	1	41,5	160	112	1,91
Layer 17	1	43	160	112	8,13	Layer 44	1	41,5	160	112	1,91
Layer 18	1	43,5	160	112	8,13	Layer 45	1	41,5	160	112	1,91
Layer 19	1	42	160	112	8,13	Layer 46	1	41,5	160	112	4,57
Layer 20	1	42,5	160	112	8,13	Layer 47	1	41,5	160	112	4,57
Layer 21	1	41,5	160	112	4,09	Layer 48	1	41,5	160	112	4,57
Layer 22	1	40	160	112	4,09	Layer 49	1	41,5	160	112	4,57
Layer 23	1	41,5	160	112	4,09	Layer 50	1	41,5	160	112	4,57
Layer 24	1	41,5	160	112	4,09	Layer 51	1	41,5	160	112	4,57
Layer 25	1	41,5	160	112	4,09	*Layer 52*	*1*	*41,5*	*160*	*112*	*1*
Layer 26	1	41,5	160	112	4,09	*Layer 53*	*1*	*41,5*	*160*	*112*	*0,2*
Layer 27	1	41,5	160	112	4,09	*Layer 54*	*1*	*41,5*	*160*	*112*	*0,2*

Table 6.4-1: Input HMTurb for the Spijkerplaat before collapse, the italic layers were added.

7 BIBLIOGRAPHY

Deltadienst. "Bescherming van de Plaat van Oude Tonge." *Deltawerken, Driemaandelijks Bericht*, February Nummer 67, 1974: 353 - 354.

Deltadienst. "Plaatval in de Roggenplaat." *Deltawerken, Driemaandelijks Bericht*, November Nummer 66, 1973: 315-323.

Groot, M.B. de, M.B. van der Ruyt, G.A. van den Ham, and D.R. Mastbergen. "Zettingsvloeiing bij ontgrondingskuil Oosterscheldekering." 2008.

Groot, M.B. de, T.P. Stoutjesdijk, T. Schweckendiek, and P. Meijers. "Verwekingsvloeiing in zand." *Geotechniek*, September 2007: 54-59.

Groot., M.B. de, M.B. van der Ruyt, D.R. Mastbergen, and G.A. van den Ham. "Bresvloeiing in zand." *GEOtechniek*, July 2009: 34-39.

Mastbergen, D. R. *Oeverstabiliteit bij verdieping waterbodems.* Delft: Delft Cluster, 2009.

Stoutjesdijk, T., and M.B. de Groot. *Verificatie SLIQ2D aan de Zeeuwse Praktijk.* Delft: Grondmechanica Delft, 1994.

Wilderom, Bakker. *Resultaten van het Vooroeveronderzoek Langs de Zeeuwse Stromen.* Vlissingen: Rijkswaterstaat, 1979.